Phosphate Removal from Wastewater by Mineral Wool Filters

N.V. van Jaarsveld

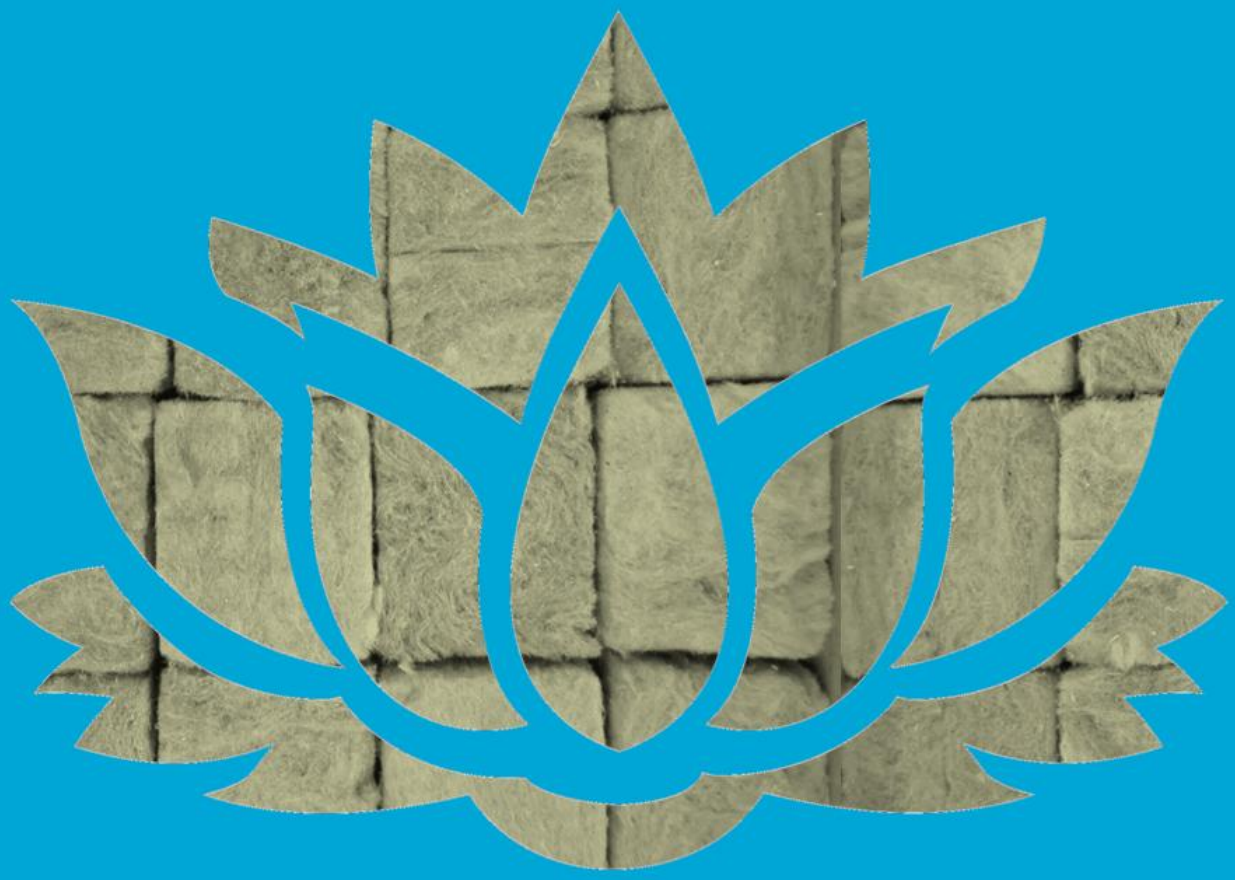

TU Delft

Delft University of Technology

Phosphate Removal from Wastewater by Mineral Wool Filters

By

N.V. van Jaarsveld

in partial fulfilment of the requirements for the degree of

Master of Science
in Environmental Engineering

at the Delft University of Technology,
to be defended publicly on Wednesday January 29, 2019 at 15:00.

Student number: 4604210

Thesis committee:

Prof. Dr.Ir. M. de Kreuk,	TU Delft, chair
Ir. S de Valk,	TU Delft, supervisor
Dr. B van Breukelen,	TU Delft
Dr. T Bogaard,	TU Delft,

TU Delft

The butterfly counts not months but moments, and has time enough.

- Rabindranath Tagore

Acknowledgement

This report is the result of my research project for my graduation as a MSc student in Environmental Engineering, with a specialization in Environmental Technology. It indicates the end of my time as a student at Delft University of Technology. A time which has led to great professional and personal development and growth.

First of all, I would like to take this opportunity to thank my daily supervisor, Ir. Steef de Valk, for his positive energy, encouragement, knowledge and time. Steef has shown me the real insights into performing scientific research and has been of great support during the process of writing a thesis. I would also like to thank the chair of my committee, Prof. Dr. Ir. Merle de Kreuk, for her valuable supervision and guidance throughout the thesis, but also during the master's degree. Merle is a true inspiration to women in science.

Furthermore, I would like to thank Dr. Boris van Breukelen and Dr. Thom Bogaard as part of my committee for their advice and recommendation given during various meetings. In addition, a special word of thanks to the lab technicians Armand Middeldorp, Patrica van den Bos, and Michel van den Brink.

Last, but not least, I would like to thank my family and friends for their support throughout my entire master's degree. Without your uplifting words, opinions, smiles and hugs, this work would not have been possible.

Nicole van Jaarsveld
January 2020, Delft

Abstract

According to the United Nations, eutrophication is the most prevalent water quality problem. Developing countries especially are struggling to manage the increasing volume of untreated wastewater. A preliminary study of a Dutch-Indian partnership, developing universal watermanagement (LOTUS^{HR}), has shown some indication of ortho-phosphate removal by mineral wool. The objective of this research is to understand the ortho-phosphate removal mechanism of mineral wool used for wastewater treatment. It was hypothesized that mineral wool dissociates ions due to biologically mediated pH changes, which subsequently interact with ortho-phosphate, forming minerals and removing ortho-phosphate from wastewater.

First of all, the chemical composition of mineral wool was determined. Secondly, the dissolution of mineral wool was quantified by batch experiments at different pH and phosphate concentrations. Furthermore, geochemical modeling with PHREEQC was used to analyze the thermodynamic potential of wastewaters to precipitation, not containing mineral wool. Additionally, the phosphate removal rates of a flow-through experiment, using mimicked Indian Drain Water and mineral wool, was compared with PHREEQC simulations.

Results showed that based on chemical analysis mineral wool contains: 188.0 g/kg silicon, 187.6 g/kg calcium, 79.3 g/kg aluminum, 43.1 g/kg iron, among other elements. The mineral wool showed no significant dissolution of ions under different pH and phosphate concentrations. Therefore, the hypothesis was rejected, as the mineral wool did not release ions when stressed with different pH. Consequently, biological conversion will not facilitate ion release from the mineral wool either. The mineral wool did show a self-buffering effect, due to its alkaline properties. Furthermore, with use of PHREEQC, amorphous tricalcium phosphate was characterized as the major mineral phase.

In conclusion, the hypothesis formulated was rejected. This research performed did not lead to the identification of the removal mechanism responsible for the ortho-phosphate removal from wastewater by mineral wool filters.

Content

List of Abbreviations

ATCP	Amorphous tricalcium phosphate
AES	Alkaline earth silicate
BOD	Biological Oxygen Demand
COD	Chemical Oxygen Demand
DCP	Dicalcium phosphate
DCPD	Brushite or dicalcium phosphate dihydrate
EBPR	Enhanced biological phosphorus removal
EC	Electrical Conductivity
G	Gibbs Energy
H	Enthaply
HAP	Hydroxyapatite
HDP	Hydroxydicalcium phosphate
IAP	Ion Activity Product
ICPOES	Inductively Coupled Plasma Optical Emission Spectrometry
Ksp	Solubility product
LCFA	Long Chain Fatty Acids
LOTUS^{HR}	Local Treatment of Urban sewage and Streams for Healthy Reuse
MON	Monetite
NEW	Newberyite
OCP	Octacalcium phosphate
PAO's	Polyphosphate-accumulating organisms
PHREEQC	pH-REdox-EQuilibrium (Geochemical model)
SCFA	Short Chain Fatty Acids
SI	Saturation Index
TCP	Tricalcium phosphate
VFA's	Volatile Fatty Acids
VSS	Volatile Suspended Solids
XRD	X-Ray powder Diffraction
XRF	X-ray Fluorescence

1. Introduction

1.1. General Background

According to the United Nations eutrophication is the most prevalent water quality problem (UNEP, 2016). Eutrophication is a result of a high nutrient loading of nitrogen and phosphorus in surface waters of which anthropogenic activities are the primary cause of high loading (EPA, 2007; UNEP, 2016; Azam *et al.*, 2019). Consequences of eutrophication are toxic algal blooms, low dissolved oxygen, and loss of biodiversity, which significantly impairs beneficial uses of water (EPA, 2007; UNEP, 2016). To combat these negative effects on aquatic ecosystems, the nutrient load needs to be controlled. Since 1990, African, Asian, and Latin American rivers experience an increase in water pollution (UNEP, 2016). Despite new investments made in wastewater treatment, developing countries especially are struggling to manage the increasing volume of untreated wastewater, produced due to population growth, increased economic activity, and expanding agriculture (UNEP, 2016).

One of such developing countries struggling to reduce water pollution is India (Lotus HR, 2016). The water quality of the Yamuna river that enters New Delhi has highly deteriorated as untreated wastewater from 22 drains from the rapid urbanized catchment area and industrial effluents are discharged into the river (Trisal, Tabassum and Kumar, 2008; Said and Hussain, 2019). The total discharge on the Yamuna river by the drains is over 2,870 mld (million liters per day), which eventually flows into the Ganga (Figure 1)(Trisal, Tabassum and Kumar, 2008). One of the drains connected to the Yamuna river is the Barapullah drain, with a volumetric contribution of 4.26% (equal to 2 m3/s) and a biological oxygen demand (BOD) load contribution of 5.97% (equal to 15.49 tons of BOD per day) (Trisal, Tabassum and Kumar, 2008). Nutrient content of phosphorus and nitrogen in the Barapullah drain vary between 1-100 mgPO_4-P/L and 2-70 mgNH_4-N/L (Lotus HR, 2018).

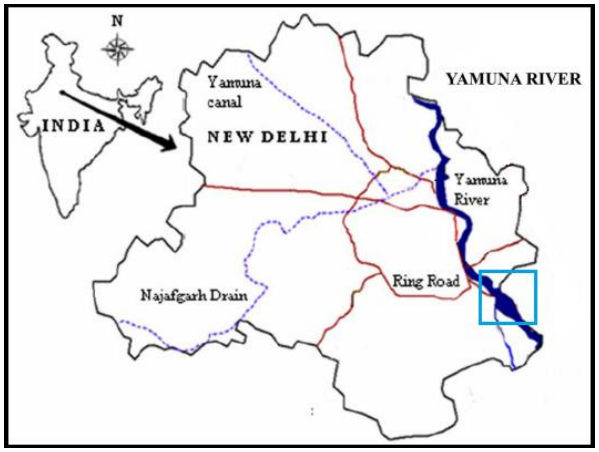

Figure 1, Yamuna River flowing through New Delhi, India. The blue box indicates the specific experimental test site of LOTUS^{HR}. Map retrieved from (Said and Hussain, 2019), adjusted by author.

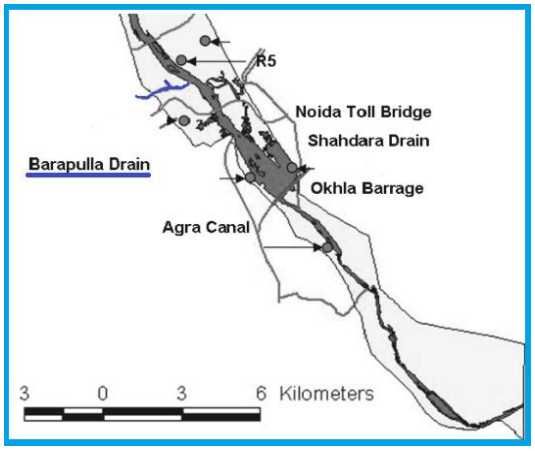

Figure 2, Location of the Barapullah Drain, tributary to the Yamuna River. Map retrieved from (Trisal, Tabassum and Kumar, 2008), adjusted by author.

The Barapullah drain is currently used as an experimental test site for the Local Treatment of Urban sewage and Streams for Healthy Reuse (LOTUS^{HR}) (Lotus HR, 2016). The goal of the project is 'to

demonstrate that by combining existing cost-effective technologies and targeting potential pollutants at the source, the sacred role of the river in Indian society can be preserved despite the anticipated rapid urbanization and associated water stress' (Lotus HR, 2016). Along these lines many different wastewater treatment technologies are being tested in both The Netherlands and in New Delhi, of which nutrient removal is one.

Mineral wool is a multipurpose material used for many different applications. Due to its high water retention capacity it is also used in water management as (storm)water retention systems, as well as a growth substrate in greenhouses, and for biological treatment of wastewaters (Drainblock, 2019). A preliminary study of the LOTUS^{HR} has shown the potential of mineral wool to function as a filter material for wastewater treatment. Mineral wool has been applied in channels in the Dutch province of Limburg and in Bandung, Indonesia (Cranenburgh, 2018; van Zandvoort, 2018). Small scale experiments with mineral wool performed in New Delhi, India indicate some ortho-phosphate (a form of phosphorus) removal, along with chemical oxygen demand (COD) conversion and nitrogen (N) removal by using biofilm (Merola, 2018).

1.2. Literature Review

Technologies that show a resemblance with the application of mineral wool in channels are: mineral based filtration, biological phosphorus uptake, and bacterially mediated mineralization. These technologies achieve P removal from wastewaters through the chemical formation of precipitates or via biological phosphorus uptake, with or without presence of biofilm.

Different mineral-based wools such as glass wool, rock/stone wool, and alkaline earth silicate (AES) wool exist. The mineral wools used in relation to water are mostly rock wools, which are chemically composed of roughly 38-46% SiO_2, 15-20% CaO, 15-19% Al_2O_3 and 6-9% Fe_2O_3 (Campopiano *et al.*, 2014). Although mineral wool is thought of to be inert, a study on the biosolubility of mineral wools showed dissolution of silicon (Si) and calcium (Ca) at different pH values, inducing calcium-phosphate (Ca-P) precipitates (Campopiano *et al.*, 2014). According to an assessment of mineral wool as support material for on-site sanitation, the mineral composition will influence the interaction between the material and the wastewater content: suggesting interaction between the mineral wool and the wastewater (Wanko *et al.*, 2016).

Mineral-based alkaline materials such as Filtra P, Polonites, natural wollastonite, and steel furnace slag are used as filter for domestic waste streams as the materials have a high phosphate binding capacity (Gustafsson *et al.*, 2008; Herrmann *et al.*, 2013; Claveau-Mallet, Courcelles and Comeau, 2014; Johansson, Ruscalleda and Colprim, 2017). These filter materials contain lime and/or alkaline calcium silicates. They have a high pH and release Ca to the water phase, leading to the removal of P from the to be treated water. The observed removal of P is explained by the formation of calcium phosphates (Gustafsson *et al.*, 2008).

Mineral wool can act as a carrier for biofilm development. The biofilm developed contains 0.015 mg P per gram of biomass and in that way fixate P and remove it from the wastewater (Metcalf & Eddy Inc., 2003). Biological reactions such as hydrolysis, nitrification and denitrification taking place in the biofilm can induce pH changes locally and temporarily as they produce acids and base (Dupraz *et al.*, 2009; Mañas *et al.*, 2012). Changes in pH induce the dissolution of cations and subsequent precipitation of minerals (Smeck, 1985; Campopiano *et al.*, 2014). This process is also referred to as biologically induced mineralization, which is one of the biologically mediated precipitation

mechanisms (Smeck, 1985; Dupraz *et al.*, 2009). This process can be further explained as metabolic activity leading to chemical modifications of the environment creating the specific circumstances needed for mineral precipitation. Extra-cellular and intra-cellular biomineralization has been previously described for calcium phosphates, magnesium carbonates and struvite (Ronteltap, Maurer and Gujer, 2007; Sánchez-Román *et al.*, 2007; Etter *et al.*, 2011; Boonrungsiman *et al.*, 2012; Mañas *et al.*, 2012; Arias, Cisternas and Rivas, 2017; Torres-Aravena *et al.*, 2018).

1.3. Problem Definition

For mineral wools used as a water treatment technology, neither the chemical nor the biological phosphate removal mechanism have been explored. The understanding of the removal mechanism is required to evaluate the potential utility of mineral wool as promising (biological) wastewater treatment technology. Therefore the purpose of this study is to understand the removal mechanism(s) of ortho-phosphate in mineral wool filters, and the role of biological activity on this removal.

1.4. Research Question

The objective of this research is to understand the ortho-phosphate removal mechanism of mineral wool used for wastewater treatment. For this purpose the main research question is:

What removal mechanism is responsible for ortho-phosphate removal from wastewater by mineral wool filters?

To answer this question, the following sub-questions should be answered first:

1. What does mineral wool consist of?
2. What is the effect of pH on the release of Ca, Al, Mg and Fe by mineral wool and on P precipitation?
3. How does mineral wool facilitate precipitation of minerals in waste- and drain waters?
4. How does biological conversion in mineral wool influence P removal rates?

1.5. Hypothesis

Literature review and a preliminary study of the LOTUS^{HR} lies at the basis of the hypothesis proposing an explanation of the removal mechanism of ortho-phosphate by mineral wool filter (see box 1.)

Box 1: Basis to formulation of the hypothesis on P removal mechanism from wastewater by mineral wool.

Mineral wool is rich in silica, calcium, aluminum and iron, and these ions may be released from the mineral wool as pH conditions change. Additionally, the mineral wool provides surface area for bacterial growth and activity. Biological activities, such as the process of (de)nitrification, can induce the localized pH change needed to release ions from the mineral wool and facilitate the reaction between those ions and the orthophosphate available in the wastewater. Phosphate removal from the aqueous phase is achieved when it reacts with the released ions from the mineral wool thereby forming a solid; the mineral phase.

It is hypothesized that *mineral wool dissociates ions due to biologically mediated pH changes, which subsequently interact with ortho-phosphate forming minerals, and in this manner removing ortho-phosphate from wastewater*. A graphical representation of the hypothesis is shown in Figure 3.

Figure 3, The three components involved in the potential biochemical removal of phosphorus.

By answering the research question and sub questions the formulated hypothesis can be confirmed or rejected, and further discussed.

1.6.Research Approach

The research performed to answer the research question and sub questions consists of a theoretical development, lab-scale experiments, and geochemical modeling. The wastewaters studied for the geochemical modeling are based upon the physiochemical composition of Indian Drain Water and Black Water. Experiments are performed in the Laboratory of Sanitary Engineering of the Delft University of Technology using mineral wool as provided by DrainBlocks.

This paper is divided into six chapters:

1. Introduction.
2. Theoretical Development. In this chapter the chemical and biological removal mechanisms are presented. A more detailed literature review on the reaction processes for potential phosphorus removal is included.
3. Method and Materials. This chapter presents the lab-scale experiments consisting of batch tests and flow-through experiments. Furthermore, the use of the geochemical modeling in PHREEQC is explained. Modeling improves understanding of biological and chemical processes and facilitate in experimental design phase (Azam *et al.*, 2019).
4. Results and Discussion. In this chapter the results are presented and discussed.
5. General Discussion and Recommendations. This chapter reflects upon the formed hypothesis in relation to the obtained results and proposes recommendations.
6. Conclusion. In this chapter the research conclusions are drawn.

2. Theoretical Development

This section contains a theoretical development on phosphates and the formation of phosphate minerals. Additionally, the different chemical and biological phosphorus removal mechanisms are explained. Furthermore, it includes an extended literature review on the reaction processes for potential phosphorus removal. A basic 'back of the envelope' calculation is performed in Appendix A, where the theoretical phosphorus removal is calculated for mineral wool for different removal mechanisms.

2.1. Natural occurrence of Phosphorus

Phosphorus is found in water, solids, and the bodies of biological organisms. Phosphorus occurs mostly as phosphates (PO_4): orthophosphates, condensed phosphates, and organic phosphates. Orthophosphate (o-PO_4) is reactive phosphate which is 'easily available' for algae, plant growth, and other biota. It is a good indicator for the availability of phosphate in waters. Condensed phosphates are phosphorus compounds that are within a structure or solids made up of salts or metals. Organic phosphates are phosphates formed in biological processes, e.g. respiration and in cell membrane (Azam *et al.*, 2019).

Important sources of phosphorus in surface waters are via run-off from lands fertilized with orthophosphate, the breakdown of organic matter in waters, and the discharge of untreated wastewater (UNEP, 2016). The available orthophosphate in surface waters can be consumed by biota but also react with other elements in the water, forming solid structures, also referred to as minerals.

2.2. Phosphate Minerals

2.2.1. Mineral Formation

The formation of phosphate minerals, as well as other minerals, can take place in different structures and phases, forming homogeneous or heterogeneous minerals.

For the formation of a homogeneous mineral, nucleation must take place, which requires energy, and the nuclei must grow to macroscopic dimensions (Nriagu and Moore, 1984). When a solution is supersaturated it contains the energy needed to form a (critical) nuclei. Supersaturated solutions have the tendency to return to an equilibrium state with respect to the solution (Nriagu and Moore, 1984). This is done by reducing its energy state through e.g., precipitation of minerals (Nriagu and Moore, 1984).

A heterogeneous reaction takes place when a foreign particle functions as an effective nucleation site upon which the crystals of a mineral phase can develop (Nriagu and Moore, 1984). A mineral phase, different from that of the seed material, can grow if the seed's surface provides a good crystal lattice match upon which the mineral phase can grow. This growth process is called epitaxy (Nriagu and Moore, 1984).

A mineral is always in a specific saturation state with respect to the solution. The degree of saturation determines a mineral will precipitate, as shown in Figure 4. In an oversaturated state minerals tend to precipitate. In between over- and undersaturation lies the metastable zone. A metastable solution is supersaturated, however precipitation might not occur for over a long period (Stumm and Morgan, 1996). A critical supersaturation value, or energy barrier, needs to be reached or overcome before crystallization can take place.

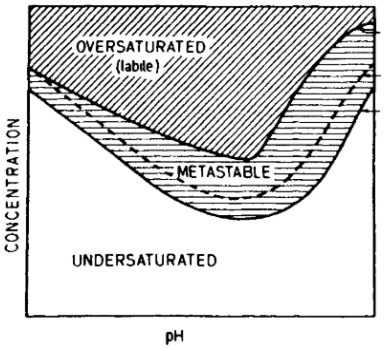

Figure 4 Solubility and saturation. A schematic solubility diagram showing concentration ranges versus pH for supersaturated, metastable, saturated, and undersaturated solutions. From Stumm Morgan 1996.

Another factor that effect the precipitation reaction for minerals is the presence of other ions. Different cat- and anions, either interacting with the crystal lattice or not, have an effect on the precipitation reaction (Nriagu and Moore, 1984). According to (Nriagu and Moore, 1984) "crystallization process is still one of the least well understood phenomena in chemistry". (Song, Hahn and Hoffmann, 2002) state that it is unclear how factors like the pH value, the temperature, the ionic strength, and the concentration of calcium and phosphates affect precipitation of calcium phosphates. These factors are also important for phosphate recovery from wastewater as shown in the following section, which briefly highlights the different research performed in the field of phosphorus removal in wastewater treatment.

2.2.2. Phosphorus Phases in Wastewater Studies

Several studies reported on the removal of phosphorus from the aqueous solution into the solid phases for wastewater treatment. Different technologies were used achieving different removal efficiencies.

- Biologically-induced precipitation of calcium phosphates in partial nitritation-anammox granules was studied by (Johansson, Ruscalleda and Colprim, 2017). Calcium precipitates likely to be encountered in the granules were: hydroxyapatite (HAP) and the precursor phases to HAP. The precursors to HAP are brushite (DCPD), octacalcium phosphate (OCP), and amorphous calcium phosphate (ATPC/ATC). The collected granules showed a high phosphate content (16 wt%), with a Ca:P molar ratio close to that of HAP.
- In (Herrmann *et al.*, 2013) mineral based sorbent as phosphate filter was tested and applied in PHREEQC. The phases ATCP, DCPD, OCP, and amorphous silica were successfully used in the PHREEQC model, simulating the removal of PO_4.
- Short term batch tests of steel slag filter material for PO_4-P removal were transposed to long term continuous flow models in PHREEQC by (Claveau-Mallet, Courcelles and Comeau, 2014). The precipitation phases modeled were monetite (MON) and HAP as the basis of the conceptual model.
- (Gustafsson *et al.*, 2008) studied the phosphate removal capacity of multiple mineral-based sorbents, namely: Filtra P, Polonites, natural wollastonite, and furnace slag. The used filter materials could hold 1.9-19 gP/kg, reaching up to removal efficiencies of over 95% for Filtra

P and Polonites. Evidence suggested ATCP to be the mineral formed in the sorbents. Other mineral phases taken into consideration were HAP, OCP, DCP and DCPC.

- Polonite was also studied by (Renman and Renman, 2010) for PO_4 influent concentrations of 5 mgP/l, reaching removal efficiencies up to 90%. In order to reach this 1-2 kg of Polonite was needed to treat 1 m^3 of wastewater.

The conditions in which these minerals are encountered are generally between pH 7-11, however most studies are performed at pH 8 and at temperatures ranging from 20 and 25 °C. For each phase the acronym, name, and chemical formula are reported in Table 1.

Table 1, Overview of all phosphate minerals as identified in the previous mentioned studies. Obtained from: (Gustafsson *et al.*, 2008; Renman and Renman, 2010; Mañas *et al.*, 2012; Claveau-Mallet, Courcelles and Comeau, 2014; Johansson, Ruscalleda and Colprim, 2017)

Acronym	Mineral name	Chemical formula
ATCP	amorphous calcium phosphate	[Ca3(PO4)2:H2O]
OCP	octacalcium phosphate	[Ca8H2(PO4)6: 5H2O]
DCPD	brushite or dicalcium phosphate dihydrate	[CaHPO4:2H2O]
TCP	(beta) tricalcium phosphate	[Ca3(PO4)2]
HAP	hydroxyapatite	[Ca5(PO4)3(OH)]
MON/DCPA	monetite	[CaHPO4]
HDP	hydroxyl dicalcium phosphate	[Ca2HPO4:2H2O]
NEW /DMPT	newberyite	[MgHPO4:3H2O]
AP	apatite	[(Ca6Na0.13Mg0.03)(PO4)6]
ClAP	chloroapatite	[Ca5(PO4)3Cl]
	calcium sulphide phosphate	[Ca10(PO4)3S]
MAP	struvite	[MgNH4PO4:6H2O]

Under acidic conditions (pH <5.5) sorption of P can take place on surfaces with a positive charge, such as aluminum (Al^{3+}) and iron (Fe^{3+}), forming amorphous Al- and Fe-phosphates (Siegrist, 2016). These phosphates can gradually change into crystalline structures forming $AlPO_4$: 2H2O (variscite) and $FePO_4$: $2H_2O$ (strengite) (Siegrist, 2016). The binding of P with Fe^{3+} can occur via two pathways: either through enhanced sorption onto ferric hydroxide ($Fe(OH)_3$) mineral surface, or through precipitation of strengite (Parkhurst, Stollenwerk and Colman, 2003; Azam *et al.*, 2019). Under anaerobic conditions, such as mineral wools inundated in water, Fe^{3+} is reduced to Fe^{2+} thus unavailable for direct precipitation of Fe-P and strengite (Parkhurst, Stollenwerk and Colman, 2003). As drain water and biomass conditions do not reach below pH 5.5, Fe-P binding such as the compounds variscite and strengtite are not taken into further consideration (Siegrist, 2016).

The Ca-P minerals that are formed occur mainly during biological removal technologies. Another mineral phase which can generate a fully recyclable product is struvite. Struvite is formed under specific conditions and the presence of Mg^{2+}, NH_4^+ and PO_4^{3-} (Le Corre *et al.*, 2007; Azam *et al.*, 2019). K-Struvite (KMgPO4:6H2O) is the potassium variant of struvite and Na-Struvite (NaMgPO4:7H2O) (Huang *et al.*, 2015).

2.2.3. Chemistry of Phosphate Minerals

The chemical reaction pathways of phosphate containing minerals frequently used in geochemical modeling are as follow (Table 2):

Table 2, Reaction pathways of phosphate containing minerals.

Solid phase	Reaction pathway	Source
ATCP	$Ca_3\,(PO_4)_2 \leftrightarrow 3Ca^{2+} + 2PO_4^{3-}$	(from Smith 2003, see Gustafsson 2008)
DCPD	$CaHPO_4 \cdot 2H_2O \leftrightarrow Ca^{2+} + PO_4^{3-} + H^+ + 2H_2O$	minteq database (from Smith 2003, see Herrmannn 2013)
DCP	$CaHPO_4 \leftrightarrow Ca^{2+} + PO_4^{3-} + H^+$	(from Smith 2003, see Gustafsson 2008) Monetite
OCP:	$Ca_3H(PO_4)_3 \leftrightarrow 4Ca^{2+} + 3PO_4^{3-} + H^+$	(from Christoffersen 1990, see Gustafsson 2008)
TCP	$Ca_3(PO_4)_2 \leftrightarrow 3Ca^{2+} + 2PO_4^{3-}$	(from Christoffersen 1990, see Gustafsson 2008)
Struvite	$NH_4\,MgPO_4 \cdot 2H_2O \leftrightarrow Mg^{2+} + PO_4^{3-} + NH_4^+ + 6H_2O + H_2PO_4^-$	
K-Struvite	$KMgPO_4 \cdot 6H_2O \leftrightarrow Mg^{2+} + PO_4^{3-} + K^+ + 6H_2O$	
Na-Struvite	$NaMgPO_4 \cdot 7H_2O \leftrightarrow Mg^{2+} + PO_4^{3-} + Na^+ + 7H_2O$	
HAP	$Ca_5(PO_4)_3OH + 4H^+ \leftrightarrow 5Ca^{2+} + 3HPO_4^{2-} + H_2O$	Phreeqc.dat database

From these reaction pathways the amount of mol of Ca needed per mol of phosphorus (Ca:P molar ratio) of the elements can be determined: ATCP 1.5, DCPD 1.0, TCP 1.5, OCP 1.33 and HAP 1.67, respectively. The reaction equations can provide preliminary information on whether the proceeding of the reaction produces or consumes acids affecting the pH, and if alkalinity is produced or not. This is of importance as during the precipitation or dissolution of a mineral returning to its equilibrium state, a change in environment can occur, leading to a shift in equilibrium of a different mineral. However, for the reaction pathways shown in Table 2, only protons are consumed during precipitation of DCPD, DCP and OCP.

2.2.4. Thermodynamics of Phosphate Minerals

The thermodynamic properties are important in the analysis of the phase changes and crystallization properties of minerals. The Gibbs free energy (G) represents the energy difference needed for a chemical reaction to proceed; the driving force (Song, Hahn and Hoffmann, 2002; Magalhães, Marques and Correia, 2007). When ΔG is positive the solution is understaturated and the reactants will predominate the equilibrium mixture (Smith, 2004; Magalhães, Marques and Correia, 2007). When ΔG is negative the solution is supersaturated and crystallization can occur as the products of the reaction equation will predominate (Smith, 2004; Magalhães, Marques and Correia, 2007). The Gibbs energy change is defined as (Song, Hahn and Hoffmann, 2002):

$$\Delta G = -\frac{2.303RT}{n}SI \qquad (1)$$

where R is the ideal gas constant and T is the absolute temperature. SI, the degree of saturation, is determined by the ratio of the ion activity product (IAP) of the dissolved mineral constituent and the solubility product (Ksp) of the mineral.

The formulas used to calculate the SI of each mineral (y):

$$SI = \log \frac{IAP_y}{K_{sp_y}} \quad (2)$$

SI is greater than zero (SI>0) when the IAP is greater than the K_{sp},. At SI>0 the system is in supersaturation with respect to the mineral, causing nucleation of the mineral after which the system will return to equilibrium (SI=0). The system is undersaturated with respect to the mineral when the IAP is smaller than the K_{sp}, SI<0 (Rivadeneyra *et al.*, 2004; Azam *et al.*, 2019). Hence, when SI=0, ΔG=0, the solution is in equilibrium; when SI<0, ΔG>0 the solution is undersaturated; when SI>0, ΔG<0 the solution is supersaturated (Song, Hahn and Hoffmann, 2002). The shift towards equilibrium of the reaction during precipitation follows Le Châtelier's Principle "*If an equilibrium is stressed, then the reaction shifts to reduce the stress*" changing the tendency to precipitate by the same and/or other phases (Smith, 2004).

An energy barrier referred to as 'critical Gibbs energy' needs to be overcome in order for nucleation and crystallization to start (Magalhães, Marques and Correia, 2007). The degree of saturation influences the driving force; when supersaturation increases, the driving force needed to meet the critical Gibbs energy needed for nucleation decreases, and the nucleation rate (at constant temperature) increases.

The enthalpy change (ΔH°) of a chemical reaction (at standard conditions of 25 °C and 1 atm pressure) can be used to define the temperature dependence of the log K (the solubility product) (Forrest, 2004). The enthalpy of reaction is used in the Van 't Hoff equation to determine the temperature dependence of the equilibrium constant (Parkhurst and Appelo, 1999). The thermodynamic solubility product of the precipitate phase (logK or logK_{sp}) and the enthalpy change (ΔH°) are shown in the Table 3:

Table 3, The thermodynamic solubility product (log_k) and the enthanlpy change (ΔH) of the precipitate phases.

Acronym	Log_k	ΔH (kcal)	Source
ATCP	-28.25	-87	(from Smith 2003, see Gustafsson 2008)
DCPD	-18.995	25	(from Smith 2003, see Herman 2013)
DCP	-19.28	31	(from Smith 2003, see Gustafsson 2008)
OCP	-47.95	-105	(from Christoffersen 1990, see Gustafsson 2008)
TCP	-25.5	-94	(from Christoffersen 1990, see Gustafsson 2008)
HAP	-3.421	-36.16	From phreeqc.dat database
Struvite	-13.46	23.62	
K-Struvite	-11.5	14.53	
Na-Struvite	-11.6	96.28	

For an endothermic reaction (ΔH>0) the solubility product increases with increasing temperature, leading to more dissolution at higher temperatures (Smith, 2004). For exothermic, ΔH<0, the solubility product decreases with increasing temperature leading to less dissolutions, thus higher SI.

2.3.Chemical Phosphorus Removal

There are different ways to remove phosphorus chemically. These processes generally involve salts of metals, such as calcium (Ca). The different mechanisms are adsorption, crystallization, and mineral precipitation. The stoichiometric reaction pathways can be used to quantify the removal. The hydro-geochemical model PHREEQC incorporates the stoichiometric reactions with the thermodynamic properties of minerals and solutions, allowing the modeling of chemical reactions of the water-gas-rock interaction in aqueous solutions, as will be explained in Section 2.3.3.

2.3.1. Mechanism

The mechanisms involved in the removal of phosphorus from aqueous solutions are adsorption, crystallization, and mineral precipitation:

- Adsorption is the attachment of charged molecules onto a surface. There are different types of forces involved which can even lead to chemical bonds between the adsorbate and absorbent (Hamdi and Srasra, 2012)(Stumm and Morgan, 1996).
- Crystallization: the formation of solid crystals from a solution, melt or the gas phase directly (Beckmann, 2013).
- Mineral precipitation: P ions reacting with cations in the environment (Azam *et al.*, 2019). It is the formation of mineral from a solution induced by a chemical or physical change, usually as a crystalline or amorphous solid.

2.3.2. Mechanism effecting factors

As previously mentioned, thermodynamics properties play a role in the formation of P minerals. However, this can be influenced by other factors such as the kinetics of mineral formation, the presence of certain ions, and the formation of precursors (Azam *et al.*, 2019).

Kinetics play a role in the formation of minerals in aqueous solutions. Even though a mineral is thermodynamically stable, it is more likely for the most soluble mineral to crystallize first (Johansson, Ruscalleda and Colprim, 2017). For example, HAP and TCP are both thermodynamically stable, but have an extremely slow kinetics formation (Celen *et al.*, 2007). Therefore they are less likely to form, compared to a mineral with faster kinetic formation. Fast reactions occur within minutes, slow phosphate mineral formations occur during a period of hours up to days (Szabó *et al.*, 2008).

Additionally, some studies report that the rate of formation of HAP and OCP are noticeably reduced by the presence of the magnesium ion; it retards the nucleation and subsequent growth by effectively blocking the mineral growth location on the surface (Nriagu and Moore, 1984; Celen *et al.*, 2007). Furthermore, OCP is formed by the hydrolysis of DCPD, both being a precursor to HAP formation. Magnesium ions do not have a noticeable effect on the rate of DCPD crystallization (Celen *et al.*, 2007).

According to several studies, one phase may act as a precursor for the final crystallized phase of HAP (Mañas *et al.*, 2012). Precursors identified are OCP, DCPD, ACTP at neutral to alkaline solutions. However, when a solution is highly supersaturated no precursor is needed for a phase to occur (Mañas *et al.*, 2012).

2.3.3. PHREEQC

PHREEQC is a hydro-geochemical modeling program which allows the modeling of chemical reactions of the water-gas-rock interaction in aqueous solutions. The species distribution is calculated from thermodynamic data sets. PHREEQC, like other frequently used models, such as MINTEQA2, WATEQ4F, EQ 3/6 etc., compute, based on the ion interaction theory, solving the non-linear set of equations resulting from equilibrium constants and mass balances in the system (Merkel and Planer-Friedrich, 2005).

The database of PHREEQC contains the definitions of chemical species, complexes, and mineral solubility's etc. Different databases exist which can be selected depending on the specific goal of the modeling. When a certain definition of, e.g. a mineral phase, is not present in a database the input file can be modified by adding the thermodynamic properties of the mineral (solubility constants and heat of reaction) (Appelo and Postma, 2006).

With the database completed PHREEQC can be used to calculate the saturation state of a solution, as well as force precipitation by setting the SI of a specific mineral phase to a value of 0 (Appelo and Postma, 2006). After running the program, the final predicted concentrations of each species can be used for calculating the potential removal of phosphorus per mineral, as well as all minerals together at different conditions (Forrest, 2004).

2.4.Biological Phosphorus Removal

2.4.1. Biological Phosphorus Content

Phosphorus is a vital cell element and plays a role in the structural and regulatory functions of microbial cells (Kulakovskaya, 2014). Ordinary heterotrophic bacteria which consume BOD can produce biomass with a P content of 0.015 gram per gram of volatile suspended solids (VSS) (Metcalf & Eddy Inc., 2003). VSS being a measure for concentration of microbial biomass. Specific technologies have been developed based on phosphorus accumulation by sludge bacteria during wastewater treatment (Kulakovskaya, 2014). For example, in enhanced biological phosphorus removal (EBPR) specific organisms can reach higher P content per gram VSS as they store ortho-phosphate in excess of their biological growth requirements (EPA, 2007). These microorganisms called phosphorus-accumulating organisms (PAO's), can achieve P content of 0.16 grams of P per gram of VSS (Falkentoft, 2000). However, this application needs specific changes in redox conditions (Falkentoft, 2000) which is not feasible for mineral wool usage.

2.4.2. Mechanisms of Bacterially Mediated Precipitation

Aside from consuming phosphorus for structural and regulatory functions, bacteria can also play a role in mineral precipitation (Dupraz *et al.*, 2009). This process is sometimes referred to as biochemical mineralization or biogenic precipitation (Smeck, 1985; Dupraz *et al.*, 2009; Arias, Cisternas and Rivas, 2017). There are three mechanisms involved in the precipitation of mineral through bacterial processes according to (Dupraz *et al.*, 2009):

- *Biologically-controlled mineralization*: the process of mineral precipitation as a result of specific cellular activity, which directs the nucleation, growth, morphology, and final location of a mineral. For example, the formation of internal or external skeletons, but also the formation of magnetite by magnetotactic bacteria (Arias, Cisternas and Rivas, 2017).
- *Biologically-induced mineralization*: the process of active mineral precipitation as a result of chemical modification of the environment through biological activity. An increase in pH can

induce oversaturated conditions leading to precipitation. Different biological activities of different bacteria lead to precipitation of biominerals from carbonates, oxides, sulfates, and phosphates (Sánchez-Román *et al.*, 2007; Benzerara *et al.*, 2011; Mañas *et al.*, 2012; Arias, Cisternas and Rivas, 2017).

- *Biologically-influenced mineralization*: the process of passive mineral precipitation as a result of the presence of organic matter, such as cell surfaces or extracellular polymeric substances (EPS) produced by microorganisms, which influence crystal morphology and composition. Biofilm and its EPS, can facilitate precipitation in different ways; i) trapping cations in negatively charged sites of the EPS or ii) trapping crystal seeds that act as nuclei for heterogeneous precipitation (Arias, Cisternas and Rivas, 2017). Among many examples, one example of biofilm related precipitation is the precipitation of calcium phosphate in microbial granules for wastewater treatment (Mañas *et al.*, 2012).

The factors that play a role in chemical phosphorus removal (Section 2.3.2) also play a role in bacterially mediated P removal. For example, during the biologically-induced precipitation of struvite the presence of calcium ions inhibit the precipitation of struvite (Sánchez-Román *et al.*, 2007). Ammonium, magnesium and carbonates influence Ca-P mineral formation and cause co-precipitation with other species (Mañas et al., 2012).

2.4.3. Biological Activity

The three identified mechanisms for bacterially mediated precipitation of minerals involve biological activity, either passively or actively. The biological activity referred to is a variety of different bioreactions by many different microorganisms. Anaerobic bioreactions convert organic pollutants into different substrates such as methane (CH_4), carbon dioxide (CO_2), ammonium (NH_3), hydrogen sulphide (H_2S) and water (H_2O) (van Lier, Mahmoud and Zeeman, 2008). In anaerobic ecosystems different microorganisms mediate different reactions and are subsequently grouped into four processes: (i) hydrolysis, (ii) acidogenesis/fermentation, (iii) acetogenesis (iv) methanogenesis, with specific bacterial groups belonging to each process. Some syntrophic reactions could induce a chemical change of the environment due to the conversion of hydrogen (H_2), protons (H^+) and HCO_3 in the biofilm (Cunha *et al.*, 2018).

The bioreactions relevant for wastewater treatment with biofilm formation within mineral wool are:

1. Hydrolysis: the breaking down of complex polymers such as proteins, carbohydrates or lipids into smaller molecules. The products formed are amino acids, sugars, fatty acids, or alcohols (Siegrist, 2016). An example reaction is the hydrolysis of lipids forming glycerol and long chain volatile fatty acids (LCFAs), and protons (Siegrist, 2016):

$$Lipids + 3H_2O \rightarrow Glycerol + LCFAs + 3H^+ \quad (3)$$

   Hydrolysis is the first and rate limiting step of biological COD removal (van Lier, Mahmoud and Zeeman, 2008).

2. Acidogenesis: the conversion of the hydrolysis products into volatile fatty acids (VFA's)(e.g., acetate, ethanol and ammonia), carbonic acid through fermentation or anaerobic oxidation (van Lier, Mahmoud and Zeeman, 2008), an example:

$$Sucrose + 9H_2O \rightarrow 4SCFAs + 4HCO_3^- + 8H^+ + 8H_2 \quad (4)$$

This process is in conjugation with the reductive de-ammonification of other amino acids consuming the produced H_2. Both reactions release NH_3 which acts as a H^+ acceptor. Therefore there is no chance of pH drop as there is no net proton production.

3. Acetogenesis: short chain fatty acids (SCFA) are further converted into acetate, hydrogen gas, and bicarbonate:

$$SCFA + H_2O \rightarrow Acetate + HCO_3^- + H_2 + H^+ \quad (5)$$

4. Methanogenesis: the conversion of the degraded organic matter to CH_4, either through acetotrophic or hydrogenotrophic methanogens (van Lier, Mahmoud and Zeeman, 2008):

$$Acetate + H_2O \rightarrow CH_4 + HCO_3^- \quad (6)$$

$$CO_2 + 4H_2 \rightarrow CH_4 + 2\,H_2O \quad (7)$$

5. Denitrification: under anoxic conditions methanol oxidation with nitrate (NO_3^-) and nitrite (NO_2^-) and occur in the following reaction (van Lier, Mahmoud and Zeeman, 2008):

$$Methanol + 6NO_3^- \rightarrow 3N_2 + 4HCO_3^- + 8\,H_2O \quad (8)$$

$$Methanol + 2NO_2^- \rightarrow N_2 + CO_3^{2-} + 2\,H_2O \quad (9)$$

At dissolved O_2 concentrations of 1 mg/l or lower (anoxic) denitrifying microorganisms use NO_3^- as an electron acceptor (van Lier, Mahmoud and Zeeman, 2008). During biological denitrification higher pH is induced (carbonate production), which contributes to the precipitation of calcium phosphates (Mañas *et al.*, 2012; Johansson, Ruscalleda and Colprim, 2017)

6. Nitrification: the oxidation of ammonia (NH_4) decreases pH as H^+ are released (Mañas *et al.*, 2012; Johansson, Ruscalleda and Colprim, 2017):

$$NH_4^+ + 1.5O_2 \rightarrow NO_2^- + 2\,H_2O + 2H^+ \quad (10)$$

In anaerobic systems reactions 1-4 take place synchronous. However, the development of balanced bacterial grouping is necessary to prevent damaging effects of environmental factors, like pH (van Lier, Mahmoud and Zeeman, 2008). The operating conditions of biological wastewater treatment are at pH of 6 - 8, for both nitrification, denitrification and COD conversion. The conversion rate of the bioreactions per gram of VSS, and the change in pH can, to a certain extent, be derived from one another by using the stoichiometric reactions equations.

3. Materials and Methods

In this section the measuring apparatus and data collection techniques are shown. Furthermore, the methods used to perform mineral wool analysis, batch- and flow-through experiments are presented. The methodology behind the performed geochemical modeling is also presented. The scripts written in PHREEQC can be found in Appendix I PHREEQC with detailed annotations.

3.1.Measuring Apparatus

3.1.1. pH

The pH was analyzed using a InoLabs IDS Multi meter 9420 and/or 3630 with an µm electrode (WTW, Germany). The multimeter and electrode were frequently calibrated by using technical buffer solutions for pH 4, 7 and 10.

3.1.2. EC

The electrical conductivity (EC) was measured using a InoLabs IDS Multi meter 9420 and/or 3630 with an electrical conductivity electrode (WTW, Germany). For calibration the Conductivity Standard 1413 µS/cm was used.

3.1.3. Temperature

The measurements were performed at room temperature which varied between 20 and 25°C. Temperature was measured by the pH and the EC electrode.

3.1.4. Titrino Titration

Titrations for alkalinity determination were performed with the Titrino 702. The results were frequently cross referenced with the Multi meter 9420 results. The Titrino 702 was also used for base, 0.1M sodium hydroxide (NaOH) and acid, 0.1M hydrochloric acid (HCl) dosing to adjust the pH of solutions, e.g. the vials of the batch experiments.

3.1.5. XRD

X-ray powder diffraction (XRD) data for mineral identification were collected with a scanning step of 0.040 ° 2θ and counting time of 2 seconds per step on a Bruker D8 Advance diffractometer θ -2θ scan 10° - 110° over a range of 10° - 110° θ -2θ. The XRD for phosphate minerals has been used repetitively (Power *et al.*, 2007; Sánchez-Román *et al.*, 2007; Renman and Renman, 2010; Mañas *et al.*, 2012; Gutierrez-Orrego, Garcia-Aristizabal and Gomez-Botero, 2017; Johansson, Ruscalleda and Colprim, 2017). Measurements were performed by the Department of Materials Science and Engineering of the Delft University of Technology.

3.1.6. XRF

X-ray fluorescence spectroscopy (XRF) analysis for chemical composition measurements were performed with a Panalytical Axios Max WD-XRF spectrometer and data evaluation was done with SuperQ5.0i/Omnian software, as done by (Gutierrez-Orrego, Garcia-Aristizabal and Gomez-Botero, 2017). Measurements were performed by the Department of Materials Science and Engineering of the Delft University of Technology.

3.1.7. ICPOES

Concentrations of Ca, P, NH_4, K, Na, Mg, S, Cl, Al and Fe, were analyzed using inductively coupled plasma optical emission spectrometry (ICPOES) as done by (Magalhães and Costa, 2018). After filtration at 0.45µm, samples were acidified to 2-3% HNO_3 concentration, before analyzed by the

ICPOES Spectro Arcos EOP. Measurements were performed by the Department of Materials Science and Engineering of the Delft University of Technology.

3.1.8. PO_4-P Test kit

Some measurements of ortho-phosphate were determined spectrophotometrically (HACH-LangeDR 3900) using the standard Test Kits of Dr. Lange Type LCK350 (Hach Lange Dusseldorf, Germany.) When needed, dilutions were made.

3.2.Data Collection Techniques

3.2.1. Sample Extraction

All aqueous samples extracted were filtered with a 0.45µm filter prior to further ICPOES and Dr. Hach test kits analysis to remove particulate material (Magalhães and Costa, 2018). Thus excluding crystals and the precipitate of the solution from the sample. By using mass balance calculations the removal of species was determined.

3.2.2. Alkalinity

Alkalinity determined according to Standard Methods (APHA *et al.*, 1998). In brief, the pH of a 100ml sample measured before reducing its pH to 4.3 with 0.1M HCl. The amount of miliequivalents (meq/l) of HCl needed to reach pH 4.3 used was multiplied by the molar mass of HCO_3^- (61,02 g/mol) or $CaCO_3$ (100,0872 g/mol) to obtain the alkalinity in mg/l of HCO_3^- or $CaCO_3$, respectively.

3.2.3. Digital Microscope

The Keyence VHX-5000 digital microscope with the VH-Z20W lens at magnification 20 - 200x was used for digital imaging of mineral wool fibers and crystal formation.

3.3.Mineral Wool Analysis

The chemical composition of the mineral wool was determined by the XRF and ICPOES providing insight on the available amount of Ca, Al and Fe, among others, to form P-precipitates, and subsequently the type of minerals that could form. Mineral wool powder was used for the XRF to determine the chemical compositions of the mineral wool in terms of percentage of total weight (Gutierrez-Orrego, Garcia-Aristizabal and Gomez-Botero, 2017). The analysis of the mineral precipitates present in the mineral wool was performed by analysis of a ground sample by the XDR. To determine the elemental composition of mineral wool, 60mg of mineral wool was dissolved in 20ml of 69% HNO_3 prior to sampling for ICPOES analysis.

3.4.Stock Solutions

3.4.1. Batch Solution

The batch experiments were performed with de-mineralized water to which potassium dihydrogen phosphate (KH_2PO_4) was added (Xu *et al.*, 2011). The concentrations used were 0, 10, 25 and 50mg PO_4-P/L. The pH was adjusted depending on the particular experiment by adding NaOH (0.1M) or HCl (0.1M).

3.4.2. Lotus Like Water

The physiochemical parameters of The Yamuna River used for the validation experiment and the flow-through experiment is shown in Table 5. As the samples are taken at different sites the physicochemical parameters have a big range. The results of chemical compositions measurements

on the total COD, NH_3, NO_3, PO_4, pH and temperature performed along the Barapullah Drain are shown in Table 4.

Table 4 Indian Drain Water. The Indian Drain Water physiochemical parameters according to [a](CPCB, 2006) and of the Barapullah Drain Water (n=23) [b](Lotus HR, 2018). The measurements by (CPCB, 2006)were performed along the Yamuna River (n=24) to which the Barapullah is a tributary.

Indian Drain Water	Average	Min	Max
pH [a]		7,4	8,46
pH (LOTUS-HR) [b]	7,24	6,88	7,93
Alkalinity ($mgCaCO_3/L$) [a]		204,7	397,7
Electrical Conductivity (µS/cm) [a]		980	2000
Temperature (°C) [b]	24,8	11,3	34,9
Total COD (mg/L) [b]	569,88	114,30	1312,50
Ammonia (mg/L) [b]	29,08	4,00	67,50
Nitrate-N (mg/L) [b]	0,18	0,00	4,20
Phosphate (mg/L) [b]	30,51	1,07	111,73

Table 5 Indian Drain Water Yamuna River, Component Analysis showing the highest measured concentrations [a](CPCB, 2006) [b](Lotus HR, 2018). Lower range can be found in Appendix B. Samples are taken from different sample sites, at different times during the time period April 2014 through February 2015, by different de (n=24). The measurements by (CPCB, 2006) were performed along the Yamuna River to which the Barapullah is a tributary.

	P[b]	NH4[b]	K[a]	Na[a]	Mg[a]	SO4[a]	Cl[a]	Ca[a]
mg/l	30	29	48	406	77	217	1424	291
mmol/l	0.97	1,62	1,2	17.71	3.,18	2.26	40.29	7.28

The highest pollution values are chosen in order to make sure reaction process will take place. The P content of the Yamuna river was far below the measured P content in the Barapullah Drain, therefore the P content was set higher for experiment and modeling. Indian Drain water composition was then mimicked in the lab to be used for the flow-through experiments. Different salts were added to de-mineralized water, mimicking the component analysis of Indian Drain water and to be referred to as Lotus Like Water. The amount of salts added to achieve the composition of Indian Drain water (Table 5):

Table 6 Lotus Like Water: salts added to demineralized water to mimic Indian Drain Water.

	Cl2Mg. 6H20	CaCl2.2H20	NH4Cl	KH2PO4	MgSO4. 7H20	NaCl
g/l	0.2	1.1	0.08	0.14	0.54	1.1
mmol/l	0.98	7.48	1.50	1.03	2.19	18.82

3.4.3. PHREEQC Input Solutions

The composition of Indian Drain Water (pH 7.2 and temperature 23 °C) was previously presented in Table 5 and Table 4. When necessary a Cl concentration of 1000mg/l was used instead if 1424mg/l in order to maintain electrical balance and the percent error close to zero.

Black Water (pH 8.8 and temperature 23 °C) was chosen to be compared to the Indian Drain water due to the resemblance in the composition. Indian Drain water mainly consists of untreated, raw effluent and is discharged directly into the drain from which it gets its name 'open sewage canal'. Black water is the effluent as it comes directly from the flushing of a toilet (non vacuum). Literature values of Black water (Table 7) were used for comparison with Indian Drain water.

Table 7, Black Water Component Analysis (De Graaff, 2010)

	P	NH4	K	Na	Mg	SO4	Cl	Ca	NO3	Alk (HCO_3^-)
mg/l	25	286	116	221	24	31.6	246	54.6	11.4	1525
mmol/l	0.81	15.89	2.97	9.64	0.99	0.33	6.96	1.37	0.18	

Both compositions were analyzed on temperature, pH and more, and compared with use of PHREEQC. The script can be found in Appendix I. III. Indian Drain Water. and I. IV. Black Water Analysis.

3.5.Batch Experiment

To test the effect of the presence of phosphorus a similar batch experiment was set up. A matrix of different phosphorus concentrations and pH was tested. The measurements were performed in duplicates and took three (o) or four weeks (x). The pH range 4.5 - 9.0, covered all possible precipitate formations. Phosphate concentrations between 0 and 50 mg P/L are representative of concentrations in real wastewater (Claveau-Mallet, Courcelles and Comeau, 2014) and Barapullah Drain water (Lotus HR, 2018). The 'pH - P matrix' was built accordingly (Table 8):

Table 8, The matrix of phosphorus and pH conditions. 'x' is 4 weeks mineral wool rectangles, '+' is four weeks of powered mineral wool and 'o' is three weeks of mineral wool rectangles.

	pH	P0: 0 mgP/l	P10: 12.6 mgP/l	P25: 25.7 mgP/l	P50: 51.5 mgP/l
Low pH	**4.5**	x		x	x
Mid pH	**7.1**	x		x	x
High pH	**8.7**	x	o	x +	x

To determine the dissolution of mineral wool under different pH conditions, 200ml vials were filled with 180ml of de-mineralized water and a 1.09 (±0.05) gram rectangular cube of mineral wool. When needed, pH was adjusted by adding NaOH (0.1M) or HCl (0.1M) depending on the experiment. The vials were vividly shaken 5 times a week to mix the samples. The duration of the experiment was 36 days.

Control samples were used to determine the effect of volume reduction on dissolution (at high pH - P10). In addition, a comparison between blank samples and samples inundated with mineral wool was made (at high pH - P10). Furthermore, the effect of rectangular cubes compared to powdered mineral wool in a sample was measured (at high pH - P25).

At the end of the experiments, the samples for ICPOES were taken and alkalinity was determined. The retrieved data was then implemented in the geochemical model PHREEQC. The script used in PHREEQC can be found in Appendix I. II. Dissolution in pH - P matrix.

3.6. Geochemical Study- PHREEQC

PHREEQC with Notepad++ as interface was used. The database phreeqc.dat was complemented with additional phases.

Exclusion of certain minerals as encountered in literature was needed for the processes as envisioned in the Barapullah Drain and for Black water. This was decided upon slow kinetics, co-precipitation, presence of magnesium or for having a precursor (see Section 2.3.2). Of the frequently modeled minerals, the mineral phases OCP and TCP were not taken into account, and neither were K-Struvite and Na-Struvite due to low formation rates. Due to the fact that aluminum and iron reactions with phosphorus occur at low pH, their mineral phases were not considered as P removing minerals in the model.

3.6.1. Model for P Removal

The concentrations of ions as measured by the ICPOES, the alkalinity, temperature and pH were used as inputs into the model. The chemical composition of Indian Drain Water and Black Water was used to make theoretical computations. The model was modified to:

- Model the degree of sensitivity of the solutions to changing temperatures (5-35 °C) and pH (4.5-11).
- Evaluate the degree of saturation of the P containing minerals after forcing precipitation (SI=0) to changing temperature and pH conditions.
- Determine the %P-removal, under the effect of changing temperature and pH conditions, by forcing precipitation (SI=0) of each P containing mineral separately, as well as together.
- Evaluate the effect of pH fixation compared to non-fixed pH conditions on the %P-removal.
- Create graphical outputs of the computations completed.

PHREEQC Keywords used were SOLUTION, EQUILIBRIUM_PHASES, REACTION_TEMPERATURE, REACTION. An annotated script is available in Appendix I. PHREEQC.

The %P removal was calculated by:

$$\frac{Initial\ P - Final\ P}{Inital\ P} \times 100 \qquad (11)$$

3.6.2. Validation Geochemical Model

In order to validate modeled results obtained from PHREEQC, a laboratory experiment was performed and compared with the model. This was done to understand precipitation of P over time and compare the theoretical P and Ca percentage removal of the model with that of the performed experiment, without the presence of mineral wool. Flasks were filled with 500ml of Lotus Like Water and kept at room temperature. Samples were taken for ICPOES analysis and alkalinity duringr an 8 day period (t0, t1, t2, t3 and t8). The pH and temperature was monitored as it was needed in the model to determine precipitation for each time step separately (Forrest, 2004).

3.7. Flow-through Experiments

In order to determine the influence of mineral wool on the P removal, two experiments were performed with use of a flow-through system (the basin in Figure 5). The first experiment covered a short time span (150 minutes), the second experiment was of longer duration (2.9 days). The pH, EC and temperature were monitored closely and used as a first indication for precipitation reactions occurring.

3.7.1. Experiment I

Two control experiments were performed: the first using a dye to assure homogeneous flow through the basin, the second to determine the breakthrough curve of the mineral wool filled basin using NaCl. Visual notations of the process of diffusion and advection of the dye were made. The EC was measured to determine the control breakthrough curve of the mineral wool filled basin. This breakthrough curve was then used as comparative measure for the breakthrough curve of Lotus Like water.

Lotus Like water was used as influent to the mineral wool basin as shown in Figure 5. At different time intervals samples of the effluent were taken for chemical analysis (e.g. Ca and P). The barrel of Lotus Like water was mixed manually and through internal re-circulation to establish homogeneous composition of the influent.

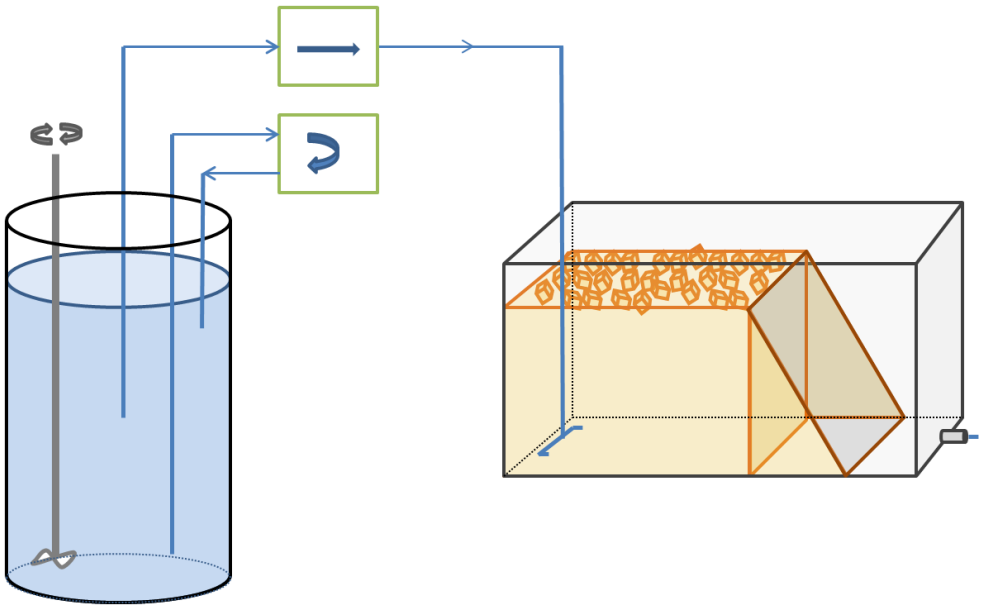

Figure 5, Set up of Experiments I performed with Lotus Like water: a barrel containing 60L of Lotus Like water, flow speed of 219ml/s, internal pump for homogeneity, 8.9L basin with small mineral wool cubes (±1.5x1.5x1.5cm), double inlet into the basin, a single outlet from an overflow fed (at 60°) discharge collection point, and a duration of 150 minutes.

3.7.2. Experiment II

Subsequently, a second experiment (Experiment II) was performed: the last 4.3 L of effluent of Experiment I was collected in a vessel, and used as influent (Figure 6). The setup was changed to a re-circulating system. This experiment was performed for 69 hours (2.9 days). Samples of the vessel were taken for chemical analysis, pH, temperature and EC were measured daily.

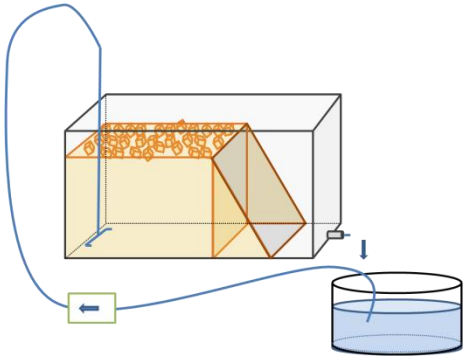

Figure 6, Set up of Experiment II performed with 4.3 L of effluent from Experiment I collected in the vessel, re-circulating in the system during 2.9 days. Flow speed of 219ml/s.

4. Results and Discussion

In this chapter the results of the mineral wool composition, dissolution experiments, flow-through experiments and the geochemical modeling are presented and discussed.

4.1.Mineral Wool Composition

4.1.1. Microscopic Imaging of Mineral Wool

Microscopic imaging of the mineral wool shows a crossed fibrous network of elongated and cylindrical manufactured mineral aggregates (Figure 7). In between the fibers are heterogeneously spread small spherical balls (Figure 8).

Figure 7, Dry mineral wool, fibrous network

Figure 8, Dry mineral wool with spherical balls highlighted by blue circles

According to (Wanko *et al.*, 2016), the balls present are formed when fiber formation is not fully achieved during the manufacturing process.

4.1.2. Minerals Found via XRD

Results from the XRD shows that the mineral wool samples are amorphous, however some crystalline iron might be present. The only element identified was iron. Making it probable that the small balls contain iron. Full analysis of the mineral wool composition by XRD can be found in Appendix D. Raw Data XRD.

4.1.3. Chemical Composition

The weight percentage distribution of the chemical composition of mineral wool determined by the XRF is given in pie chart (Figure 9). Mineral wool mainly consists of silicon (34%), calcium (33%), aluminum (14%), magnesium (9%) and iron (8%).

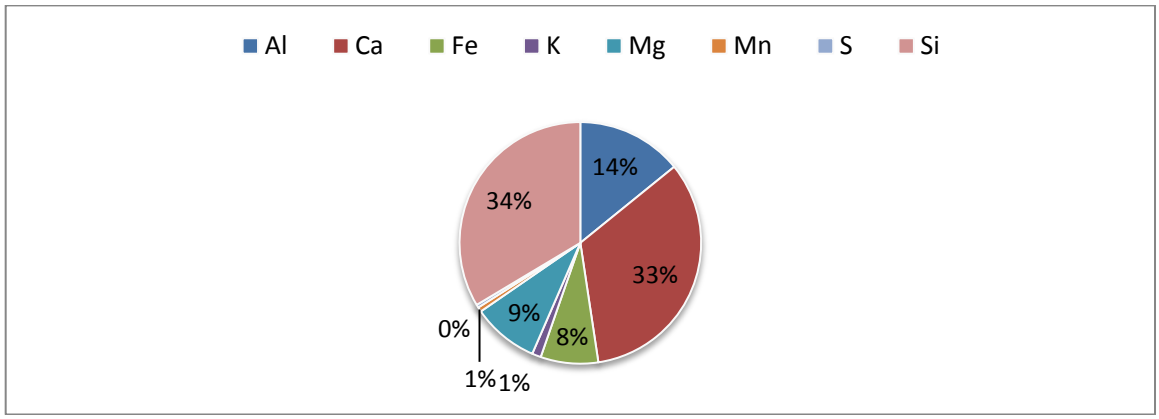

Figure 9, Mineral wool chemical composition wt% as measured by the XRF. The trace elements measured are shown in the full analysis in Appendix C. Raw Data XRF. Al: aluminium, Ca: calcium, Fe :iron, K: potassium, Mn: manganese, S: sulfur, Si: silicon.

As sodium (Na) is not detected by the XRF and silicon (Si) is not detected by ICPOES analysis, both data collection techniques were compared. Table 9 shows that the elements detected in both methods are of similar mass.

Table 9, Chemical Composition of Mineral Wool by XRF and ICPOES analysis in mg/g mineral wool. Only the major elements are shown. The trace elements present in very small concentrations are shown the full analysis in Appendix C. Raw Data XRF.

mg/gram	Al	Ca	Fe	K	Mg	Mn	Na	S	Si
XRF	79.29	187.35	43.18	6.70	49.76	3.48	0.00	2.23	188.02
ICPOES	95.66	175.43	33.97	6.33	56.37	2.83	15.24	4.03	-

In general, all the elements are of the same order of magnitude between both measuring methods. The mineral wool is not homogeneous in fibers distribution; some fibers are more white in color than the usual yellow, some fibers have small balls surrounding the fibers. This could be a reason for the slight deviation between method results.

Comparing the results with mineral wool studies in literature, the chemical composition as determined by XRF is very similar to the 'traditional rock wool 2' as defined by the research of (Campopiano *et al.*, 2014) (Table 10).

Table 10, Chemical composition (wt%) of mineral wool in this study compared to traditional mineral wool according to (Campopiano *et al.*, 2014)**.**

Mineral Wool	SiO_2	CaO	Al_2O_3	MgO	Fe_2O_3
This study	39	23	15	9	6
T. Rock wool 2	46	14	15	11	8.4

The differences in composition may be due to the variation of the geographic source of the basaltic material which is melted and spun forming mineral wool (Bunsell, 2009).

4.2.Mineral Wool Dissolution

To measure the potential of mineral wool in contributing ions for P precipitation, the dissolution of the mineral wool was measured under different circumstances, such as different pH conditions and different P concentrations.

4.2.1. Lab Experiment

4.2.1.1. Dissolution

With the batch test, the dissolution of the mineral wool was tested at different pH during a period of 36 days. As the pH was not kept constant through acid or base dosing, the pH of the solutions in the batch experiments changed over time (Table 11), reaching a steady pH of 7 for all tested pH conditions.

Table 11, The initial and final pH conditions during mineral wool dissolution experiment. Elemental analysis of the batch solutions after four weeks of exposure to mineral wool, tested at different pH conditions. One gram of mineral wool was added to 180ml vials. *Cl release from the measuring electrodes used. ** K release from the measuring electrode used, as well as from the mineral wool. nd, not detected. Si was not measured.

	pH		Concentration mg/l								
pH	Initial	Final	Al	Ca	Cl *	Fe	K**	Mg	Mn	Na	S
Low	4.7	7.0	nd	0.2	114.8	nd	68.0	0.6	nd	2.6	1.9
Mid	5.7	7.0	nd	0.18	104.3	nd	68.2	0.5	nd	2.5	2.0
High	7.7	7.1	nd	0.2	98.1	nd	66.6	0.5	nd	3.6	2.0

From the results in Table 11 it appears that the composition of the solution containing mineral wool barely changed. Traces of Ca and Mg were measured. Neither Fe, nor Al was detected, even though mineral wool is composed of both elements (8% and 14%, respectively). For K it is unclear what fraction of the measured concentration is due to dissociation from the mineral wool or due to the electrode. Similar amount of traces of K (~1.6 mg/l), Mg (~0.7 mg/l) and Ca (~2 mg/l) were measured at low pH conditions by (van Noordwijk, 1979). However, these results were obtained with different solution compositions (e.g. KCl, $CaCl_2$, $MgCl_2$), at a lower solution to mineral wool ratio, and with different sample extraction methods, possibly leading to higher dissolution concentrations.

The dissolution of 'T. Rock wool 2' (at pH 7.4 1mgCa/l, at pH 4.5 5 mgCa/l) (Campopiano *et al.*, 2014) shows a higher final Ca concentration than tabulated results (~0.2 mgCa/l). Other alkaline silicate materials tested showed even higher Ca release at pH 7.4 and pH 4.5 as can be shown in Graph 1 and Graph 2 (Campopiano *et al.*, 2014).

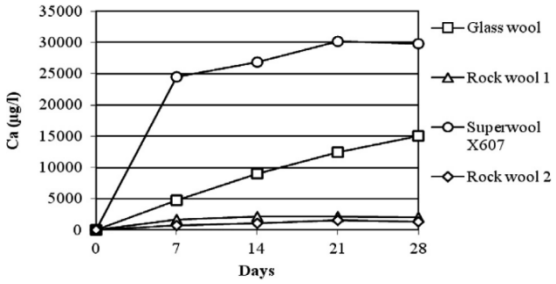

Graph 1, Dissolution of Ca at pH 7.4 From (Campopiano *et al.*, 2014)**. The chemical composition of the mineral wools can be found in Appendix H Composition Mineral Wools.**

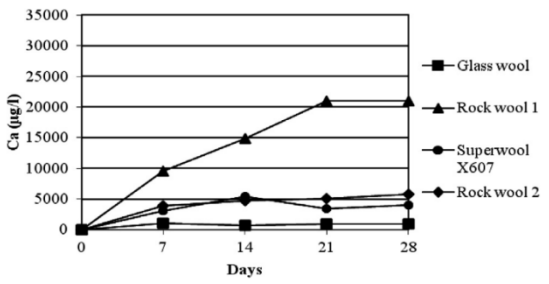

Graph 2, Dissolution of Ca at pH 4.5. From (Campopiano *et al.*, 2014)**. The chemical composition of the mineral wools can be found in Appendix H Composition Mineral Wools.**

These graphs indicate that the mineral wool tested show lower dissolution than T. Rock wool 2 to which it is similar in composition. Furthermore, the graphs also show that there are other mineral wools such as Superwool and Rock wool 1, that dissociate more Ca (up to 30mg/l) in similair pH conditions after four weeks.

The obtained results also show that the mineral wool appears to have a self-buffering capacity as the final pH of the samples converged to a pH of 7 independent of the initial pH condition. The buffering capacity indicates that there is an exchange of ions with H^+ and OH^-. In the case of a high initial pH the pH decreases. This trend is comparable to a water sample without mineral wool which is exposed to air (CO_2-buffer, carbonate equilibrium). Water exposed to CO_2 in the air is in

equilibrium at a pH of 5.8, but with the presence of $CaCO_3$ the pH increases to 7 (van Noordwijk, 1979), as also shown by the final pH reached in Table 11.

In the lower pH region the pH increases to 7. The exchange of H^+ for Ca^{2+}, among other cations, could be an explanation as suggested, but not confirmed, by (van Noordwijk, 1979).

Another, more plausible cause, could be the dissolution of free calcium oxide (CaO), releasing hydroxide(OH^-) :

$$CaO + H_2O -> Ca^{2+} + 2OH^- \quad (12)$$ (Park *et al.*, 2017)

A third cause could be the dissolution of calcium carbonate ($CaCO_3$) by water and CO_2, leading to an increase of pH as the release of bicarbonate (HCO_3^-) influences the carbonate equilibrium. The reaction equations of $CaCO_3$ and the carbonate equilibrium are as follow:

$$H_2O + CO_2 + CaCO_3 \leftrightarrow Ca^{2+} + HCO_3^- \quad (13)$$ (Stumm and Morgan, 1996)

$$H_2O + CO_2 <-> H_2CO_3 \leftrightarrow H^+ + HCO_3^- \leftrightarrow 2H^+ + CO_3^{2-} \quad (14)$$ (Stumm and Morgan, 1996)

The dissolution of $CaCO_3$ consumes CO_2(↓), and produces HCO_3^-(↑), causing a stress on the carbonate equilibrium and driving it to the left, producing more carbonic acid (H_2CO_3) and CO_2, consuming some H^+.

These suggestions will be considered in greater depth in Chapter 5, General Discussion and Recommendations.

Nevertheless, from these results, it is unclear if this self-buffering effect has an effect on the dissolution of mineral wool. Therefore further testing is performed while applying an acid/dose to overcome the self-buffering effect and measuring the dissolution.

4.2.1.2. pH and P matrix

Measurements following a 'pH - P matrix' were performed to test the effect of P in solution with mineral wool on dissolution and subsequent precipitation. For these measurements the pH was kept constant to overcome the self-buffering effect by two weekly acid dosing for low and mid pH, and base dosing for high pH, as shown in Table 12:

Table 12, pH conditions and average dosing in the 'pH and P matrix'. HCl 0.1M was added to low and mid pH, NaOH to the high pH. All samples were tested during four weeks, except P10, which was tested during three weeks. The pH is as follow: low is 4.7, mid pH is 7.1, high pH is 8.5. Phosphate concentrations: P0 is 0 mg/l , P10 is 10.4mg/l, P25 is 25.7 mg/l, P50 is 51.5 mg/l as the amount of phosphate in the solution mg/l as measured by the ICPOES. * P10 was only tested at high pH and during 3 weeks, not 4 weeks.

pH	Average pH	+/- pH	ml of HCl/NaOH dosing for each P concentration			
			P0	P10	P25	P50
Low	4.7	0.7	0.47		1.94	3.30
Mid	7.1	0.3	0.00		0.44	1.46
High	8.5	0.8	0.21	0.14	0.45	0.42

More acid was needed at lower pH-P50 (3.30 ml) than at mid pH-P50 (1.46 ml). This can be explained by the P-containing solution which is prepared with KH_2PO_4, behaving as a buffer at pH 6-8. To decrease the pH to 4.7, which is lower than the buffer range, the buffer capacity needs to be

overcome, thus a high amount of acid dosage is needed before little buffering capacity is left. With increasing P content, the dosing of both acid and base was higher. This is due to the molar strength of the KH_2PO_4 buffer; a diluted solution has a lower buffering capacity. Little dosing was needed to keep the pH around 7.1 and little deviation occurred: affirming the self-buffering capacity of the mineral wool.

The concentrations of the elements Al, Ca, Mg and Si in the solutions after inundation with mineral wool following the 'pH - P matrix' are shown in Table 13.

Table 13, Elemental analysis for Al, Mg, Ca and Si, of the batch solutions after four weeks of exposure to mineral wool, tested at within the 'pH - P matrix'. One gram of mineral wool was added to 180ml vials. The pH is as follow: low is 4.7, mid pH is 7.1, high pH is 8.5. Phosphate concentrations: P0 is 0 mg/l , P10 is 10.4 mg/l, P25 is 25.7 mg/l, P50 is 51.5 mg/l as the amount of phosphate in the solution mg/l as measured by the ICPOES. A full elemental analysis is shown in Appendix E Dissolution of mineral wool pH - P matrix. *P10 was only tested at high pH and during 3 weeks, not 4 weeks.

		Concentration mg/L						Concentration mg/L			
Compound	pH	P0	P10*	P25	P50		pH	P0	P10*	P25	P50
Aluminum	low	0.38		0.09	0.11	**Calcium**	low	3.06		3.02	3.49
	mid	0.04		0.01	0.01		mid	2.32		1.75	1.69
	high	0.63	1.65	0.35	0.35		high	3.18	3.64	1.82	1.69
Magnesium	low	1.00		0.94	1.12	**Silicon**	low	1.70		1.26	1.52
	mid	0.78		0.60	0.56		mid	1.13		0.64	0.61
	high	1.19	1.29	0.73	0.69		high	3.22		2.06	2.07

The results show very little dissolution of the mineral wool. In general, for the four elements, the highest dissolution takes place when mineral wool is exposed to P content of zero mg/l. At high pH conditions relatively more dissolution takes place, although concentrations are still low. The difference in dissolution between P25 and P50 is minimal. A reason for the lower dissolution at both high pH and P content could be explained by the higher ion strength of the solution the mineral wool is in which decreases the dissolution.

The results do show dissolution of silicon which was previously not measured (Table 11). Most likely this was due to the measurement setting of the ICPOES. The results presented here are in partial agreement with (Campopiano *et al.*, 2014). 'T. Rock wool 2' reached final Si concentrations of 10mg/l and 1 mg/l under pH conditions of at pH 4.5 and 7.5 respectively (Campopiano *et al.*, 2014). This research shows highest Si dissolution at 3.22mg/l at pH 7.1, being slightly higher than measured by (Campopiano *et al.*, 2014). Possibly the slight difference is due to the composition of the mineral wool or different extraction method of the samples.

The Ca concentrations increased to ~2-3mg Ca/l: values similar to those measured by (van Noordwijk, 1979) at low pH. Comparing the results without acid/base addition (Table 11) with the 'pH - P matrix' (Table 13), slightly higher Ca concentrations were measured. This is most likely due to the dosing of acid to overcome the self buffering effect.

4.2.1.3. The 'pH - P matrix ' per week

In order to determine if the P was removed from the aqueous phase into the solid phase by precipitation, the PO_4-P concentration was measured for all batches in the matrix during four weeks (Graph 3).

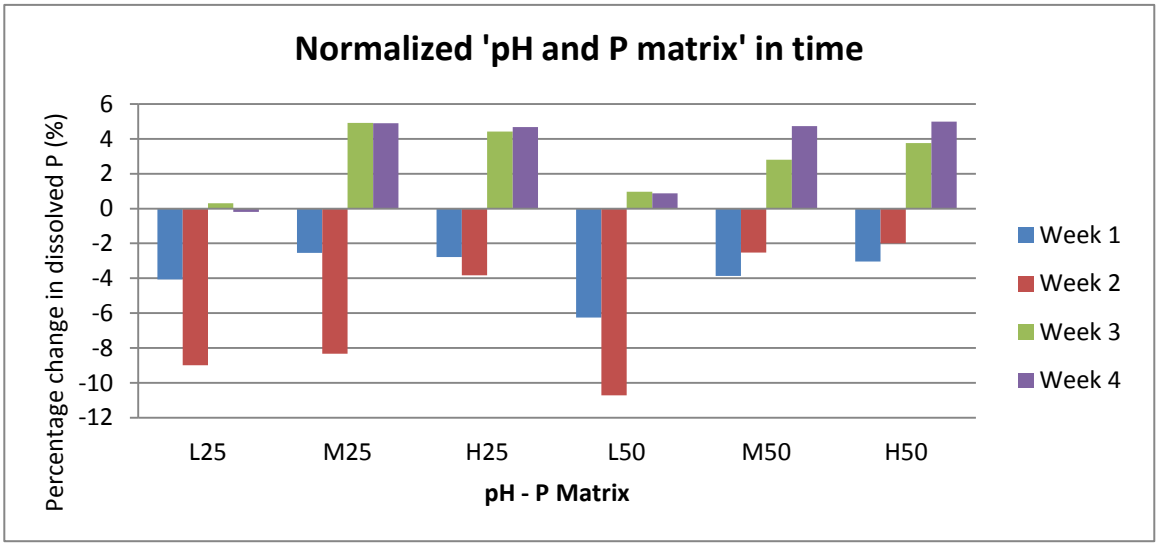

Graph 3, Normalized phosphate concentrations with respect to the stock solution, after 1, 2, 3 and 4 weeks. A decrease in %P concentration indicates a removal of P from the solution, thus suggesting precipitation of P-containing minerals due to interaction with the solute. The pH is as follow: L(low) is 4.7, M(mid) pH is 7.1, H (high) is 8.5. Stock phosphate concentrations: P25 is 25.7mg/l, P50 is 51.5mg/l as the amount of phosphate in the solution mg/l as measured by the ICPOES. The average of duplicate measurements are shown.

The results show an increase in % change in dissolved P in weeks three and four, suggesting an increase in P content compared to its stock solution. However, this is not possible considering the mass balance as no additional P was added during the experiment.

Evaluation of the P concentration over time was expected to show evidence of gradual decreasing P concentrations. However, the presented results did not show this. For all measurements the P content dropped consistently in the first two weeks. In order to find a cause for the decreased P measurements in the second week, the ICPOES results were compared with the Test kits results (Graph 4).

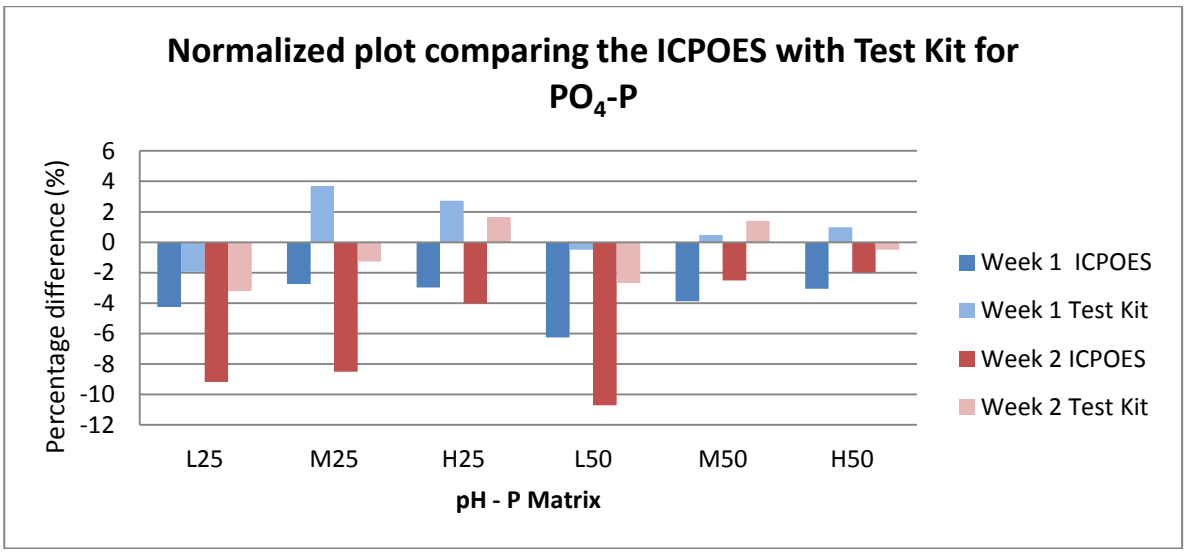

Graph 4, Normalized phosphate concentrations with respect to the stock solution, after 2 weeks, comparing the ICPOES results with the Dr. HACH Lange Test Kits. The pH is as follow: low is 4.7, mid pH is 7.1, high pH is 8.5. The pH is as follow: L(low) is 4.7, M(mid) pH is 7.1, H (high) is 8.5. Stock phosphate concentrations: P25 is 25.7 mg/l, P50 is 51.5 mg/l as the amount of phosphate in the solution mg/l as measured by the ICPOES. The average of duplicate measurements are shown.

The amount of P measured by the Test Kit were more or less the same as with the stock solution (<4% difference). The ICPOES result showed greater deviations in week one and two compared to the Test kit, especially for week 2. From these findings, it is clear that the P content in week one and two do not differentiate distinctively from each other, nor does the P content decrease significantly. Based on these differences it is clear that the P decrease in week two is due to the ICPOES measurements rather than P removal. Therefore, also considering the positive mass balance, the reliability of the ICPOES results in week three and four (Graph 3) are questioned as well.

4.2.1.4. Blank Compared to Mineral Wool Samples

In order to assure that any P reactions taking place were solely due to the presence of mineral wool and not due to the interaction with the vial, control samples were compared to mineral wool incubated samples (Graph 5).

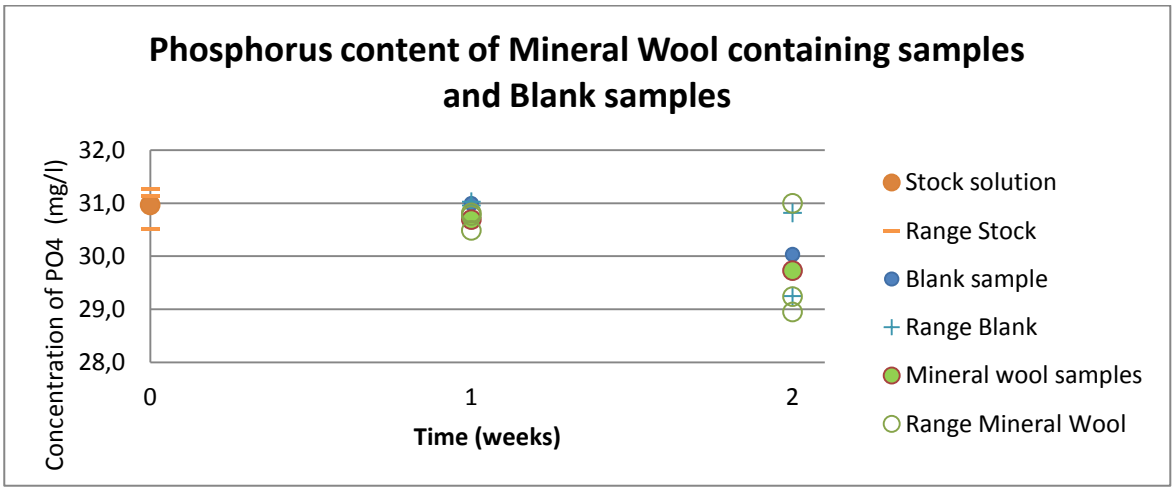

Graph 5, Phosphorus content of mineral wool containing samples and blank samples after two weeks. Week three was excluded due to PO_4 calibration settings of the ICPOES. Batches containing a stock solution of 10 mgPO_4-P/l, were kept at a pH of 8.5. The average values of duplicate measurements are show, as well as both measurements. The green measurement points resemble the batches containing mineral wool. The blue are batches containing solely the stock solution.

The results show that the PO_4-P concentration slightly decreased over time. The spread between the blank and mineral wool sample is relevant for comparison: the blank samples and the mineral wool samples do not significantly differ from each other. From these findings it is clear that the vial does not interact with P removal.

4.2.1.5. Volume Controlled Samples

To explore the effect of volume decrease due to sample extraction a comparison was made between volume controlled samples and samples reduced in volume (Table 14).

Table 14, Dissolution of selected mineral wool element in their P containing solution after three weeks, for samples with controlled and decreasing (variable) volume. Measurements performed at pH 8.5- P10, in duplicate.

mg/l	Al	Ca	Mg	PO4-P
Constant V	1.49	3.22	1.15	12.59
Variable V	1.65	3.64	1.30	12.64
% Difference	10.7	13.0	12.8	0.4

The dissolution concentrations measured for samples constant in volume (Constant V) showed lower concentrations compared with decreasing volume (Variable V) due to weekly extraction. As solution is extracted the concentration may increase as the mineral wool to solution ratio decreases. This is also shown by the difference in dosing needed for both samples: for Constant V a dosing of 0.19 ml of NaOH (0.1M) was applied, compared to 0.14 ml of NaOH (0.1M) for Variable V sample. From these findings it is clear that there is a slight deviation between constant and variable volume in dissociation of ions from the mineral wool to the solution. However, this effect shrinks to insignificance given minimal dissolution of mineral wool and precipitation of P.

4.2.1.6. Powdered Mineral Wool

To explore the effect of fiber size and surface area, on the dissolution a comparison was made between non powdered samples and powdered samples. In general, the average dissolution of the four minerals Al, Ca, Mg and Si was slightly higher for the powdered samples compared to the non powdered samples, in 'high pH - p50 matrix'. Only for the first week the dissolution of the powdered sample was higher (18%), in the subsequent weeks the difference between the samples decreased to 7.5% (See Appendix F for further details.) However, as mentioned before, dissolution rates are low thus the difference may be ignored.

4.2.2. Implemented in PHREEQC

Of the 'pH - P matrix' (Section 4.2.1.2) the concentrations of ions as measured by the ICPOES, the alkalinity, temperature and pH after four weeks were used as inputs into the PHREEQC. The Saturation Indices (SIs) for the different P containing minerals were calculated by PHREEQC to show the thermodynamic potential of the different pH-P solutions to the formation of different Ca-P minerals (Table 15):

Table 15, SIs for minerals all media tested at different pH and phosphate concentrations after 4 weeks. Results are from the geochemical computer program PHREEQC. The pH is as follow: low is 4.7, mid pH is 7.1, high pH is 8.5. Phosphate concentrations: P0 is 0 mg/l , P10 is 10.4 mg/l, P25 is 25.7 mg/l, P50 is 51.5 mg/l according the amount of phosphate in the solution mg/l as measured by the ICPOES. Samples without P (P0) are not shown as they have no tendency to saturation with P containing minerals. *10 mg/l P was only tested at high pH and during 3 weeks, not 4 weeks.

Saturation Index							
pH	**Low pH**		**Mid pH**		**High pH**		
Mineral	**P25**	**P50**	**P25**	**P50**	**P10***	**P25**	**P50**
DCPD	-3.3	-2.9	-1.4	-1.2	-1.1	-1.1	-1.1
ATCP	-11.7	-10.5	-3.1	-2.7	**1.1**	**1.1**	**0.4**
TCP	-14.4	-13.3	-5.9	-5.5	-1.7	-1.7	-2.4
HAP	-16.9	-15.1	-1.8	-1.2	**6.2**	**6.2**	**4.8**
OCP	-14.3	-12.7	-3.8	-3.2	**0.7**	**0.7**	-0.0

Only at high pH the thermodynamic tendency to precipitate is the highest for HAP, followed by ATCP and OCP. The latter shows a slight potential to saturation as the SI is between 0 and 1. The SIs at low and mid pH showed a systematic undersaturation of the minerals to the tested conditions. The previous findings showed no reduction of P. However, the SIs>1 do suggest that Ca-P has the tendency to precipitate.

The potential P removal forcing precipitation of HAP (SI 6.2, high pH-P25) is calculated by PHREEQC to be 0.62mg/l, equivalent to -2.4% when normalized. With Ca being the restricting element. The measured normalized P reduction (Graph 3, high pH-P25) after four weeks was +4%. These measurements do not align. Additionally, an explanation of the decrease of 0.62 mgP/l can lie within the measurement error of both ICPOES measurements as well as Dr. Hach test kits due to dilution for sampling. On the other hand, a reason why this difference is not measured previously (in Graph 3) could also be due to the critical Gibbs energy needed for crystallization not being overcome. Perhaps the obtained SI values >1 are not high enough to provide the critical Gibbs energy for the formation of HAP, ATCP or OCP. However, this is not likely as other studies do measure Ca-P precipitation at similar SIs (Mañas *et al.*, 2012; Johansson, Ruscalleda and Colprim, 2017).

Nevertheless, the modeling of final composition of the pH - P matrix solutions show that even though the Ca concentrations are very low (~2-3 mg/l, Table 13) removal of P is thermodynamically possible, as shown by the example of HAP high pH-P25. In regard to this latter, it is most likely that if the Ca concentrations would have been higher, the SI values would have been higher and a higher P removal percentages would have occurred.

4.3.Geochemical Model PHREEQC

A geochemical analysis was performed of the solutions of Indian Drain Water and Black Water, as defined in Sections 3.4.2 and 3.4.3, respectively. The saturation state of different mineral phases, under different circumstances, such as pH and temperature were tested. These effects are further studied in the next sections. First for Indian Drain Water, then for Black Water, after which they are compared.

4.3.1. Saturation State

Results on the Indian Drain Water showed supersaturation for all mineral phases except the struvite phases. The mineral phases ATCP, TCP, HAP and OCP showed greater thermodynamic tendency to

precipitation in Black Water compared to Indian Drain Water (Table 16). The only wastewater with a (slightly) positive SI for Struvite was Black water.

Table 16, Saturation Index values (SI) for minerals in Indian Drain Water and Black Water. Results are from the geochemical computer program PHREEQC. The temperature and pH for the Indian Drain Water: 24.8°C and 7.24 respectively. The temperature and pH of Black Water: 23.0°C and 8.8, respectively.

Mineral	DCP	DCPD	ATCP	TCP	HAP	OCP	Stuvite	K-Struvite	Na-Struvite
Indian Drain	0.66	0.37	3.5	0.74	9.69	4.53	-0.75	-2.85	-1.55
Black Water	-0.01	-0.3	3.73	0.97	10.82	4.08	0.96	-1.67	-1.02

4.3.2. Indian Drain Water Saturation State

The SIs without precipitation for a temperature range and pH range showed the sensitivity of the Indian Drain Water to these changing conditions. Graph 3 illustrates the SIs of the selected P containing minerals for a range in temperature relevant to that of Indian Drain Water (11-34 °C).

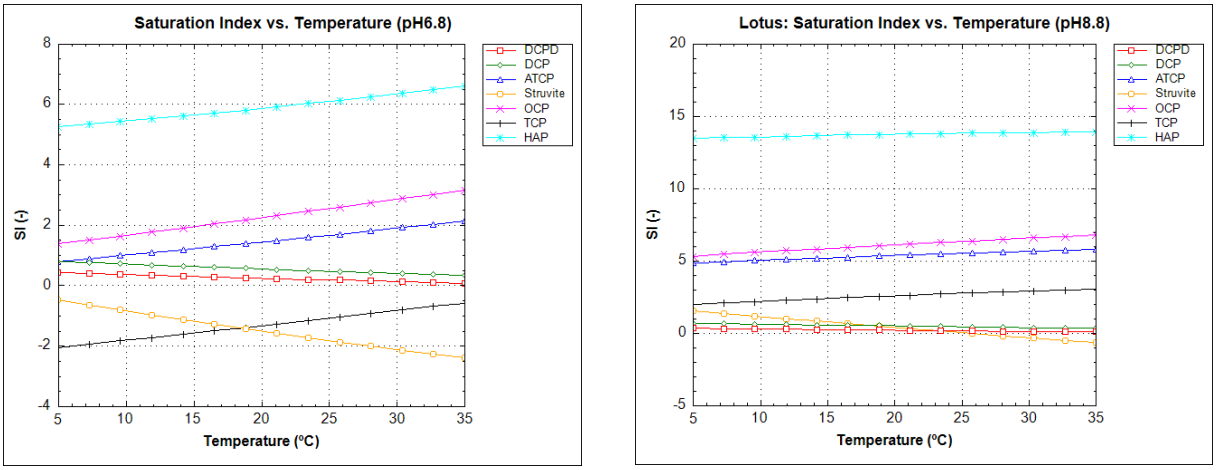

Graph 6, Saturation Index of minerals for temperature: A) Indian Drain Water at pH 6.8. B) Indian Drain water at pH 8.8.

When comparing Graph 6A with Graph 6B it is clear that at pH 6.8 (Graph A) the mineral phases are more sensitive to temperature than at pH 8.8 (Graph B). Accordingly, the three phases (Struvite, DCP and DCPD) with a thermodynamically negative enthalpy change ($\Delta H<0$) show a decrease in SI with increasing temperature, independent of the pH. For struvite the conditions in which $SI>0$ is reached, is at low temperatures 5-10°C and pH around 9-10.

Graph 7 illustrates the SIs of the selected P containing minerals as addressed in Section 2.3.2.

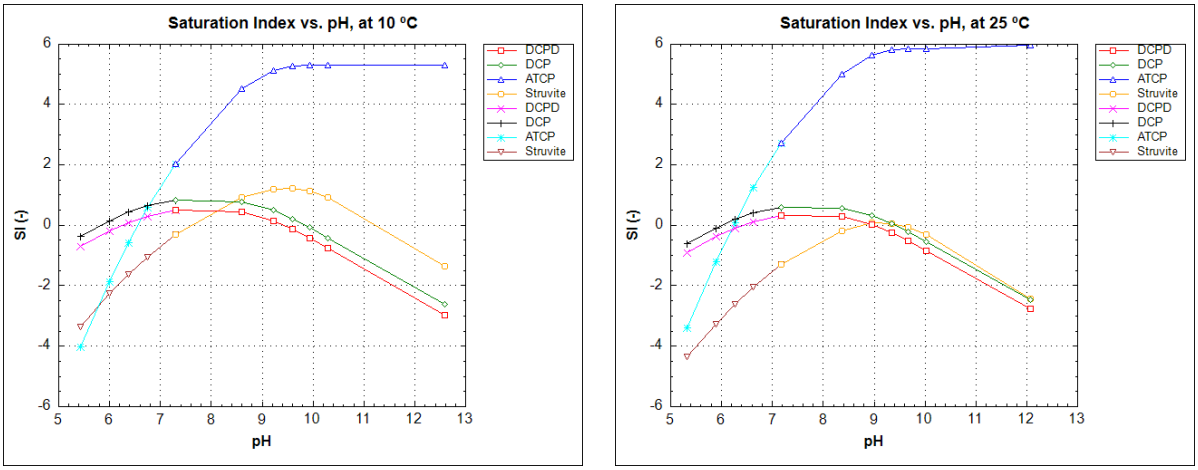

Graph 7, Saturation Index of minerals for pH: A) Indian Drain Water at 10 °C for only DCPD, DCP, ATCP and Struvite. B) Lotus like water at 25 °C for only DCPD, DCP, ATCP and Struvite. Different colors for the same minerals are used as base was added to increase pH to deviate from the initial condition, and acid was added to simulate pH decrease. The pH of the Barapullah Drain varies between 6.6 and 7.9 (Table 4).

When looking at the complete range of pH conditions tested in Graph 6A and B there is no linear relationship between pH and SI. For mineral phases with a positive enthalpy change (ΔH>0) an increase in temperature leads to a shift into a higher saturation state.

In general, in Graph 6 and 7 DCDP and DCP run almost parallel to each other. ATCP has the highest SI of the minerals modeled from pH 6 onwards. It has a higher SI at a higher temperature: the max SI is 4 at 10 °C (Graph 6A) and 8 at 25 °C (Graph 6B). At low temperatures the SI of struvite is larger than the SI at high temperature. Thermodynamically this means that ATCP has the highest tendency to precipitate as its SI>0, struvite could precipitate as well but at lower temperatures.

The development of the SI of ATCP with increasing pH conditions is in line with research of (Mañas *et al.*, 2012), stating that the SI of the mineral ACTP increases proportionally with pH in the solution.

4.3.3. Indian Drain Water Precipitation

The following simulations include the forced precipitation (SI=0) of the selected mineral phases all together. The effect of temperature and pH are illustrated. As the model only permits continuous modeling, the pH conditions have been fixed. Continuous modeling being an increase of temperature with 5 units every step, starting from the lowest temperature, instead of decreasing or increasing the temperature for each step separately, starting from the initial temperature conditions. The continuous modeling especially is of influence during the addition of base or acid, this is further explored in paragraph 4.3.3.4.

4.3.3.1. Precipitation: Temperature

At pH 6.8 and low temperature, DCP is thermodynamically the mineral phase most likely to precipitate (SI=0) (Graph 8A).

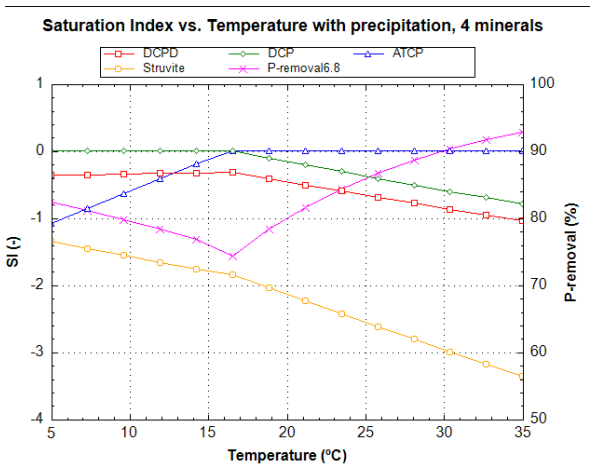

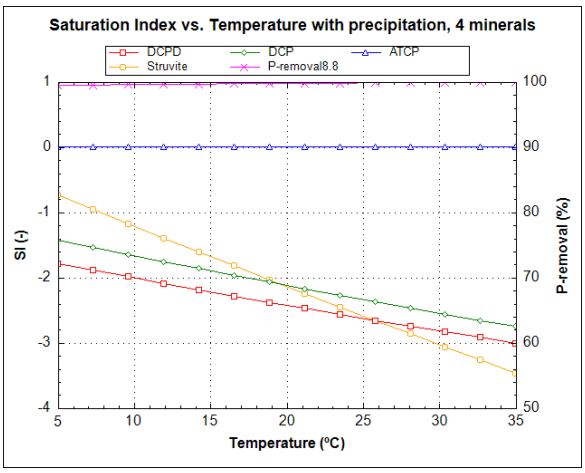

Graph 8, Simultaneous precipitation of phosphorus minerals DCPD, DCP, ATCP and Struvite for different temperatures A) Indian Drain Water at pH of 6.8 B) Indian Drain Water at pH of 8.8

At 10°C both ATCP and DCP precipitate. As temperature increases ATCP starts to precipitate (SI=0) and DCP becomes understaturated (SI>0). Struvite does not play a role as it is understaturated (SI<0) at all conditions. It is important to know which mineral precipitates as all minerals have different elemental ratio's which effect the %P removal given the specific composition of the solution. Graph 8A with Graph 8B shows that at pH 8.8 compared to pH 6.8, the P removal through precipitation is higher. The removal efficiencies at all temperatures are >99%. As precipitation of ATCP occurs, Ca is removed from the aqueous phases, resulting in a decrease in level of saturation of the other phases.

4.3.3.2. Precipitation: pH

The SIs of the mineral phases and the total %P removal are shown in Graph 9 for changing pH conditions. The total %P removal with the subsequent chemical dosing of HCl or NaOH are shown in Graph 10.

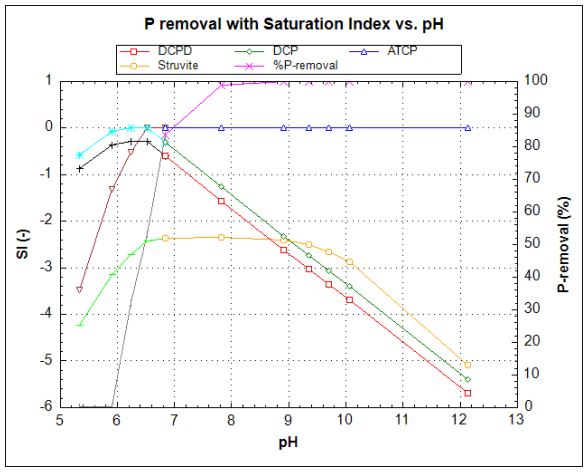

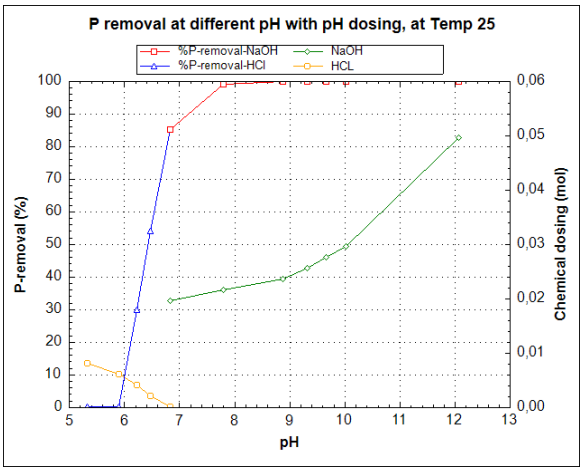

Graph 9, Simultaneous precipitation of phosphorus minerals DCPD, DCP, ATCP and Struvite at different pH values for 25 °C, Indian Drain water.

Graph 10, P removal by simultaneous precipitation at different pH values for 25°C, including the amount of NaOH and HCl added to fixate the pH, Indian Drain water.

Looking at P removal (grey and pink line) depicted in both graphs, the removal starts at pH 5.8, at 25 °C. ATCP (brown) and quickly rises in SI at higher pH conditions, becoming the dominant mineral phase and precipitating. Almost 100% P removal is achieved at pH 7.9 and higher. Graph 10

confirms that pH seriously influences Ca-P precipitation: an acid dosing of 0.05 mol/l, lowering the pH by 0.5 units, theoretically leads to a P percentage reduction from 85% to 10%, which is in line with PHREEQC modeling of Ca-P precipitation by (Mañas *et al.*, 2012).

4.3.3.3. Precipitation: Temperature and pH

The effect of pH on the removal efficiency is significant. As supported by Graph 11 and 12, P removal is sensitive to a change in the pH. This effect is greater at lower temperature than a high temperatures.

The %P removal greatly depends on the pH. At high pH great %P removals are achieved. At low pH of 6.8 (red line) the variation in removal is strongly affected by the temperature. While at high pH (8.8, yellow top line) temperature has less effect.

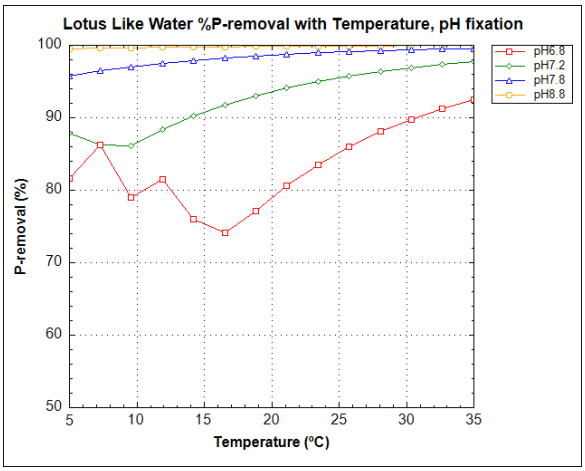

Graph 11, Graphical representation of the course of P removal (%) with increasing temperature for different pH conditions.

4.3.3.4. Role of pH Fixation

For the Graphs 7, 10, 11 and 12 the pH was fixated by a function in the model. The fixation of pH was used to construct graphs from which the potential P removal at a certain temperature and pH could be read off.

A non pH fixed equilibrium phase, driving the simulation of a continuous batch solution, leads to different P removal results compared to fixed pH equilibrium. This is clearly represented in Graph 12. The percentage P removal at fixed pH (red line) is higher than the percentage P removal for the non fixed pH system (blue) at all temperatures. This can lead to a %P removal up to 12%.

The pH of the non fixed pH curve (yellow), decreases at each increment in temperature, as precipitation occurs and the pH drops.

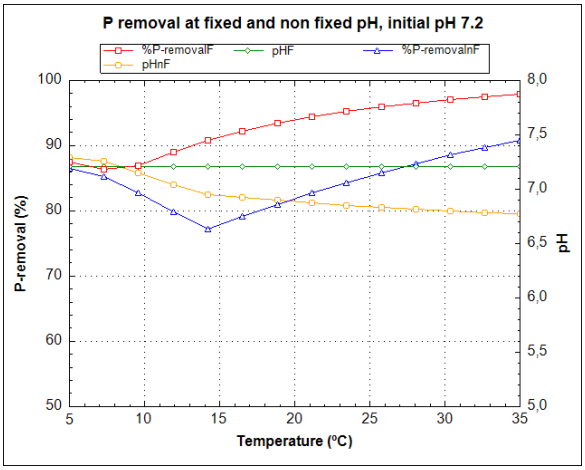

Graph 12, P removal (%) at fixed and non fixed pH, where the initial pH is set to 7.2. The course of the P removal changes as temperature increases. Red line: %P-removal non fixed pH. Green line: fixed pH. Blue line: %P-removal non fixed pH. Yellow line: non fixed pH.

Graph 13 shows the removal of Cl which is a representation of the consumption of NaOH. By the equilibrium phase chosen the model adjusts as follow: if a pH increase is needed (thus NaOH is needed), then NaCl dissolves and HCl is removed, leaving Na^+ and OH^- in solution. Thus the concentration of Cl is reduced.

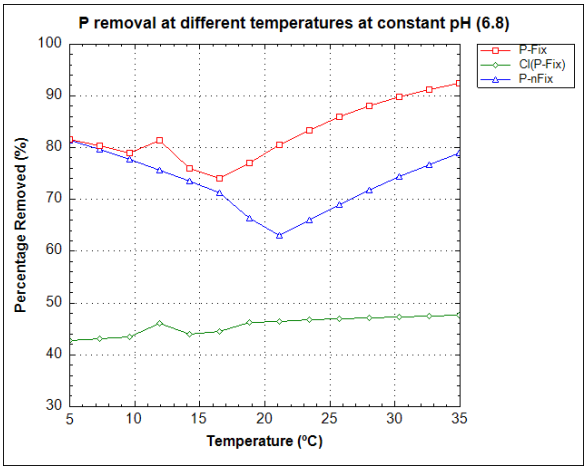

Graph 13, P removal (%) at fixed and non fixed pH, including the amount of HCL (%) removed which resembles the amount of NaOH released.

4.3.4. Indian Drain Water Solution Composition Changes

This section shows the results of modeling of the Indian Drain Water with different compositions in P, Ca and NH_4 concentration at fixed pH.

4.3.4.1. Phosphate Concentration

At fixed pH, an increase in P concentration leads to higher P removal (Graph 14).

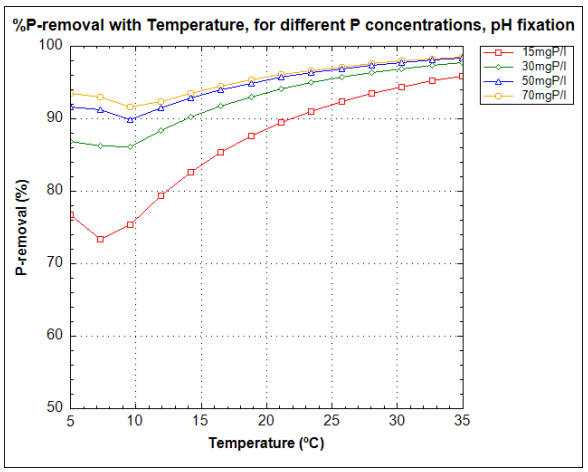

Graph 14, P removal (%) with temperature at different P concentrations including pH fixation at pH 7.2, temperature 23 °C. The P content in Indian Drain water is 30mgP/l.

4.3.4.2. Calcium Concentration

Graph 15 demonstrates the effect of Ca concentration at different pH conditions. Increased Ca concentrations lead to higher P removal percentages. At a high pH (7.8) the same amount of Ca added leads to a higher increase in P removal compared to a low pH (6.8).

Ca-P minerals precipitate best at higher pH (>7.2). If the Ca:P molar ratio is optimal, 100% P removal can be obtained. If there is a deficit to this ratio, 100% P removal cannot be obtained. There is not yet a 100% P removal for middle pH 7.2 and 7.8. An increase in temperature could lead to higher P removal as demonstrated in Graph 11.

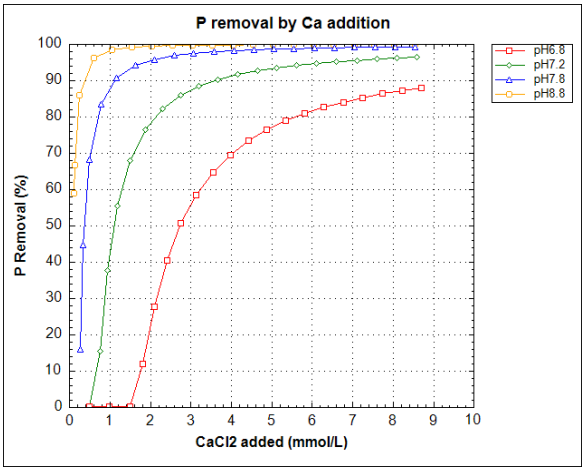

Graph 15, %P removal with increasing CaCl2 at different pH concentrations, including pH fixation, temperature 23 °C. The Ca of Indian Drain water is 7.28 mmol/l

4.3.4.3. Ammonium Concentration

The addition of ammonium at different pH conditions as shown in Graph 16 has no effect on the P removal. Only the SI of struvite increases slightly but remains undersaturated (SI<0). Under the tested temperature and pH conditions struvite is thermodynamically not inferior to precipitation compared to ATCP, DCP or DCPD. Thus, regardless of the increase in ammonium struvite will not precipitate.

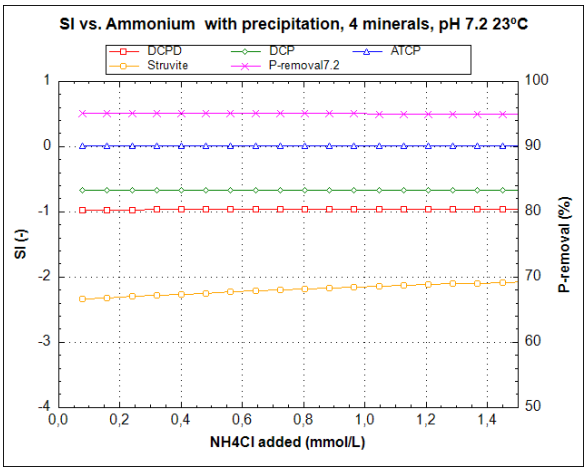

Graph 16, Representing the effect of increased ammonium on the P removal (%) and the SI of DCPD, DCP ATCP and Struvite, at temperature 23 °C.

4.3.5. Black Water Analysis

Black water was modeled at similar conditions as the Indian Drain water. The saturation state and effect of pH and temperature on the saturation state with respect to different mineral phases was made graphical.

4.3.5.1. Black Water Saturation State

Both ATCP and HAP, as well as struvite have an SI>0 at pH 8.8 (Graph 17). Struvite's SI decreases as temperature increases according to its positive enthalpy change. As shown in Graph 18, ATCP reaches its highest SI from pH 9 onwards; SI = 4. Struvite reaches positive saturation values between pH 7.8 and 10.9; SI ~1..

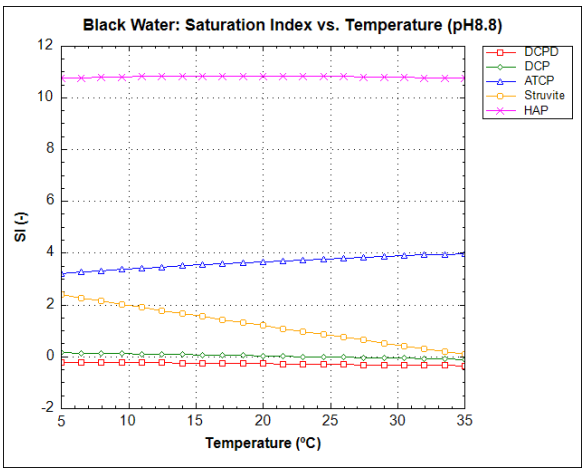

Graph 17, Saturation Index of minerals for increasing temperature at pH 8.8.

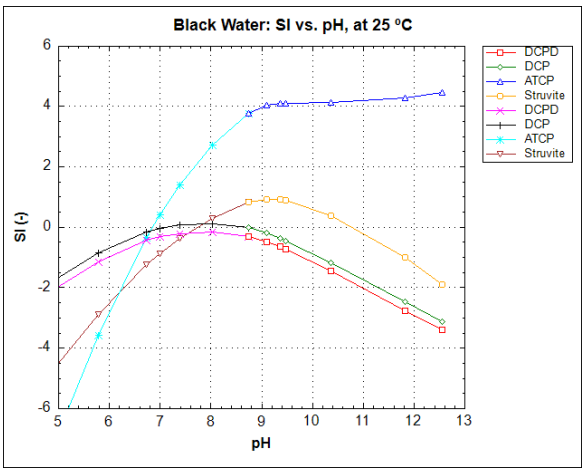

Graph 18, Saturation Index of minerals for increasing pH at temperature 25 °C.

4.3.5.2. Precipitation: Temperature

During forced precipitation of DCPD, DCP, ATCP, and struvite, at fixed pH conditions of 8.8, the %P removal is high (Graph 19). ATCP and struvite both precipitate (SI=0). However as temperature increases to above 25 °C, struvite becomes understaturated and the %P removal decreases slightly.

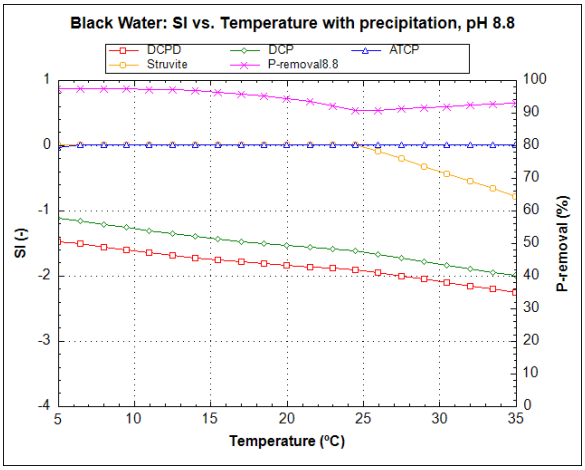

Graph 19, SI of Black water at pH 8.8 for increasing temperature at forced precipitation.

Graph 20 shows the %P removal for different pH conditions. Very little P removal occurs at low pH (red line). With increasing temperature ATCP starts to precipitate (S=0) and P removal increases. At high pH, temperature shows to have little effect on the %P removal. As temperature increases a slight decrease in P removal noted, which continues up to the point where struvite, aside ATCP, does not precipitate anymore (SI<0).

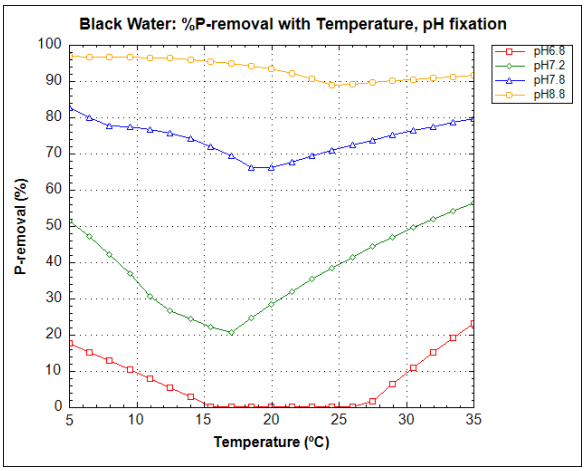

Graph 20, %P removal with increasing temperature under fixed pH conditions for Black Water, at forced precipitation.

4.3.5.3. Precipitation: pH

The SIs of the mineral phases and the total percentage of P removal are shown in Graph 21. The P removal (grey and pink line) starts at pH 6.8, at 25 °C. ATCP (brown and blue) quickly rises in SI at higher pH conditions, becoming the dominant mineral phase and precipitating. Around pH 9 struvite precipitation also contributes to the total P removal. Near 100% P removal is not achieved for Black Water at temperature of 25°C.

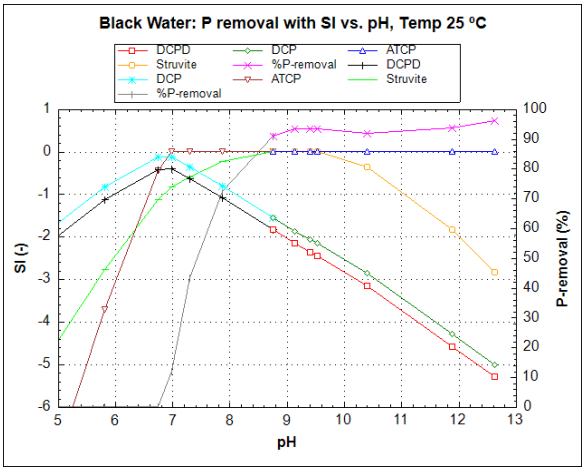

Graph 21, Simultaneous precipitation of phosphorus minerals DCPD, DCP, ATCP and Struvite at 25 °C, Black Water

The total %P removal with the subsequent chemical dosing of HCl or NaOH is shown in Graph 22. As indication, if Black Water were more acidic, the percentage P removal from could be 10% (pH 7.9), instead of 90% at pH 8.8.

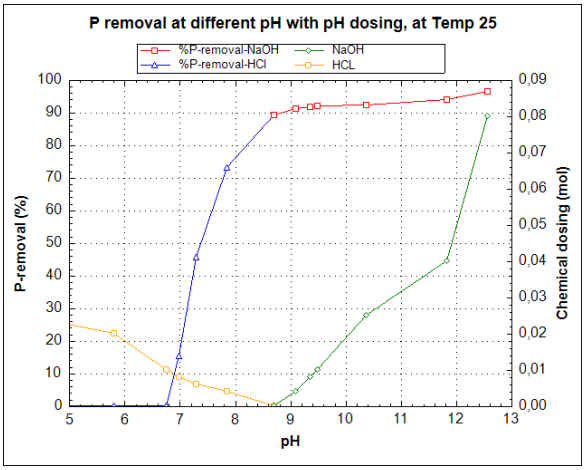

Graph 22, P removal (%) by simultaneous precipitation at different pH at 25°C, including the amount of NaOH (mol) and HCl (mol) added to fixate the pH, Black Water.

4.3.6. Comparison of Indian Drain Water and Black Water

When comparing the PHREEQC graphical output of Indian Drain Water with Black Water several observations stand out:

Indian Drain Water

- P removal starts at pH 5.9 at 25°C (Graph 10).
- ATCP is the most dominant mineral responsible for P removal.
- 100% P removal achieved at pH 8.8 (Graph 14).
- Over 85% P removal at pH 7.2 (Graph 11).
- More sensitive to a shift in pH with respect to its P removal capacity. This is also shown by the effect of acid and base addition on the P removal curve (Graph 8)
- Struvite does not play a role in P removal as it does not precipitate.

Black Water

- P removal starts at pH 6.8 at 25°C (Graph 20).
- ATCP is a dominant mineral responsible for P removal.
- Less than 100% P removal at pH 8.8 (Graph 20)
- Less than 60% P removal at pH 7.2 (Graph 20).
- Higher alkalinity, thus a buffering effect, reducing its sensitivity to pH shifts (Graph 22).
- Struvite does play a role in the P removal as it co-precipitates with ATCP under specific conditions.

This shows that even though the composition of Indian Drain water and Black Water share resemblance in composition, different minerals may form at different conditions, affecting the P removal.

4.4.Validation Geochemical Model

The chemical composition of Lotus Like water was implemented in PHREEQC to start the validation of the geochemical model. After the input parameters were implemented in PHREEQC, four different runs were performed:

1) precipitation of DCP, ATCP and HAP ('all minerals')
2) forced precipitation of 'only DCP'
3) forced precipitation of 'only ATCP'
4) forced precipitation of 'only HAP'

In this way the removal percentage of Ca and P was determined for each run performed by PHREEQC.

The removal percentage of Ca and P of the verification experiment was determined by comparing the composition of the stock solution (Day 1) with the final composition (Day 5). The amount of Ca and P removed was 8.6 %P and 33.0 %Ca (Table 17).The Ca:P molar ratio of 1.98 was calculated based upon the removal percentages.

Table 17, Comparison of PHREEQC modeling with verification experiment for different mineral phases for Ca and P removal. The first part of the table shows the measured parameters and the Ca and P results (ICPOES) on Day 1 and Day 2. The second part shows the Input parameters for modeling in PHREEQC. The third part shows the Output of this PHREEQC modeling. For each part the Ca and P concentrations are shown, as well as the Ca and P removal (%). The output also shows the amount of mol/l of a mineral that has precipitated at forced precipitation (Si=0).

	pH	EC uS/cm	Temp °C	Ca	P	DCP	ATCP	HAP	% Ca - rem	% P - rem
						mol/l				
Measured parameters and ICPOES result										
Day 1 - Stock	7,16	4680	19,7	8,79	1,19					
Day 5 - Final	**6,24**	**4670**	17,9	8,04	0,79				**8.6**	**33.0**
Input to PHREEQC										
Solution	7,16	4134	17,9	8,79	1,19					
Output of PHREEQC										
All minerals	6,58	3919	17,9	7,93	0,31	0,86			9,8	73,4
DCP only	6,58	3919	17,9	7,93	0,31	0,86			9,8	73,4
ATCP only	**6,40**	**3940**	17,9	8,22	0,79		0,19		**6,4**	**33,0**
HAP only	**5,89**	3930	17,9	8,05	0,73			0,15	**8,4**	**38,3**

From the mineral formation at different runs it becomes clear that even though all minerals are allowed to precipitate, it is only DCP that is thermodynamically favorable to form, no co-precipitation is favored. 'Only ATCP' precipitation showed that, at the final temperature of 17.9 °C, the C and P removal was 6.4% and 33.0% respectively, which is close to the experimental removal percentages achieved (8.6% and 33.0%). However, there are some discrepancies: the modeled pH reached after ATPC precipitation is slightly higher than that of the measured final sample, pH 6.40 vs 6.24, respectively, and the reduction in the EC is not the same.

In addition, 'only HAP' also values shows close to the experimental removal efficiencies of Ca and P (8.4% and 38.3%, respectively).The measured Ca:P molar ratio (1.98) is closer to the Ca:P molar ratio of HAP (1.67) compared to the Ca:P molar ratio of ATCP (1.5). Even though PHREEQC does not consider the reactions to co-precipitate, this could still have occurred in the experiment, as often precursor minerals (such as OCP and ATCP) are identified together with the final crystallized phase (Mañas *et al.*, 2012). Furthermore, impurities or the presence of certain ions such as Mg can notably reduce the formation of HAP (Celen *et al.*, 2007). However, this does not justify why the measured Ca:P molar ratio is 1.98.

In search for an explanation why the Ca:P molar ratio of the experiment does not peer with the runs, the mineral phases and processes should be reconsidered. One study proposes the formation of HAP-precursor HDP (hydroxyl dicalcium phosphate [Ca2HPO4(OH)2]) (Maurer and Boller, 1999). The Ca:P molar ratio of HDP is 2.0 (Maurer and Boller, 1999). However, (Mañas *et al.*, 2012) opposes the formation of HDP as they suggest that ATCP is formed and co-precipitation of $CaCO_3$ occurs, explaining the Ca:P molar ratio of 2. Since the formation of ATCP is independent of the $CaCO_3$ precipitation (when Ca is in excess), and the %P removal measured for ATCP and the experiment are both 33%, it is plausible to say that according to PHREEQC it is ATCP that forms in the experiment. Nonetheless, PHREEQC modeling of HDP and the precipitation of $CaCO_3$ is encouraged to obtain a better understanding of the P removal mechanism.

4.5.Flow-through Experiments

Two flow-through experiments were performed to determine the influence of mineral wool on the P removal. Short term influences were determined by monitoring EC and P during a breakthrough of the influent passing through a mineral wool filled basin (Experiment I, Figure 5, Section 3.7). The long term influences were determined by monitoring of the recirculation of the effluent through the same mineral wool filled basin (Experiment II, Figure 6, Section 3.7).

4.5.1. Lab Experiment I, Lotus Like water

A flow-through experiment of which the breakthrough was monitored by EC and P concentration was performed (Graph 23):

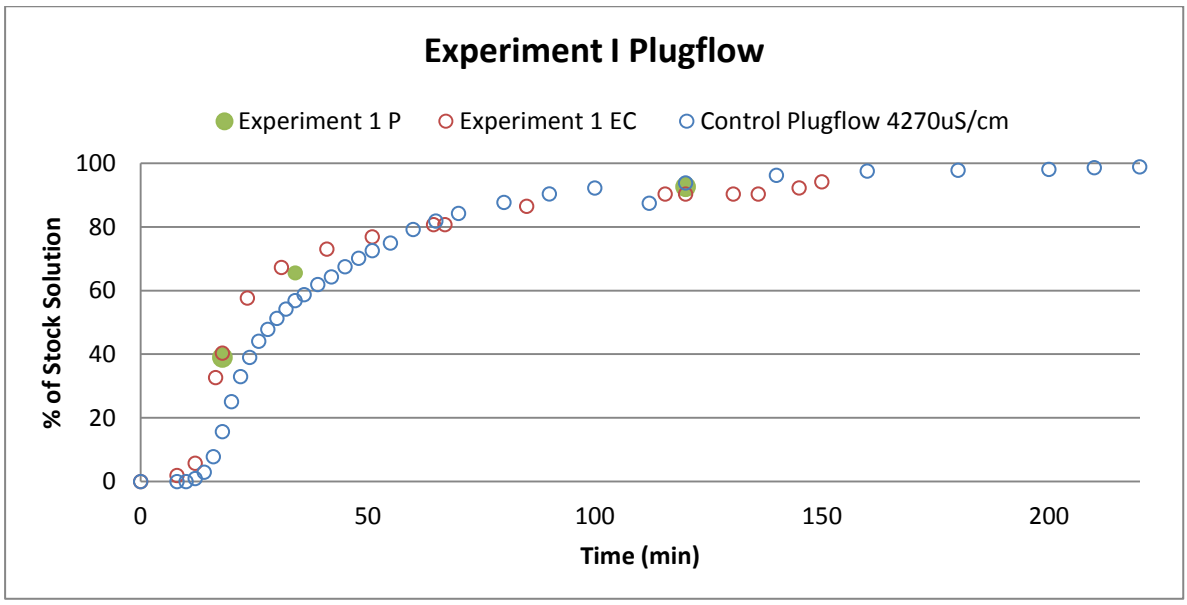

Graph 23, Experiment: breakthrough curve of the EC and P measured, compared to the control plug flow (normative). The blue circles show the control performed. The red circles show the experiment EC. The influent pH and temperature were 6.8 and 21.8 °C, respectively. The effluent pH and temperature was 8.3 and 25 °C, respectively.

Comparing the control breakthrough curve with the measured P and EC curve there is a slight but not significant difference in shape of the curve. The normative % of P does not differ from the normative % of EC. This is also the case for the last measured P point. Considering these results there appears to be no indication the P removal by mineral wool at first encounter (short term).

4.5.2. Lab Experiment II, Lotus Like water

A second experiment performed collected effluent from Experiment I and was re-circulated through the mineral wool basin. The PHREEQC solution input used was corrected for composition change, and included temperature and pH at each measuring interval. The pH increased gradually over time, as well as the temperature.

The modeling included the forced precipitation (SI=0) of Ca-P minerals. Since the Experiment II setup lead to aeration of the re-circulated solution, the CO_2 equilibrium with air was modeled by equilibrating the solution to 400ppm of CO_2 (P_{CO2} $10^{-3.4}$ atm). The stripping of CO_2 from the solution increases the pH, which significantly influences the Ca-P precipitation as modeled in Section 4.3.

Additionally, the model included a correction for the initial Ca concentration, as compared to Experiment I, because P removal is very dependent on the Ca concentration of the solution. Unfortunately, measurement of the initial composition of the solution of Experiment II determined by the ICPOES was incorrect, thus the initial Ca concentration for Experiment II was based upon the reduction of P and Ca as measured in Section 3.5. The amount of P measured by the Test Kit showed a reduction of 6.1% compared to the initial stock concentration in Experiment I, leading to a Ca reduction of 1% (see Appendix G). Therefore, the new Ca concentration used in the model was 287 mg/l.

Furthermore, as done in Section 4.4, different runs for different Ca-P minerals were performed. Overall, the modeling lead to the percentage P removal for each run which could then be compared to the measured (experiment) P reduction in time (Graph 24.)

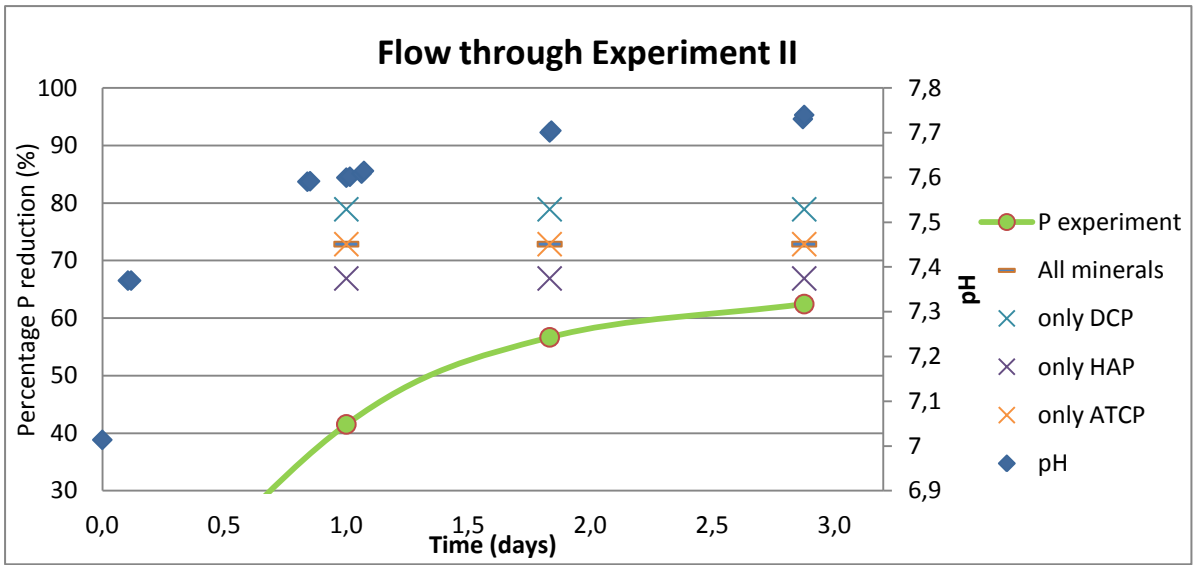

Graph 24, Experiment II: Comparison of the experimentally obtained % P removal (green line) with the % P removal as modeled for four different runs in PHREEQC (colored crosses). The runs performed: 1) Letting DCP, ATCP and HAP precipitate ('all mineral'), 2) 'only DCP' precipitate, 3) 'only ATCP' precipitate, and lastly 4) 'only HAP' precipitate. The pH (blue diamond) of the experiment solution increased. The script of the input can be found in Appendix I. V. Validation PHREEQC and Experiment II.

According to this graph all model runs overestimated the amount of P removed compared to the experimental %P removal (green line).

As time passes more P is reduced, but in the performed model runs P reduction is leveled. This is due to the difference in equilibrium state of the measured and modeled solutions. The measured sample is still returning to its equilibrium state, while the model results are at equilibrium after forcing precipitation.

If the measured P reduction exceeded the modeled results, there would be a reason to consider whether the mineral wool has an effect on the P removal from the solution. However, as this is not the case, and previous experiments with mineral wool have also shown no additional P removal, the results of this section affirm that there is no direct effect of mineral wool on the P removal.

Nonetheless, an observation that needs discussion is the presence of white crystal-like flocks formed in both the basin as well as in the collection barrel. As the P removal increased, more flocks formed, mainly floating on the surface or attached to any surface present, on both the mineral wool and the barrel itself. Consequently, it was unclear what the role of the mineral wool was in filtering out the crystal-like flocks formed as they formed in all places. Thus, it is encouraged that more experiments are performed with a slightly different setup, improving the testing conditions with respect to filtration.

Furthermore, a factor not incorporated in the PHREEQC model is the self buffering effect of mineral wool. This could be incorporated by adding calcium oxide (CaO) and wollastonite ($CaSi_3$) as 'dissolve only' phases to the model, supplying the Ca^{2+} and OH^- needed as done for modeling of mineral-based material Filtralite (Herrmann *et al.*, 2013)

4.5.3. Microscope Imaging

Observation during the flow-through experiment was the formation of crystal-like flocks (Figure 10) on the top of the influent/effluent barrel as well as on the solution passing through the mineral wool basin.

The flocks appear similar to the dendritic growth of calcium phosphate as identified by (Mañas *et al.*, 2012).

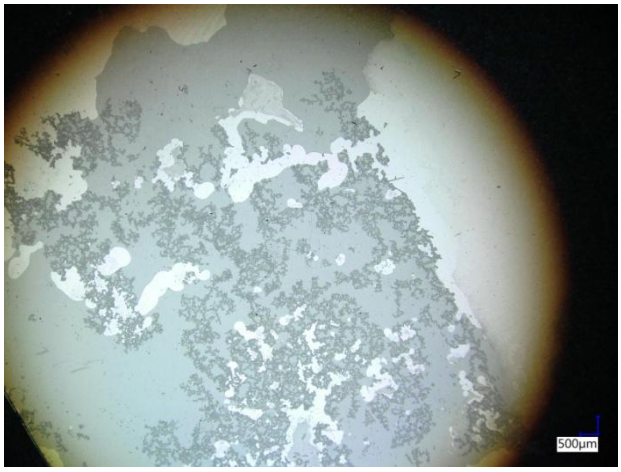

Figure 10, Digital Microscope Imaging of Formation of Crystals on the Lotus Like Water.

5. General Discussion and Recommendations

The hypothesis proposed in this research stated that mineral wool dissociates ions due to biologically mediated pH changes, which subsequently interact with orthophosphate forming minerals and in this way removing orthophosphate from wastewater. This research focused specifically on the dissolution of the mineral wool under different pH conditions and the subsequent precipitation mechanism for P removal.

The presented results showed that there was no significant dissolution of mineral wool under different pH and P concentrations (the pH-P matrix) to precipitate with P in wastewater. Other studies did report dissolution of mineral wool, at somewhat higher concentrations (van Noordwijk, 1979; Kipp, Wever and de Kreij, 1999; Campopiano *et al.*, 2014). These studies differ slightly in mineral wool composition as well as the experiments performed to measure concentrations.

The mineral wool did show a self-buffering effect. At high pH the CO_2 buffer plays a role, as well as the formation of CaCO3 (van Noordwijk, 1979). For low initial pH, three different reasons for increasing pH can be suggested: i) an exchange of cations with H^+ as reported by (van Noordwijk, 1979). However, the charge-balance was not conserved. Therefore it is questionable whether the exchange of ions is the main process responsible for the self buffering effect. ii) The dissolution of free CaO in water releasing OH^- and thus increasing the pH (Herrmann *et al.*, 2013). iii) The dissolution of $CaCO_3$ releasing HCO_3^- and Ca^{2+}, subsequently influencing the carbonate equilibrium and increasing the pH (Stumm and Morgan, 1996). Interestingly, the measured Ca concentration (~0.2mg Ca/l) was still very low, thus it is not exactly clear which dissolution reactions (ii or iii) area responsible for the self-buffering effect at low pH. In addition, a report on the method to measure pH buffering capacity in mineral wools simply addresses the pH increase due to the alkaline properties of the mineral wool, without further explanation on which reactions take place (Blok and Kaarsemaker, 2008).

It is recommended that the self-buffering effect is incorporated in the geochemical modeling, taking into consideration the different plausible mechanisms. To further improve the PHREEQC model, simulating P removal, more research is needed on the effects, controlling, and influencing of the precipitation of P minerals. As previously mentioned, the presence of $CaCO_3$, CaO, CO_2, and other complexes, such as HDP, should be studied. In addition, the effect of surface complexation and exchange should be studied and incorporated (Maurer and Boller, 1999; Mañas *et al.*, 2012; Azam *et al.*, 2019). Moreover, the ionic composition and presence of proteins and specific amino acids must be considered, since this can hinder the availability of the ions for precipitation (Song, Hahn and Hoffmann, 2002; Stelt, Temminghoff and Riemsdijk, 2005).

Returning to the hypothesis, ideally, mineral wool would predominantly contain a high amount of easily dissolvable Ca to react with P, while maintaining its substrate properties for bacterial activity. Since dissociation of ions could lead to fiber deterioration, it is desirable that precipitation of the minerals occur on the fibers, strengthening the fibers (Campopiano *et al.*, 2014). To increase the Ca content of the mineral wool to levels such as in Filtralite and Superwool, it is suggested to add more limestone ($CaCO_3$) at the manufacturing stage (Herrmann *et al.*, 2013; Campopiano *et al.*, 2014). The repetition of the experiment performed is encouraged, with different mineral wool compositions, to test the hypothesis and gain more understanding of the role of mineral wool composition.

The hypothesis assumed release of ions from the mineral wool due to biologically induced pH changes. However, a different mechanism influencing the release of ions could be chelating agents. When the bioavailability of iron is low microorganisms produce siderophores, which are iron chelating (Ferreira *et al.*, 2019). Siderophores have a high affinity and selectivity to bind and complex iron (Fe(III))(Ferreira *et al.*, 2019). In this manner, being an effective iron chelating compound, obtaining iron from the environment. Perhaps this, or a similar biologically-induced process extracting ions occurred at the sites tested with mineral wool (Limburg, India, Indonesia). This encourages further onsite research concerning mineral wool, carrying biomass.

There is also a positive aspect to the insignificant dissolution of mineral wool. When mineral wool stays intact, it can act as carrier for microorganisms, and as substrate for plant growth. If mineral wool were to dissociate ions it would reach exhaustion at a certain point and replacement would be needed. Given that the mineral wool appears to be inert, high P removal rates may not be achieved, but biological conversions decreasing excessive nutrient levels can still occur.

An additional recommendation concerns the future use of mineral wool in its current composition. If mineral wool containing biofilm for biological nutrient conversion is to be used, further investigation is encouraged focusing mainly on biological activities taking place (microbial growth, denitrification, nitrification, CO_2 exchange), rather than focusing on the self-buffering capacity of mineral wool. According to research on mineral wool as substrate for root growth, mineral wool is only responsible for 10% of the pH change (Blok and Kaarsemaker, 2008). The presence of microorganisms can affect the pH up to 5 - 10 times more than mineral wool, therefore playing an essential role in providing environmental conditions for biological conversions and/or desired precipitation of minerals. Therefore, consequently, the geochemical model should include more aspects: biological activities, kinetic rates, self buffering capacity, mineral precipitation and biological conversions responsible for changing solution composition.

6. Conclusion

This research set out **what removal mechanism was responsible for the ortho-phosphate removal from wastewater by mineral wool filters.** It was hypothesized that mineral wool dissociates ions due to biologically mediated pH changes, which subsequently interact with orthophosphate forming minerals and in this way removing orthophosphate from wastewater. To accomplish the research objective four sub-questions were formulated for which both laboratory experiments with mineral wool, as well as geochemical modeling in PHREEQC was performed.

- The first sub-question being: **'What does mineral wool consist of?'**

Mineral wool is classified as an alkaline material. According to chemical analysis, the mineral wool contains: 188.0 g/kg silicon, 187.6 g/kg calcium, 79.3 g/kg aluminum, 43.1 g/kg iron, and 9.3 g/kg magnesium. It is made of a fibrous network of elongated and cylindrical manufactured mineral aggregate. In between the fibers small spherical balls are spread throughout heterogeneously.

- Sub-question 2: **'What is the effect of pH on the release of Ca, Al, Mg and Fe by mineral wool and on P precipitation?'**

Batch experiments performed showed that there was no significant dissolution of any ion from the mineral wool stressed under different pH and P concentrations. The experiments performed also showed that the effect of mineral wool on P precipitation at different pH and P concentrations was not significant. The mineral wool did appear to have a self-buffering mechanism indicating some exchange of protons and hydroxide. The carbonate equilibrium plays a role at reducing the pH at high pH levels to equilibrium pH (~7). The increase of pH at low pH levels is most likely due to the alkaline properties of mineral wool in combination with the carbonate equilibrium. Other studies have shown that other mineral wools do show significant dissolution of ions and precipitation of P due to the effect of pH. Thus the limited release of ions is most likely due to the used mineral wool itself.

- Sub-question 3: **'How does mineral wool facilitate precipitation of minerals in waste- and drain waters?'**

The geochemical model PHREEQC was used to determine the thermodynamic potential of wastewaters to precipitation, independent of the presence of mineral wool, under different pHs and temperatures. Validation of this model for wastewater characterized amorphous tricalcium phosphate (ATCP) as the mayor crystallized mineral phase. The comparison of the model with the performed flow-through experiment showed consistent overestimation of P precipitation by the model, with respect to the experiment. Considering the insignificant dissolution of Ca, Al, Mg and Fe ions from the mineral wool, it is unlikely that the used mineral wool chemically facilitates precipitation of minerals through interaction with the wastewater. Furthermore, this research could neither affirm nor reject the role of mineral wool filtering out crystal-like flocks formed in the wastewater. Perhaps the presence of chelating organisms could extract other ions, which would otherwise not be dissociated from the mineral wool, increasing P removal rates.

- Sub-question 4: **'How does biological conversion in mineral wool influence P removal rates?'**

Although no experiment was performed with mineral wool containing biomass, a theoretical approach did lead to preliminary conclusions on this sub-question. As the hypothesis was rejected

as mineral wool does not release ions when stressed with different pH, biological conversion will not facilitate ion release from the mineral wool either. Thus, there will also be no increase of reactant from the mineral wool to further induce precipitation of P. Nevertheless, the theoretical development identified three bacterially-induced mechanisms of which two could influence P removal rates namely, *biologically-induced mineralization* and *biologically-influenced mineralization*.

In conclusion, the research performed did not lead to the identification of the removal mechanism responsible for the ortho-phosphate removal from wastewater by mineral wool filters. There was no significant dissolution of any ions from the mineral wool stressed under different pH and P concentrations However, this research does provide valuable information on the theoretical background of both chemical and biological precipitation. In addition, the research resulted in a model of P removal of wastewater in PHREEQC and developed a method for determining P precipitation from wastewater by mineral wool.

7. References

APHA *et al.* (1998) *Standard methods for the examination of water and wastewater*. 20th edn. Washington DC.

Appelo, C. A. J. and Postma, D. (2006) *Geochemistry, Groundwater and Pollution, 2nd Edition*, *Vadose Zone Journal*. doi: 10.2136/vzj2005.1110br.

Arias, D., Cisternas, L. and Rivas, M. (2017) 'Biomineralization Mediated by Ureolytic Bacteria Applied to Water Treatment: A Review', *Crystals*, 7(11), p. 345. doi: 10.3390/cryst7110345.

Azam, H. M. *et al.* (2019) 'Phosphorous in the environment: characteristics with distribution and effects, removal mechanisms, treatment technologies, and factors affecting recovery as minerals in natural and engineered systems', *Environmental Science and Pollution Research*. Environmental Science and Pollution Research, 26(20), pp. 20183–20207. doi: 10.1007/s11356-019-04732-y.

Beckmann, W. (2013) *Crystallization: Basic Concepts and Industrial Applications*. Wiley-VCH Verlag GmbH & Co. doi: https://doi.org/10.1002/9783527650323.ch9.

Benzerara, K. *et al.* (2011) 'Importance, mécanismes et implications environnementales de la biominéralisation par les microorganismes', *Comptes Rendus - Geoscience*. doi: 10.1016/j.crte.2010.09.002.

Blok, C. and Kaarsemaker, R. (2008) *De pH buffer bepaling van teeltmedia: opkweek in steenwol en perlietpotten*. Wageningen.

Boonrungsiman, S. *et al.* (2012) 'The role of intracellular calcium phosphate in osteoblast-mediated bone apatite formation', *Proceedings of the National Academy of Sciences of the United States of America*, 109(35), pp. 14170–14175. doi: 10.1073/pnas.1208916109.

Bunsell, A. R. (2009) 'Structure and properties of glass fibres 15', in Huff, N. T. and Jones, F. R. (eds) *Handbook of Tensile Properties of Textile and Technical Fibres*. Cambridge: Woodhead Publishing Limited, pp. 529–569. doi: 10.1533/9781845696801.2.529.

Campopiano, A. *et al.* (2014) 'Dissolution of glass wool, rock wool and alkaline earth silicate wool: Morphological and chemical changes in fibers', *Regulatory Toxicology and Pharmacology*. Elsevier Inc., 70(1), pp. 393–406. doi: 10.1016/j.yrtph.2014.05.023.

Celen, I. *et al.* (2007) 'Using a chemical equilibrium model to predict amendments required to precipitate phosphorus as struvite in liquid swine manure', *Water Research*, 41, pp. 1689–1696. doi: 10.1016/j.watres.2007.01.018.

Claveau-Mallet, D., Courcelles, B. and Comeau, Y. (2014) 'Phosphorus removal by steel slag filters: Modeling dissolution and precipitation kinetics to predict longevity', *Environmental Science and Technology*, 48(13), pp. 7486–7493. doi: 10.1021/es500689t.

Le Corre, K. S. *et al.* (2007) 'Kinetics of Struvite Precipitation: Effect of the Magnesium Dose on Induction Times and Precipitation Rates.', *Environmental Technology,* 28(12), pp. 1317–1324.

CPCB (2006) 'Water quality status of Yamuna River, Assessment and Development of River Basin', pp. 1–115. Available at: www.cpcb.nic.in.

Cranenburgh, L. Van (2018) *The impact of a Drainblock filter on water quality improvement of highly polluted Indonesian water streams A study on how Drainblock can be applied for turbidity*.

Delft University of Technology.

Cunha, J. R. *et al.* (2018) 'Calcium addition to increase the production of phosphate granules in anaerobic treatment of black water', *Water Research*, 130, pp. 333–342. doi: 10.1016/j.watres.2017.12.012.

Dash, A., Zhang, H. and Srinivas, V. (2019) 'Direct and indirect estimation of biomass density in mineral wool biofilters used for nitrification and', pp. 1–23.

Drainblock (2019) *Drainblock*. Available at: http://www.drainblock.nl/en (Accessed: 1 February 2019).

Dupraz, S. *et al.* (2009) 'Experimental and numerical modeling of bacterially induced pH increase and calcite precipitation in saline aquifers', *Chemical Geology*. Elsevier B.V., 265, pp. 44–53. doi: 10.1016/j.chemgeo.2009.05.003.

EPA (2007) *Biological Nutrient Removal Processes and Costs*. Washington DC. doi: EPA-823-R-07-002.

Etter, B. *et al.* (2011) 'Low-cost struvite production using source-separated urine in Nepal', *Water Research*. Elsevier Ltd, 45(2), pp. 852–862. doi: 10.1016/j.watres.2010.10.007.

Falkentoft, C. M. (2000) *Simultaneous removal of nitrogen and phosphorus in a two-biofilter system: The aspect of diffusion.*, *Water Science and Technology*. doi: 10.2166/wst.2000.0249.

Ferreira, C. M. H. *et al.* (2019) 'Comparison of five bacterial strains producing siderophores with ability to chelate iron under alkaline conditions', *AMB Express*. Springer Verlag, 9(1). doi: 10.1186/s13568-019-0796-3.

Forrest, A. L. (2004) *Process Optimization of a Technical Scale Phosphorus Recovery System Through Struvite Crystallization at the City of Penticton Advanced Wastewater Treatment Plant*. The University of British Columbia.

De Graaff, M. S. (2010) *Resource recovery from black water*. Wageningen University.

Gustafsson, J. P. *et al.* (2008) 'Phosphate removal by mineral-based sorbents used in filters for small-scale wastewater treatment', *Water Research*, 42, pp. 189–197. doi: 10.1016/j.watres.2007.06.058.

Gutierrez-Orrego, D. A., Garcia-Aristizabal, E. F. and Gomez-Botero, M. A. (2017) 'Mechanical and Physical Properties of Soil-Cement Blocks Reinforced with Mineral Wool and Sisal Fiber.', *Journal of Materials in Civil Engineering*, 29(3), pp. 1–12. doi: 10.1061/(ASCE)MT.1943-5533.0001753.

Hamdi, N. and Srasra, E. (2012) 'Removal of phosphate ions from aqueous solution using Tunisian clays minerals and synthetic zeolite', *Journal of Environmental Sciences*. doi: 10.1016/S1001-0742(11)60791-2.

Herrmann, I. *et al.* (2013) 'Modeling phosphate transport and removal in a compact bed filled with a mineral-based sorbent for domestic wastewater treatment', *Journal of Contaminant Hydrology*. Elsevier B.V., 154, pp. 70–77. doi: 10.1016/j.jconhyd.2013.08.007.

Huang, W. *et al.* (2015) 'Identification of inorganic and organic species of phosphorus and its bio-availability in nitrifying aerobic granular sludge', *Water Research*. Elsevier Ltd, 68, pp. 423–431. doi: 10.1016/j.watres.2014.09.054.

Johansson, S., Ruscalleda, M. and Colprim, J. (2017) 'Phosphorus recovery through biologically induced precipitation by partial nitritation-anammox granular biomass', *Chemical Engineering Journal*. The Authors, 327, pp. 881–888. doi: 10.1016/j.cej.2017.06.129.

Kipp, J. A., Wever, G. and de Kreij, C. (1999) *Substraat: Analyse, Eigenschappen, Advies*. Doetichem: Elsevier.

Kulakovskaya, T. (2014) 'Phosphorus storage in Microorganisms: Diversity and Evolutionary Insight', *Biochemistry & Physiology: Open Access*, 04(01), pp. 1–4. doi: 10.4172/2168-9652.1000e130.

van Langerak, E. P. A. *et al.* (1998) 'Effects of high calcium concentrations on the development of methanogenic sludge in upflow anaerobic sludge bed (UASB) reactors', *Water Research*, 32(4), pp. 1255–1263. doi: 10.1016/S0043-1354(97)00335-7.

van Lier, J. B., Mahmoud, N. and Zeeman, G. (2008) *Biological wastewater treatment: principles, moddeling and design - Chapter 16: Anaerobic wastewater treatment*, *Biological Wastewater Treatment : Principles, Modelling and Design*. doi: 10.1021/es00154a002.

Lotus HR (2016) *About - Lotus HR*. Available at: https://lotushr.org/about/ (Accessed: 17 January 2020).

Lotus HR (2018) 'Barrapullah Drain Data 2018-27-09'. Delft University of Technology.

Magalhães, M. C. F. and Costa, M. O. G. (2018) 'On the solubility of whitlockite, Ca9Mg(HPO4)(PO4)6, in aqueous solution at 298.15 K', *Monatshefte fur Chemie*, 149(2), pp. 253–260. doi: 10.1007/s00706-017-2129-z.

Magalhães, M. C. F., Marques, P. A. A. P. and Correia, R. N. (2007) *Calcium and Magnesium Phosphates: Normal and Pathological Mineralization*, *Biomineralization - Medical Aspects of Solubility*. doi: 10.1002/0470092122.ch3.

Mañas, A. *et al.* (2012) 'Parameters influencing calcium phosphate precipitation in granular sludge sequencing batch reactor', *Chemical Engineering Science*, 77, pp. 165–175. doi: 10.1108/IJCST-01-2018-0012.

Maurer, M. and Boller, M. (1999) 'Modelling of phosphorus precipitation in wastewater treatment plants with enhanced biological phosphorus removal', in *Water Science and Technology*. No longer published by Elsevier, pp. 147–163. doi: 10.1016/S0273-1223(98)00784-7.

Merkel, B. J. and Planer-Friedrich, B. (2005) *Groundwater Geochemistry*. Edited by D. K. Nordstrom. Krips, Meppel.

Merola, C. (2018) *Performance of mineral wool as filter medium for the treatment of contaminated drain water in the urban context of Delhi, India .* Delft University of Technology.

Metcalf & Eddy Inc. (2003) *Wastewater engineering: treatment and reuse*. 3rd edn. Edited by G. Tchobanoglous and F. L. Burton. McGraw-Hill; New York.

van Noordwijk, M. (1979) *Fysische en chemische eigenschappen van steenwol als substraat voor plantenteelt zonder aarde*. Haren.

Nriagu, J. O. and Moore, P. B. (1984) 'Phosphate Minerals', in *Phosphate Minerals*. Berlin Heidelberg: Springer-Verlag.

Park, J. H. *et al.* (2017) 'Phosphate removal in constructed wetland with rapid cooled basic

oxygen furnace slag', *Chemical Engineering Journal*. Elsevier B.V., 327, pp. 713–724. doi: 10.1016/j.cej.2017.06.155.

Parkhurst, B. D. L. and Appelo, C. A. J. (1999) *User's Guide to PHREEQC (Version 2)—A Computer Program for Speciation, Batch-Reaction, One-Dimensional Transport, and Inverse Geochemical Calculations. U.S. Geological Survey Water-Resources Investigations Report 99-4259*.

Parkhurst, D. L. (2019) *PHREEQC Users, recourse for geochemists, Forum*. Available at: https://phreeqcusers.org/index.php/topic,1334.msg4174.html#msg4174.

Parkhurst, D. L., Stollenwerk, K. G. and Colman, J. a (2003) 'Reactive-Transport Simulation of Phosphorus in the Sewage Plume at the Massachusetts Military Reservation, Cape Cod, Massachusetts', *Water-Resources Investigations Report 03-4017*.

Power, I. M. *et al.* (2007) 'Biologically induced mineralization of dypingite by cyanobacteria from an alkaline wetland near Atlin, British Columbia, Canada', *Geochemical Transactions*, 8, pp. 1–16. doi: 10.1186/1467-4866-8-13.

Renman, A. and Renman, G. (2010) 'Long-term phosphate removal by the calcium-silicate material Polonite in wastewater filtration systems', *Chemosphere*. Elsevier Ltd, 79(6), pp. 659–664. doi: 10.1016/j.chemosphere.2010.02.035.

Rivadeneyra, M. A. *et al.* (2004) 'Biomineralization of carbonates by Halobacillus trueperi in solid and liquid media with different salinities', *FEMS Microbiology Ecology*, 48(1), pp. 39–46. doi: 10.1016/j.femsec.2003.12.008.

Ronteltap, M., Maurer, M. and Gujer, W. (2007) 'Struvite precipitation thermodynamics in source-separated urine', *Water Research*, 41(5), pp. 977–984. doi: 10.1016/j.watres.2006.11.046.

Said, S. and Hussain, A. (2019) 'Pollution mapping of Yamuna River segment passing through Delhi using high-resolution GeoEye-2 imagery', *Applied Water Science*. Springer International Publishing, 9(3), pp. 1–8. doi: 10.1007/s13201-019-0923-y.

Sánchez-Román, M. *et al.* (2007) 'Biomineralization of carbonate and phosphate by moderately halophilic bacteria', *FEMS Microbiology Ecology*, 61(2), pp. 273–284. doi: 10.1111/j.1574-6941.2007.00336.x.

Siegrist, R. L. (2016) *Decentralized water reclamation engineering: A curriculum workbook*, *Decentralized Water Reclamation Engineering: A Curriculum Workbook*. doi: 10.1007/978-3-319-40472-1.

Smeck, N. E. (1985) 'Phosphorus dynamics in soils and landscapes', *Geoderma*, 36(3–4), pp. 185–199. doi: 10.1016/0016-7061(85)90001-1.

Smith, E. B. (2004) *Basic Chemical Thermodynamics*. Fifth Edit. London: Imperial College Press.

Song, Y., Hahn, H. H. and Hoffmann, E. (2002) 'Effects of solution conditions on the precipitation of phosphate for recovery: A thermodynamic evaluation', *Chemosphere*, 48(10), pp. 1029–1034. doi: 10.1016/S0045-6535(02)00183-2.

Stelt, B. van der, Temminghoff, E. J. M. and Riemsdijk, W. H. van (2005) 'Measurement of ion speciation in animal slurries using the Donnan Membrane Technique'. 83, , , 552(1–2), pp. 135–140. Available at: https://edepot.wur.nl/20651.

Stumm, W. and Morgan, J. J. (1996) 'Precipitation and dissolution', *Aquatic chemistry. Chemical Equilibra and Rates in Natural Waters*, 3, pp. 329–424.

Szabó, A. *et al.* (2008) 'Significance of Design and Operational Variables in Chemical Phosphorus Removal', *Water Environment Research*, 80(5), pp. 407–416. doi: 10.2175/106143008x268498.

Torres-Aravena, Á. *et al.* (2018) 'Can Microbially Induced Calcite Precipitation (MICP) through a Ureolytic Pathway Be Successfully Applied for Removing Heavy Metals from Wastewaters?', *Crystals*, 8(11), p. 438. doi: 10.3390/cryst8110438.

Trisal, C., Tabassum, T. and Kumar, R. (2008) 'Water quality of the River Yamuna in the Delhi stretch: Key determinants and management issues', *Clean - Soil, Air, Water*, 36(3), pp. 306–314. doi: 10.1002/clen.200700044.

UNEP (2016) *A Snapshot of the World's Water Quality: towards a global assessment*. Nairobi, Kenya. Available at: en.unesco.org/emergingpollutants.

Wanko, A. *et al.* (2016) 'Assessment of rock wool as support material for on-site sanitation: Hydrodynamic and mechanical characterization', *Environmental Technology (United Kingdom)*, 37(3), pp. 369–380. doi: 10.1080/09593330.2015.1069901.

Xu, K. *et al.* (2011) 'Simultaneous removal of phosphorus and potassium from synthetic urine through the precipitation of magnesium potassium phosphate hexahydrate', *Chemosphere*. Elsevier Ltd, 84(2), pp. 207–212. doi: 10.1016/j.chemosphere.2011.04.057.

van Zandvoort, R. (2018) *'Combi van stro en Drainblock in sloot is ideaal'*, *Nieuwe Oogst*. Available at: https://www.nieuweoogst.nl/nieuws/2018/07/03/combi-van-stro-en-drainblock-in-sloot-is-ideaal (Accessed: 16 January 2020).

8. Appendix

A. Theoretical Phosphorus Removal

In order to determine the conditions in which P can be chemical or biologically removed the following elements and biological P removal mechanism are looked into; calcium, aluminum and biological phosphorus removal. The parameters used to test for different conditions, such as the water composition, will be based upon wastewater composition of the Indian Drain Water (See section 3.4.2 tables 5 and 6). P removal through iron is not considered as possible removal mechanism as experiments show no iron release from the mineral wool when at a range of pH conditions.

For every P removal mechanism a potential treatment capacity was determined per 1 m^3 of mineral wool for the removal of 90% P from a wastewater containing 10mgP/l. This potential treatment capacity was set as standard measure for comparison, and a summary is provided in Section 0. The potential treatment capacity is based upon simplified calculations in which the component of time is not taken into consideration.

A. I. Coagulation: Aluminum

According to (Metcalf & Eddy Inc., 2003) and estimate on the addition of Aluminum for P removal by coagulation can be made with the following formula:

$$Al_{dose} = \left(\frac{Al}{P}\right)\left(C_{P,in} - C_{P,res}\right)\frac{\left[55.85\frac{g}{mole\ Al}\right]}{\left[30.97\frac{g}{mole\ P}\right]} \qquad (15)$$

Where $C_{P,in}$ is the initial P concentration and $C_{P,res}$ the desired final P concentration in the solution. Leading to the Graph 25 for different removal percentages at several P concentrations.

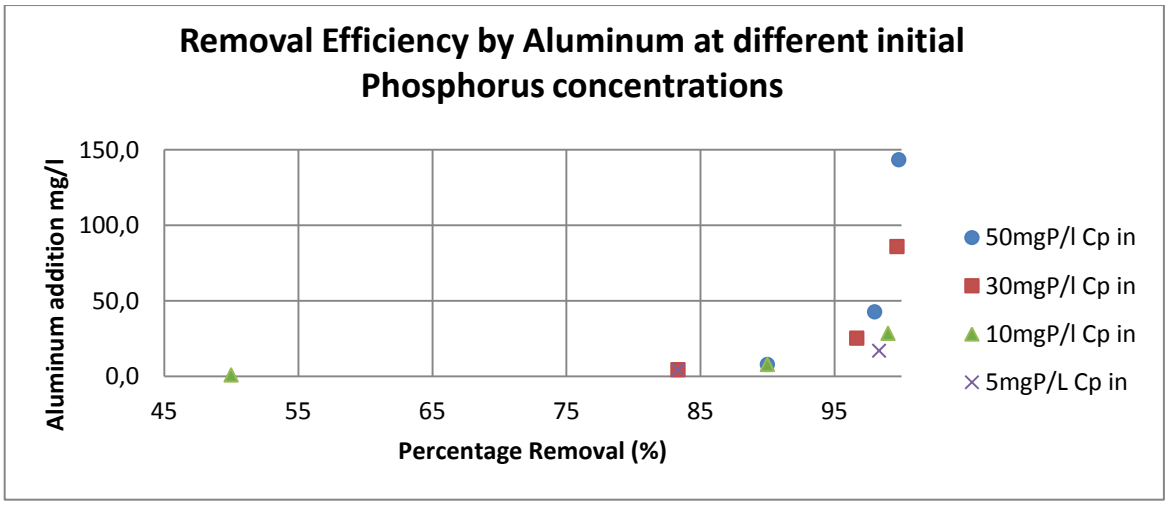

Graph 25, Phosphorus removal efficiency by aluminum at different initial phosphorus concentrations

Graph 25 illustrates that lower initial phosphorus concentrations need relatively less aluminum addition than solutions with high initial phosphorus concentration. When high removal efficiencies are desired, the aluminum addition required seems to increase almost exponentially.

As an example and for further comparison to other P removal mechanisms,

With the assumptions:

- The Al content of mineral wool is 80g/kg of mineral wool;
- The density of mineral wool is 120kg/m^3;
- All the Al in the mineral wool would dissolves and reacts with the P in the wastewater;
- A 90% P removal is desired to P content of 1 mgP/l;
- No interaction with other ions, organics or inorganics takes place;

the amount of aluminum needed is 7.8 mg/l to treat a liter of wastewater, thus the amount of wastewater that can be treated is about 1200 m^3 per cubic meter of mineral wool.

A. II. Precipitation with calcium

Optimal P precipitation with calcium can be calculated with use of the calcium phosphorus molar ratio. Every mineral phases has its specific molar ratio as defined in section 2.23. Thus, in the abundant presence of calcium and under perfect pH and temperature conditions, phosphate would theoretically precipitate up to 100% P removal.

For ATCP the molar ratio is 1.5 mol Ca per mol of P. Thus, at different ratio's full P removal can be achieved (Ca:P >1.5) or not (Ca:P <1.5). Table 18 shows the potential percentage of P removal at different C and P concentrations for ATCP.

Table 18 , Potential %P removal at different Ca:P molar ratio's assuming ATCP precipitation

	Phosphate (mg/l)			
Calcium (mg/l)	**10**	**30**	**50**	**70**
30	100	52	31	22
50	100	86	52	37
100	100	100	100	74
300	100	100	100	100

Assuming that:

- The calcium content in mineral wool is 180 gCa/kg of mineral wool
- The density of mineral wool is 120kg/m^3;
- A 90% P removal is desired to P content of 1 mgP/l;
- Only ATPC precipitation could take place;
- All Ca in the mineral wool dissolves and reacts with the P in the wastewater;
- No interaction with other ions, organics or inorganics takes place;

the amount of wastewater that can be treated by 1m^3 of mineral wool is 1240 m^3.

A. III. Biological Phosphorus Removal

According to (Metcalf & Eddy Inc., 2003) biomass production by ordinary heterotrophic bacteria consuming BOD may produce biomass with a P content of 0.015 gram P per gram VSS. In order

to achieve high P removal the biomass production needs to be high. Graph 26 illustrates the amount of biomass that needs to be produced to achieve a certain P removal efficiency (%).

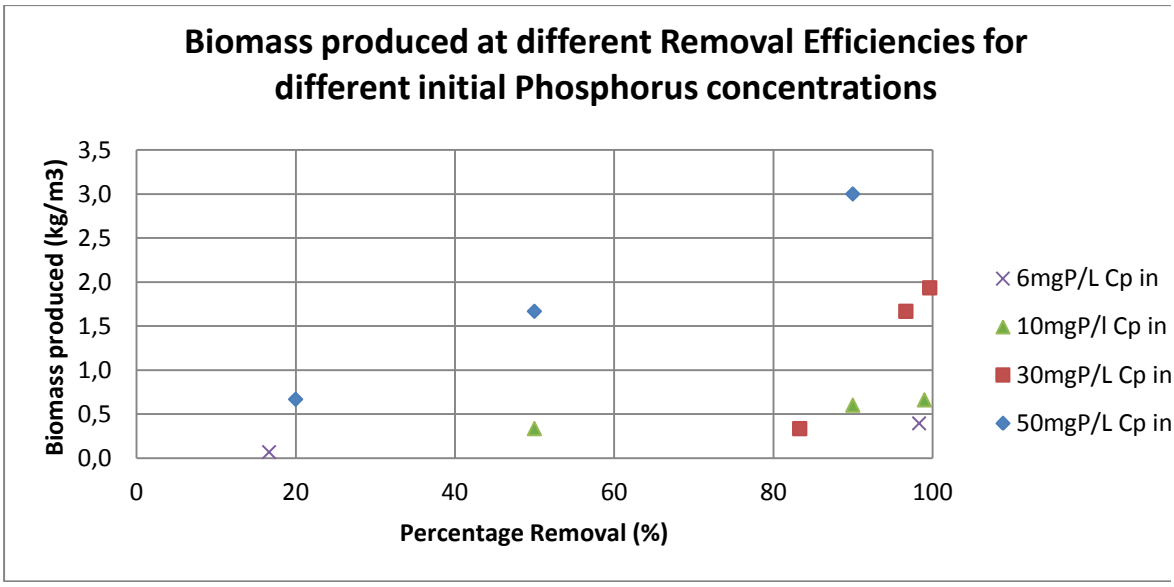

Graph 26, Biomass produced at different removal efficiencies for different initial phosphorus concentrations. Cp in, is the initial P concentration.

Based upon a preliminary study on the biomass content in mineral wool during nitrification and denitrification, the biomass density can be roughly estimated to be 15 kg per cubic meter of mineral wool (Dash, Zhang and Srinivas, 2019).

With the assumption that the biomass density is 15 kg/m^3 of mineral wool among these other assumption:

- 1 m^3 of mineral wool can hold 15kg of biomass (Dash, Zhang and Srinivas, 2019);
- Initial P concentration is 10mg/l;
- 90% of P is desired to be removed;
- thus 600g biomass produced per 1m^3 of treated water (from graph 2);

the amount of wastewater that can be treated is 27m^3 per cubic meter of mineral wool.

bCOD Consumption is necessary to achieve biomass production. By rearranging the formula 12 and following a few assumptions, an estimation can be made on how much bCOD is consumed for each P removal efficiency given its initial P concentration. The biomass produced can be quantified by :

$$Biomass\ produced\ = \left[\frac{Y}{1 + b(SRT)}\right] bCOD \qquad (16)$$

This formula takes into account the Bacteria Synthesis Yield, Y, the Endogenous decay coefficient, b, and the Solids Retention Time, SRT. Assuming: $Y = 0.45\ g\frac{VSS}{g}COD$, $b = 0.08\ g/g \cdot d$, $SRT = 5d$, the amount of bCOD that needs to be consumed to be able to produce the amount of biomass for specific P removal efficiencies can be calculated. The amount of bCOD needed in order to achieve a certain P removal efficiency is shown in Graph 27:

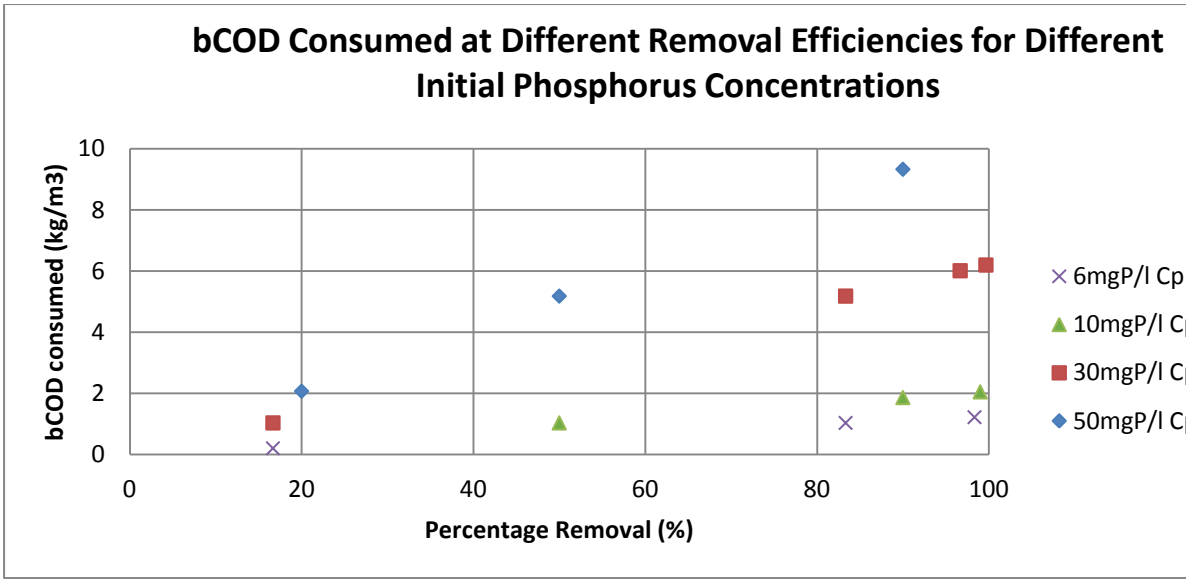

Graph 27, bCOD consumed at different removal efficiencies for different initial phosphorus concentrations.

Assuming that :

- Initial P concentration is 10mg/l;
- 90% of P is desired to be removed;
- thus 600g biomass produced per 1m3 of treated water (from graph 3);
- thus 27m^3 of wastewater can be treated per cubic meter of mineral wool;

the amount of bCOD that is to be consumed is 1900 g bCOD/m^3 of treated wastewater (Graph 27). However, the amount of COD per cubic meter present in the Barrapullah drain is between 115 and 1310 gCOD/m^3 with an average of 570 gCOD/m^3 (Lotus HR, 2018). Thus, it is not even taking into account the biodegradable fraction of the total COD in the drain water.

The theoretical calculations show that; (i) for low P content of 10mgP/l only 27m^3 of water can be treated per cubic meter of mineral wool to achieve 90% removal and (ii) for this removal efficiency and initial P content a higher bCOD concentration is needed than the maximum amount of COD measured. Considering these calculations biomass in the mineral wool is unlikely to have a significant effect on the P removal at high P concentrations.

A. IV. Bacterially Mediated Precipitation

With use of the biomass density of the mineral wool and the P content of biomass under similar conditions the amount of P removal through biologically induced precipitation can be calculated.

According to upflow anaerobic sludge blanket reactor (UASB) experiments run with Black water the P content of the biomass in the granular sludge reactor ranged from 144mgP/gVSS to 284mgP/gVSS (De Graaff, 2010). UASB experiments under high calcium concentration wastewaters (600mg-1200mg Ca/l, 30mgP/l) showed P-contents from 30 mgP/VSS up to 192 mgP/gVSS (van Langerak *et al.*, 1998). Both studies reported that precipitation and co-precipitation of Ca-P minerals took place.

As it is roughly estimated that 15kg of biomass can grow in one cubic meter of mineral wool and a range of P content per gram of VSS is known the amount of P per cubic meter of mineral can be determined. As done in the sections before: assuming 90% of P removal to 1 mgP/l, the biomass in 1 m^3 of mineral wool can contain 0,45 - 4,3 kg of P. Leading to the amount of wastewater that can be treated to be 50 to 473 m^3 per cubic meter of mineral wool.

A. V. Potential Removal Capacity of Mineral Wool

The potential treated volume of wastewater by 1 m^3 of mineral wool to obtain a P removal of 90% for a wastewater containing 10 mP/l was calculated for coagulation with aluminum, precipitation with calcium, biological phosphorus removal and biologically induced precipitation. A summary of the potential treatment capacity per 1 m^3 of mineral wool is given in the Table 19:

Table 19, Summary of the volume of wastewater that could potentially be treated when reducing the P content of water by 90% for a 10 mgP/l containing wastewater.

Method	Volume of treated water (m^3)
Al release from mineral wool	1200
Ca release from mineral wool	1240
P uptake in biomass	27
Bacterially mediated precipitation	50-473

As previously mentioned, these results are based on simplified calculations and ideal conditions apply, such as optimal calcium and aluminum release from the mineral wool, perfect kinetics, instant growth of mineral wool, single process in the absence of any interfering component, no component of time. These results give an indication of the potential of mineral wool to facilitate P removal if it were to release its Ca and Al subsequently precipitate with P in the wastewater.

B. Raw Data India Lotus

Overview of the chemical composition of Indian Drain water as reported by the (CPCB, 2006). These values were used in PHREEQC as input solution as well as the base for Lotus Like water used in the experiments.

Table 20, Chemical Composition of Yumanu River, Dehli (CPCB, 2006)

S. No.	Parameters	Minimum			Maximum		
		Value (mg/l)	Location	Year	Value (mg/l)	Location	Year
1.	Total Dissolved Solids	83	Hathnikund	2000	1357	Etawah	2002
2.	Chloride	2	Hathnikund Sonepat Kalanaur	2001	424	Agra d/s (½)	2005
3.	Sulphate	7	Etawah	2005	217	Nizamuddin Bridge	1999
4.	Sodium	6	Hathnikund Sonepat	2001 2003 2004	406	Agra d/s (¼)	2004
5.	Calcium	7	Kalanaur	2001	291	Agra d/s (½)	2005
6.	Magnesium	0.4	Sonepat	2004	77	Agra canal (½)	2004
7.	Total Hardness	46	Hathnikund	2005	792	Agra u/s	2005
8.	Alkalinity	40	Hathnikund	2000	425	Mazawali	2004 2005
9.	Phosphate	0.02	Palla	2005	2.00	Mathura u/s	2004
10.	Potassium	1.0	Hathnikund	2000	48	Agra D/s	1999

Table 21 shows the maximum measured concentrations in mmol/l.

Table 21, Conversion table between mg/l and mmol/l of the maximum measured concentrations of Yumanu River (CPCB, 2006)**. The P and NH_4 concentrations are set as in measured in** (Lotus HR, 2018)**.**

	P	NH4	K	Na	Mg	SO4	Cl	Ca
mg/l	30	29	48	406	77	217	1424	291
mmol/l	0.97	1,62	1,2	17.71	3.,18	2.26	40.29	7.28

C. Raw Data XRF

The results of the XRF for two mineral wool blocks that were powdered before measured.

X-RAY FACILITIES GROUP

Dr. Amarante Böttger *A.J.Bottger@tudelft.nl*
phone +31(0)1527·82243
Dhr. Ruud Hendrikx *R.W.A.Hendrikx@tudelft.nl*
Drs. Richard Huizenga *R.M.Huizenga@tudelft.nl*

Delft University of Technology, Faculty of 3mE
Department o+f Materials Science and Engineering
Mekelweg 2, NL-2628 CD Delft, the Netherlands, phone +31(0)1527·82255/89459

XRD identification of mineral wool samples

Author	:	Ruud Hendrikx
Date	:	22 feb 2019
Researcher	:	Nicole van Jaarsveld, CITG
Research question	:	Phase identification

Samples
The samples are blocks of mineral wool. The blocks were powdered by pressing in a pellet press. They were labeled : "NvJ 0.1" and " NvJ 0.2".

Specimens
The sample powder was deposited as a thin layer on a Si510 wafer.

Experimental
Instrument: Bruker D8 Advance diffractometer Bragg-Brentano geometry and Lynxeye position sensitive detector. Cu Kα radiation. Divergence slit V12, scatter screen height 5 mm, 45 kV 40 mA. Sample spinning. Detector settings LL 0.11 W 0.14.

Measurements
Coupled θ -2θ scan 10° - 110°, step size 0.040 ° 2θ, counting time per step 2 s.

Data evaluation
Bruker software DiffracSuite.EVA vs 5.0

Results
Figure 1 shows the measured XRD patterns in black and red, after background subtraction.The colored sticks give the peak positions and intensities of the possibly present phases, using the ICDD pdf4 database. Not all small peaks could be identified. The samples are amorphous, however some crystalline iron might be present.

sample	*compound*	
NvJ 0.1	amorhous	
NvJ 0.2	Fe	iron

Table 1.

D. Raw Data XRD

The experimental conditions of the XRD measurements and the results of the XRD measurement and of the mineral wool analysis

Materials Science and Engineering
TUDelft, Faculty of 3mE
Mekelweg 2
2628CD Delft, The Netherlands
Tel. 015 27 82244/89459
Email: R.W.A. Hendrikx@tudelft.nl

X- ray diffraction facilities

Experimental conditions:

For XRF analysis the measurements were performed with a Panalytical Axios Max WD-XRF spectrometer and data evaluation was done with SuperQ5.0i/Omnian software. 18/12/2015 09:37:03

20/02/2019 13:46:56

PANalytical

Quantification of sample N. v. Jaarsveld. sample "mineral wool Nv J0.1", 20feb19

Sum before normalization: 86.0 wt%

Normalised to: 100.0 wt%

Sample type: Pressed powder

Initial sample weight (g): 2.000

Weight after pressing (g): 2.500

Oxygen validation factor: 0.00

Correction applied for medium: No

Correction applied for film: No

Used Compound list: Oxides

Results database: omnian 4kw 27mm

Results database in: c:\panalytical\superq\userdata

	Compound Name	Conc. (wt%)	Absolute Error (wt%)
1	SiO2	39.546	0.1
2	CaO	23.602	0.1
3	Al2O3	15.982	0.1
4	MgO	9.339	0.09
5	Fe2O3	5.562	0.07
6	TiO2	1.994	0.04
7	Na2O	1.934	0.04
8	K2O	0.798	0.03
9	MnO	0.38	0.02
10	SO3	0.364	0.02
11	P2O5	0.17	0.01
12	SrO	0.066	0.008
13	CeO2	0.056	0.007
14	ZrO2	0.037	0.006
15	Cr2O3	0.037	0.006
16	BaO	0.032	0.005
17	V2O5	0.029	0.005
18	Cl	0.023	0.005
19	Rb2O	0.022	0.004
20	ZnO	0.009	0.003
21	NiO	0.008	0.003
22	CuO	0.007	0.002
23	Nb2O5	0.005	0.002

E. Dissolution of mineral wool pH - P matrix

The final concentration of the 'pH -P Matrix' tested vials for all measured elements. Performed 4 weeks long. 1 gram of mineral wool was inundated in vials with 180ml of solution.

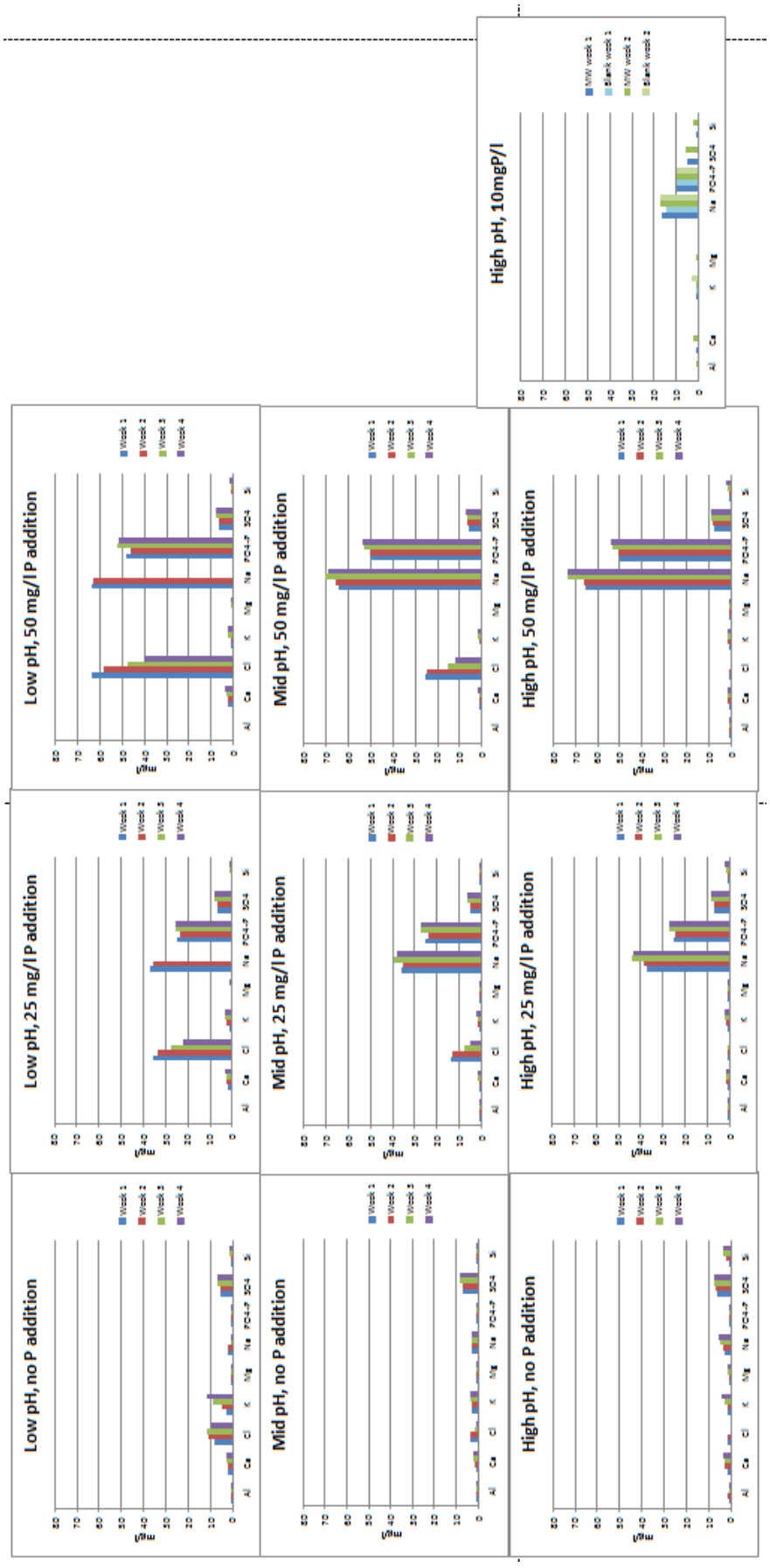

F. Powdered non Powdered mineral wool

The difference in dissolution of calcium and silicon from the mineral wool at high pH and 25 mgP/l for both mineral wool blocks and powdered form are shown in Graph F28 and Graph F29

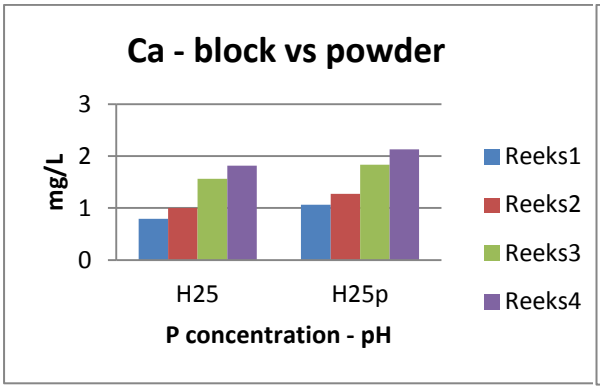

Graph F28 Calium release in four weeks time by mineral wool

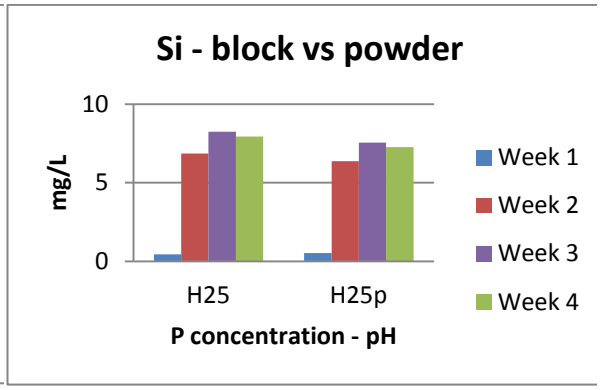

Graph F29 Silica release in four weeks time by mineral wool

G. Validation Results Ca and P removal

Graph 30, has been produced during the experiment for the validation of the PHREEQC model was used to estimate the amount of calcium still left in the stock solution used for Experiment II based upon the 6% P removal measured.

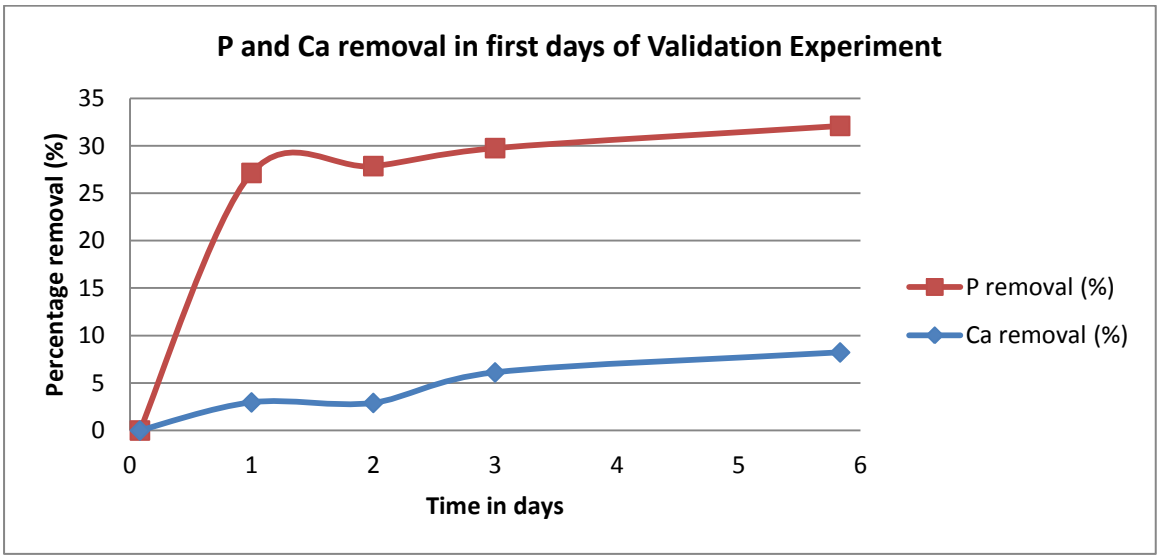

Graph 30, P and Ca removal(%) in first days of Validation Experiment

H. Composition Mineral Wools

Chemical composition (% weight) of mineral wools studied

	Glass wool[a]	Rock wool 1[a]	Superwool X607[a]	Traditional rock wool 2[a]	Electric arc furnace (EAF) slag[b]	Lapinus® 503K4, Rockwool [d]	Filtralite(R)[c]
SiO2	62–67	38-43	58.3	45.8	16	42.7	
Al2O3	1–4	16-19	1.3	14.9		18.5	
Fe2O3	0–1	5-8	0.1	8.4	33	7.7	
MgO	3	28-34	0.4	10.9	12	6.0	
CaO	7		38.7	14.3	30	20.5	
Na2O	16	2-5	0.3	2.0		2.2	
K2O1	1		0.1	1.0		0.6	
B2O3	3-6	-	-	-			
TiO2	-	<2	0.05	1.6		1.3	
P2O5	0-1	-	0.4	0.4		0.2	
MnO	-	-	-	<0.1		0.2	

[a](Campopiano *et al.*, 2014) on biosolubility and biopersitance of earth silicate wools. [b](Claveau-Mallet, Courcelles and Comeau, 2014) phosphorus removal by steel slag (granuale/aggregate material). [c]Filtralite(R) mineral based sorbent as phosphate filter (lightweight expanded clay aggregates). According to chemical analysis, the material contains: 269 g/kg silicon, 86.1 g/kg aluminum, 56.5 g/kg iron, 35.7 g/kg calcium and 28.3 g/kg magnesium. (Herrmann *et al.*, 2013) [d]Lapinus® 503K4 product data sheet Lapinus. Comparable compositon as mineral wool to be used in this research. (Source Email, Lapinus and Hydrorock)

The two rock wool samples showed an extremely low dissolution of calcium at pH 7.4 (Graph 1). At acid pH the contrary was true and Rock wool 1 released the greater amount of calcium (Graph 2). The high concentration of dissolved calcium in the solution at pH 7.4 and the phosphate in Gamble's solution caused calcium phosphate precipitates to form on the surface layers of the Super- wool X607 fibers. (Campopiano *et al.*, 2014).

I. PHREEQC

I. I. Phases

The phases and their thermodynamic properties added to the phreeqc.dat database were:

```
PHASES
# Defining phases that are not in the phreeqc.dat database:
ATCP            # Amorphous tricalcium phosphate: Ca3(PO4)2(am2)
(from Smith 2003, see Gustafsson 2008)
Ca3(PO4)2 = 3 Ca+2 + 2 PO4-3
log_k   -28.25
delta_h -87     #kJ/mol

DCPD            # CaHPO4:2H2O(s) from minteq database (from Smith
2003, see Herman 2013) Brusite
CaHPO4:2H2O = 1 Ca+2 + H+1 + 1 PO4-3 + 2 H2O
log_k   -18.995
delta_h 25      #kJ/mol

DCP             # CaHPO4 (from Smith 2003, see Gustafsson 2008)
Monetite
CaHPO4 = Ca+2 + PO4-3 +H+
log_k -19.28
delta_h 31      #kJ/mol

OCP             # Ca4H(PO4)3 (s) <--> 4Ca+2 + 3 PO4-3 + H+ (from
Christoffersen 1990, see Gustafsson 2008)
Ca4H(PO4)3 =  4 Ca+2 + 3 PO4-3 + H+
log_k   -47.95
delta_h -105    #kJ/mol


TCP             # Ca3(PO4)2 (s) = 3Ca+2 + 2PO4-3 (from
Christoffersen 1990, see Gustafsson 2008)
Ca3(PO4)2 = 3Ca+2 + 2PO4-3
log_k -25.5
delta_h   -94   #kJ/mol
```

```
Struvite
AmmHMgPO4:6H2O = Mg+2 + PO4-3 + AmmH+ + 6H2O
log_k   -13.46
delta_h 23.62 kcal      #kcal

K-Struvite
KMgPO4:6H2O = Mg+2 + PO4-3 + K+ + 6H2O
log_k -11.5
delta_h 14.53 kcal      #kcal

Na-Struvite
NaMgPO4:7H2O = Mg+2 + PO4-3 + Na+ + 7H2O
log_k -11.6
delta_h 96.28 kJ        #kJ

Fix_pH
   H+=H+
   logK 0
END
```

I. II. Dissolution in pH - P matrix

The ICPOES results of the dissolution of mineral wool following the 'pH - P matrix'. The results of the equilibrium phases and the saturation indices along with Ca and P concentrations are output to an Excel sheet for futher processing. Part of these results are depicted in Table 15.

```
SOLUTION SPREAD    1 # Week 4 results batch tests
-units  mg/l

Number  Al      Ca      Cl      K       Mg      Mn      Na      P       S(6)    Si      pH      temp    Alkalinity      Description
                                                                                                        as HCO3
1       0.38    3.06    9.19    11.40   1.00    0.05    2.42    0.01    6.80    1.70    4.62    23.40   8.27
2       0.09    3.02    21.83   3.45    0.94    0.05    38.40   25.65   7.82    1.26    4.55    23.40   9.36
3       0.11    3.49    40.12   2.63    1.12    0.06    69.26   51.95   8.09    1.52    4.66    23.40   12.33
4       0.04    2.32    0.24    3.67    0.78    0.03    3.00    0.02    8.64    1.13    6.64    23.40   15.85
5       0.01    1.75    4.87    2.02    0.60    0.02    38.13   26.96   6.35    0.64    7.02    23.40   44.91
6       0.01    1.69    11.98   1.67    0.56    0.02    69.34   53.94   7.06    0.61    7.04    23.40   75.36
7       0.63    3.18    0.00    4.20    1.19    0.02    5.20    0.02    7.74    3.22    7.80    23.40   29.35
8       0.35    1.82    0.00    2.21    0.73    0.01    43.13   26.90   8.24    2.06    8.31    23.40   74.62
9       0.35    1.69    0.00    1.73    0.69    0.01    73.75   54.07   9.02    2.07    8.55    23.40   125.46
10      0.33    2.13    0.00    1.84    0.79    0.01    44.91   27.10   7.55    2.27    8.36    23.40   83.30   powdered P25 - high pH
11      1.82    3.96    0.75    1.02    1.41    0.00    22.20   12.53   7.28    3.56    8.58    24.70   44.17   Decreasing volume P10 - high pH
12      1.49    3.22    1.14    1.30    1.15    0.00    23.81   12.59   8.62    2.99    8.79    24.70   43.91   Constant volume P10 - high pH
END
```

```
SELECTED OUTPUT 1
-file              2019_8_1_BatchTest.xls
-reset             false
-solution          true
-totals            P Ca
-pH                true
-SI                Hydroxyapatite ATCP DCPD DPC OCP TCP
-temp              true
-equilibrium_phases    ATCP DCPD DPC
END

RUN CELLS
-cells 1-12
END

EQUILIBRIUM_PHASES 1-12
ATCP                    0 0
DCPD                    0 0
DCP                     0 0
```

```
Struvite                0 0
 END

RUN CELLS
-cells 1-12
END
PRINT
-selected output        true
END
```

With the use of RUN_CELLS the 12 solutions as shown in the solution spread will be run, first without precipitation and afterwards with precipitation of ATCP, DCPD, DCP and Struvite. By using PRINT the selected output will be added for all run outputs.

I. III. Indian Drain Water

Solution input of Indian Drain Water

```
SOLUTION  1 Indian Drain Water
-units  mg/l
-temp    23          # Chiara
pH       7.2         # NOTE ALSO CHANGE Fix_pH #Afzal et al 2000 8.5,
L/Chi 7.6 mgP/l
P        30          # mgPO4-P/l Lotus/Chiara      30, 50 average, 15-
111 mgP/l
Amm      29          # mgN/l     Lotus/Chiara      average 28, 2-
104mgN/l
K        48          #48   CPCB 2006 2007 ## 22 #Afzal et al 2000,
Hudiara Drain June 1998, 22 mg/l
Na       406         #406  CPCB 2006 2007 ##250 # Afzal et al 2000,
Hudiara Drain india-pakistan June 1998, 255mg/l
Mg       77          #77   CPCB 2006 2007 ##  Afzal et al 2000,
Hudiara Drain June 1998, 24mg/l
S(6)     217         #217  CPCB 2006 2007
Cl       1000        #1424 CPCB 2006 2007
Ca       291         #291  CPCB 2006 2007 ## 56 Afzal et al 2000,
Hudiara Drain June 1998, 56mg/l
Alkalinity     452       #mg/l as HCO3-
SAVE Solution 1
END

SOLUTION  2
-units  mg/l
-temp    23          # Chiara
pH       6.8         # NOTE ALSO CHANGE Fix_pH #Afzal et al 2000 8.5,
L/Chi 7.6 mgP/l
P        30          # mgPO4-P/l Lotus/Chiara      30, 50 average, 15-
111 mgP/l
Amm      29          # mgN/l     Lotus/Chiara      average 28, 2-
104mgN/l
K        48          #48   CPCB 2006 2007 ## 22 #Afzal et al 2000,
Hudiara Drain June 1998, 22 mg/l
Na       406         #406  CPCB 2006 2007 ##250 # Afzal et al 2000,
Hudiara Drain india-pakistan June 1998, 255mg/l
Mg       77          #77   CPCB 2006 2007 ##  Afzal et al 2000,
Hudiara Drain June 1998, 24mg/l
S(6)     217         #217  CPCB 2006 2007
Cl       1424        #1424 CPCB 2006 2007
Ca       291         #291  CPCB 2006 2007 ## 56 Afzal et al 2000,
Hudiara Drain June 1998, 56mg/l
Alkalinity     452
SAVE SOLUTION  2
END
```

```
SOLUTION 4
-units  mg/l
-temp    23          # Chiara
pH       8.8         # NOTE ALSO CHANGE Fix_pH #Afzal et al 2000 8.5,
L/Chi 7.6 mgP/l
P        30          # mgPO4-P/l Lotus/Chiara      30, 50 average, 15-
111 mgP/l
Amm      29          # mgN/l     Lotus/Chiara      average 28, 2-
104mgN/l
K        48          #48   CPCB 2006 2007 ## 22 #Afzal et al 2000,
Hudiara Drain June 1998, 22 mg/l
Na       406         #406  CPCB 2006 2007 ##250 # Afzal et al 2000,
Hudiara Drain india-pakistan June 1998, 255mg/l
Mg       77          #77   CPCB 2006 2007 ##  Afzal et al 2000,
Hudiara Drain June 1998, 24mg/l
S(6)     217         #217  CPCB 2006 2007
Cl       1424        #1424 CPCB 2006 2007
Ca       291         #291  CPCB 2006 2007 ## 56 Afzal et al 2000,
Hudiara Drain June 1998, 56mg/l
Alkalinity     452
SAVE SOLUTION 4
END
```

Temperature settings

```
REACTION_TEMPERATURE 1
5.0 35.0 in 14 steps #increase in temperature by degree Celcius
END

REACTION_TEMPERATURE 10
10
END

REACTION TEMPERATURE 15
15
END

REACTION TEMPERATURE 25
25
END
```

Reactions, dosing of NaOH and HCl

```
REACTION 1  #NaOH Addition
NaOH
0.0 0.004 0.004 0.006 0.006 0.008 0.008 0.01 0.03 0.03 0.03 0.03
#003 0.003 0.003 0.004 0.004 0.005 0.01        #increases the pH in
```

```
14 steps by adding a total of 1.4M NaOH
END

REACTION 2 #HCl Addition
HCl
0.0 0.004 0.004 0.006 0.006 0.008 0.008 0.01 0.01
END
```

The different forced precipitation phases at fixed and non fixed pH

```
EQUILIBRIUM_PHASES 1     #pH 6.8
ATCP                     0 0
DCPD                     0 0
DCP                      0 0
Struvite                 0 0
Fix pH                   -6.8 HCl #10
-force
Halite                   -10  10
END

EQUILIBRIUM_PHASES 2     #pH 7.2
ATCP                     0 0
DCPD                     0 0
DCP                      0 0
Struvite                 0 0
Fix_pH                   -7.2  HCl #10
-force
Halite                   -20  20
END

EQUILIBRIUM_PHASES 3     #pH 7.8
ATCP                     0 0
DCPD                     0 0
DCP                      0 0
Struvite                 0 0
Fix_pH                   -7.8  HCl #10
-force
Halite                   -20  20
END

EQUILIBRIUM_PHASES 4     #pH 8.8
ATCP                     0 0
DCPD                     0 0
DCP                      0 0
Struvite                 0 0
Fix pH                   -8.8  HCl #10
-force
Halite                   -20  20
```

```
END

EQUILIBRIUM_PHASES 15    #4 minerals non-fixed pH X
ATCP                     0 0
DCPD                     0 0
DCP                      0 0
Struvite                 0 0
END
```

Graph development for SI of all minerals without precipitation at pH 6.8 and pH 8.8 (Graph 6A and B)

```
#Graph showing SI of all minerals, no precipitation
USE SOLUTION 2                          #pH 6.8
USE REACTION TEMPERATURE 1              #5 to 35degC
USER_GRAPH 2  SIall_noPrecip_68_LotusT.png
-active                 True
-batch G2a_SIall_noPrecip_68_LotusT.png False True
-headings Temperature   DCPD DCP ATCP Struvite OCP TCP HAP
-axis_titles            "Temperature (C)" "SI (-)"
-chart_title            "Saturation Index vs. Temperature (pH6.8)"
-initial_solutions      false
-axis_scale x_axis      5 35            # X Temperature
-axis_scale y_axis      auto auto       # Y SI
-connect_simulations    true
-start
20 GRAPH_X TC
30 GRAPH_Y SI ("DCPD")
45 GRAPH_Y SI ("DCP")
50 GRAPH_Y SI ("ATCP")
60 GRAPH_Y SI ("Struvite")
70 GRAPH_Y SI ("OCP")
80 GRAPH_Y SI ("TCP")
90 GRAPH_Y SI ("Hydroxyapatite")
  -end
END
USER GRAPH 2
-detach

USE SOLUTION 4                          #pH 8.8
USE REACTION TEMPERATURE 1
USER GRAPH 2    SIAll NOPrecip 88 LotusT.png
-batch G2b_SIall_noPrecip_88_LotusT.png  False True
-active                 True
-headings Temperature   DCPD DCP ATCP Struvite OCP TCP HAP
-axis_titles            "Temperature (C)" "SI (-)"
-chart_title            "Lotus: Saturation Index vs. Temperature
(pH8.8)"
```

```
-initial_solutions       false
-axis_scale x_axis       5 35            # X Temperature
-axis_scale y_axis       auto auto       # Y SI
-connect_simulations     true
-start
20 GRAPH_X TC
30 GRAPH_Y SI ("DCPD")
45 GRAPH_Y SI ("DCP")
50 GRAPH_Y SI ("ATCP")
60 GRAPH_Y SI ("Struvite")
70 GRAPH_Y SI ("OCP")
80 GRAPH_Y SI ("TCP")
90 GRAPH_Y SI ("Hydroxyapatite")
  -end
END
USER_GRAPH 2
-detach
```

Graph showing all SI of 4 minerals at equilibrium phases and P removal. (Graph 8A)

```
#Graph showing all SI of 4 minerals at equilibrium_phases and P
removal.
USE SOLUTION 1                          #pH 7.2
USE REACTION TEMPERATURE 1
USE EQUILIBRIUM PHASES 1                #6.8
USER_GRAPH 4 SI4_Precip6.8F_Prem_LotusT.png         #Shows the P
removal at different temperatures and the SI values of the
corresponding phases
-active                 True
-batch G4a_SI4_Precip6.8F_Prem_LotusT.png  False True
-headings                Temperature DCPD DCP ATCP Struvite P-
removal6.8
-axis_titles            "Temperature (C)" "SI (-)" "P-removal (%) "
-chart_title            "Saturation Index vs. Temperature with
precipitation, 4 minerals"
-initial_solutions      false
-axis_scale x_axis       5 35           #Temperature
-axis_scale y_axis       -4 1           #SI
-axis_scale sy_axis     50 100,         #P removal %
-connect_simulations    true
-start
110 GRAPH_X TC                          #TC temperature in Celcius
130 GRAPH_Y SI("DCPD")
140 GRAPH_Y SI("DCP")
150 GRAPH_Y SI("ATCP")
160 GRAPH_Y SI("Struvite")
190 P0  = 9.714e-04                     #initial amount of P
200 GRAPH_SY ((P0-tot("P"))/P0)*100     #%P removal
  -end
END
USER_GRAPH 4
-detach
```

Graph showing all SI of 4 minerals at equilibrium phases and P removal. (Graph 8B)

```
USE SOLUTION 1                          #pH 7.2
USE REACTION TEMPERATURE 1              #5 to 35degC
USE EQUILIBRIUM_PHASES 4                #8.8
USER_GRAPH 4 SI4_Precip8.8F_Prem_LotusT.png #Shows the P removal at
different temperatures and the SI values of the corresponding phases
-active                 False
-batch G4b_SI4_Precip8.8F_Prem_Lotus.png  False True
-headings                Temperature DCPD DCP ATCP Struvite P-
removal8.8
-axis_titles            "Temperature (C)" "SI (-)" "P-removal (%)"
-chart_title            "Saturation Index vs. Temperature with
precipitation, 4 minerals"
-initial_solutions      false
-axis_scale x_axis       5 35           #Temperature
-axis_scale y_axis       -4 1           #SI
-axis_scale sy_axis      50 100,        #P removal %
-connect_simulations    true
-start
110 GRAPH_X TC                          #TC temperature in Celcius
130 GRAPH_Y SI("DCPD")
140 GRAPH_Y SI("DCP")
150 GRAPH_Y SI("ATCP")
160 GRAPH_Y SI("Struvite")
190  P0  = 9.714e-04                    #initial amount of P
200 GRAPH_SY ((P0-tot("P"))/P0)*100     #%P removal
  -end
END
USER_GRAPH 4
-detach
```

Graph 12, P removal (%) at fixed and non fixed pH, where the initial pH is set to 7.2. The course of the P removal changes as temperature increases.

```
### Constant pH versus changing pH
# P removal at fixed and non fixed pH"
USE SOLUTION 1                          #pH 7.2
USE REACTION_TEMPERATURE 1              #5 to 35degC
```

```
USE EQUILIBRIUM PHASES 2                #4 minerals Fixed pH 7.2
USER GRAPH 5 Prem FpH nFpH LotusT.png
-active                  True
-batch G5_Prem_FpH_LotusT.png  False True
 -headings               %P-removalF Temperature pHF
 -axis_titles            "Temperature (C)" "P-removal (%) " "pH" #
 -initial_solutions      false
 -chart_title            "P removal at fixed and non fixed pH,
initial pH 7.2 "
  -connect_simulations   true
 -axis_scale x_axis       5 35           # TC
 -axis_scale y_axis       50 100         # %P removal
 -axis_scale sy_axis      5 8            # pH
 -start
05 P0  = 9.714e-04
10 Na0 = 1.771e-02
15 Cl0 =4.029e-02                       # initial P in moles
20 pH = -LA("H+")
40 GRAPH_X   TC                         # Temperature
30 GRAPH_Y  ((P0-tot("P"))/P0)*100      # P removal in %
50 GRAPH_SY  pH                         # pH
 -end
END

# non Fixed pH "
USE SOLUTION 1                          #7.2
USE REACTION_TEMPERATURE 1
USE EQUILIBRIUM PHASES 15               #4 minerals non fixed pH X
USER GRAPH 5
-headings  Temperature %P-removalnF pHnF
-start
05 P0  = 9.714e-04                      # initial P in moles
20 pH = -LA("H+")                       # definition of pH
30 GRAPH X   TC                         # Temperature
40 GRAPH Y  ((P0-tot("P"))/P0)*100      # P removal in %
50 GRAPH_SY  pH                         # pH
 -end
END
 USER GRAPH 5
 -detach
```

Graph 11, Graphical representation of the course of P removal (%) with increasing temperature for different pH conditions.

```
## P removal with fixed pH and with 4 Minerals precipitating at same
time
USE SOLUTION  1
USE REACTION TEMPERATURE 1
```

```
USE EQUILIBRIUM PHASES 1                #pH Fix 6.8
USER GRAPH 7 Prem FpH 4pH LotusT.png    #Shows the P removal at
different temperatures and the SI values of the corresponding phases
-active                  True
-batch G7_Prem_FpH_4pH_LotusT.png  False True
-headings                Temperature  pH6.8 pH7.2 pH7.8  pH8.8 #
Struvite  #OCP TCP HAP
-axis_titles             "Temperature (C)" "P-removal (%)"
-chart_title             "Lotus Like Water %P-removal with
Temperature, pH fixation"
-initial_solutions       false
-axis_scale x_axis       5 35           #Temperature
-axis_scale y_axis       50 100         #P removal %
-connect_simulations     false
-active                  true           #true or false, to publish
graph or not
-start
10 GRAPH X TC                           #TC temperature in Celcius
20 P0  = 9.714e-04                      #initial amount of P
30 GRAPH_Y ((P0-tot("P"))/P0)*100       #%P removal
  -end
END

USE SOLUTION  1
USE EQUILIBRIUM_PHASES 2                #pH Fix 7.2
USE REACTION_TEMPERATURE 1
USER_GRAPH 7                            #Shows the P removal at
different temperatures and the SI values of the corresponding phases
-start
10 P0 = 9.714e-04                       #initial amount of P
20 plot_xy TC, ((P0-tot("P"))/P0)*100,  #TC temperature in Celcius,
%P removal
-end
END

USE SOLUTION  1
USE EQUILIBRIUM_PHASES 3                #pH Fix 7.8
USE REACTION_TEMPERATURE 1
USER GRAPH 7     #Shows the P removal at different temperatures and
the SI values of the corresponding phases
-start
10 P0  = 9.714e-04                      #initial amount of P
20 plot_xy TC, ((P0-tot("P"))/P0)*100,  #TC temperature in Celcius,
%P removal
-end
END

USE SOLUTION  1
USE EQUILIBRIUM_PHASES 4                #pH Fix 8.8
```

```
USE REACTION TEMPERATURE 1
USER GRAPH 7                              #Shows the P removal at
different temperatures and the SI values of the corresponding phases
-start
10 P0  = 9.714e-04                        #initial amount of P
20 plot_xy TC, ((P0-tot("P"))/P0)*100,    #TC temperature in Celcius,
%P removal
-end
END
USER GRAPH 7
-detach
END
```

Graph 13, P removal (%) at fixed and non fixed pH, including the amount of HCL (%) removed which resembles the amount of NaOH released.

```
##
USE SOLUTION 2                            #6.8
USE REACTION_TEMPERATURE 1
USE EQUILIBRIUM_PHASES 1
 USER GRAPH 9 Prem HClrelease 68 LotusT.png
-active                  true
-batch G9_Prem_HClrelease_68_LotusT.png False True
 -headings               Temperature P-Fix Cl(P-Fix)
 -axis_titles            "Temperature (C)" "Percentage Removed (%)" #
 -initial_solutions      false
 -chart_title            "P removal at different temperatures at
constant pH (6.8)"
  -connect_simulations   true
 -plot_concentration_vs  x                # xy plot where dosage of
chemicals added are plotted versus x defined further below as
calculated P removal
 -axis_scale x_axis      5 35             # TC
 -axis_scale y_axis      auto auto        # %P removal
  -start
05 P0  = 9.714e-04                        # initial P in moles
10 Na0 = 2.346e-17                        # initial Na in moles
15 Cl0 = 4.029e-02                        # initial Cl in moles
20 pH = -LA("H+")
25 GRAPH_X   TC                           # Temperature
30 GRAPH_Y ((P0-tot("P"))/P0)*100         #%P removal
35 GRAPH_Y ((Cl0-tot("Cl"))/Cl0)*100      # FinalCl- Initial Cl
 -end
END

USE SOLUTION 2                            #pH 6.8
USE EQUILIBRIUM_PHASES 15                 #4 minerals nF pH
USE REACTION TEMPERATURE 1
```

```
USER GRAPH 9     #Shows the P removal at different temperatures and
the SI values of the corresponding phases
-headings                                 Temperature P-nFix
10 GRAPH_X TC                             #TC temperature in Celcius
20 P0  = 9.714e-04                        #initial amount of P
30 GRAPH Y ((P0-tot("P"))/P0)*100         #%P removal
END
USER GRAPH 9
-detach
```

Graph 7A and B

```
### pH VARIABILITY
USE SOLUTION 1
USE REACTION_TEMPERATURE 25
USE REACTION  1 #NaOH
USER_GRAPH 10   G10a_SI4_noPrecip_T25_LotuspH.png
-active True
-batch G10a_SI4_noPrecip_T25_LotuspH.png False True
-headings pH DCPD DCP ATCP Struvite
-axis_titles              "pH" "SI (-)"
-chart_title              "Saturation Index vs. pH, at 25 C"
-initial_solutions        false
-axis_scale x_axis        5 13     # X pH
-axis_scale y_axis        -6 6     # Y SI
-connect_simulations      true
-start
10 pH = -LA("H+")
20 GRAPH_X pH
30 GRAPH_Y SI ("DCPD")
45 GRAPH_Y SI ("DCP")
60 GRAPH_Y SI ("ATCP")
70 GRAPH_Y SI ("Struvite")
-end
END

USE SOLUTION 1
USE REACTION_TEMPERATURE 25
USE REACTION  2 #HCL
USER_GRAPH 10   G10a_SI4_noPrecip_T25_LotuspH.png
-headings                 pH DCPD DCP ATCP Struvite
-initial_solutions        false
-axis_scale x_axis        5 13     # X pH
-axis_scale y_axis        -6 6     # Y SI
-connect_simulations      false
-start
10 pH = -LA("H+")
20 GRAPH X pH                       #pH
30 GRAPH_Y SI ("DCPD")
```

```
45 GRAPH_Y SI ("DCP")
60 GRAPH_Y SI ("ATCP")
70 GRAPH_Y SI ("Struvite")
-end
END
USER GRAPH 10
-detach


USE SOLUTION 1
USE REACTION TEMPERATURE 10      # 10 degC
USE REACTION  1                  #NaOH
USER_GRAPH 10   G10b_SI4_noPrecip_T10_LotuspH.png
-active True
-batch G10b_SI4_noPrecip_T10_LotuspH.png False True
-headings               pH DCPD DCP ATCP Struvite
-axis_titles            "pH" "SI (-)"
-chart_title            "Saturation Index vs. pH, at 10 C"
-initial_solutions      false
-axis_scale x_axis      5 13     # X pH
-axis_scale y_axis      -6 6     # Y SI
-connect_simulations    true
-start
10 pH = -LA("H+")
20 GRAPH_X pH                    #pH
30 GRAPH_Y SI ("DCPD")
45 GRAPH_Y SI ("DCP")
60 GRAPH_Y SI ("ATCP")
70 GRAPH_Y SI ("Struvite")
-end
END

USE SOLUTION 1
USE REACTION TEMPERATURE 10      # 10 degC
USE REACTION  2                  # HCL
USER_GRAPH 10   G10b_SI4_noPrecip_T10_LotuspH.png
-headings               pH DCPD DCP ATCP Struvite
-initial_solutions      false
-axis_scale x_axis      5 13     # X pH
-axis_scale y_axis      -6 6     # Y SI
-connect_simulations    false
-start
10 pH = -LA("H+")
20 GRAPH_X pH                    #pH
30 GRAPH_Y SI ("DCPD")
45 GRAPH_Y SI ("DCP")
60 GRAPH_Y SI ("ATCP")
70 GRAPH_Y SI ("Struvite")
-end
```

```
END
USER GRAPH 10
-detach
```

Graph 9, Simultaneous precipitation of phosphorus minerals DCPD, DCP, ATCP and Struvite at different pH values for 25 °C, Indian Drain water.

```
USE SOLUTION 1
USE REACTION 1
USE EQUILIBRIUM PHASES 15       #4 minerals non-fixed pH X
USER GRAPH 11 G11 SI4 Prem Precip T25 LotuspH.png
-active True
-batch G11_SI4_Prem_Precip_T25_LotuspH.png False True
-headings pH  DCPD DCP  ATCP Struvite %P-removal #HAP TCP OCP
-axis_titles            "pH" "SI (-)" "P-removal (%)"
-chart_title            "P removal with Saturation Index vs. pH"
-initial_solutions      true
-axis_scale x_axis      5 13            # pH
-axis_scale y_axis      -6 1            # SI
-axis_scale sy_axis     0 100           # %P removal
-connect_simulations    true
  -start
10 pH = -LA("H+")
20 GRAPH_X pH
30 GRAPH_Y SI("DCPD")
40 GRAPH_Y SI("DCP")
50 GRAPH_Y SI("ATCP")
60 GRAPH_Y SI("Struvite")
70 P0  = 9.714e-04                      # initial P in moles
80 GRAPH_SY ((P0-tot("P"))/P0)*100,     # P removal in %
  -end
END

USE SOLUTION 1
USE REACTION 2
USE EQUILIBRIUM_PHASES 15       #4 minerals non-fixed pH X
USER GRAPH 11 G11 SI4 Prem Precip T25 LotuspH.png
-initial_solutions      true
-headings pH  DCPD DCP  ATCP Struvite %P-removal
-start
10 pH = -LA("H+")
20 GRAPH_X pH
30 GRAPH_Y SI("DCPD")
40 GRAPH_Y SI("DCP")
50 GRAPH_Y SI("ATCP")
60 GRAPH_Y SI("Struvite")
70 P0  = 9.714e-04                      # initial P in moles
80 GRAPH_SY ((P0-tot("P"))/P0)*100,     # P removal in %
```

```
  -end
END
USER_GRAPH 11
-detach
```

Graph 10, P removal by simultaneous precipitation at different pH values for 25°C, including the amount of NaOH and HCl added to fixate the pH, Indian Drain water.

```
USE SOLUTION  1
USE REACTION  1
USE REACTION TEMPERATURE 25
USE EQUILIBRIUM PHASES 15       #4 minerals non-fixed pH X
USER_GRAPH 12 G12_NaOH_Precip_T25_LotuspH.png
-active                 True
-batch G12_NaOH_noPrecip_T25_LotuspH.png False True
-headings %P-removal pH NaOH
-axis_titles            "pH" "P-removal (%)" "NaOH added (mol)" #
-initial_solutions      false
-chart_title "          P removal at different pH with NaOH dosing,
at Temp 10 and 25"
-connect_simulations    true
-axis_scale x_axis      5 13            # pH
-axis_scale y_axis      0 100           # %P removal
-axis_scale sy_axis     0 auto          # NaOH added in M
-start
05 P0  = 9.714e-04                      # initial P in moles
10 Cl0 = 2.828e-02                      # initial Cl in moles
20 pH = -LA("H+")
30 GRAPH Y    ((P0-tot("P"))/P0)*100    # P removal in %
40 GRAPH_X    pH
50 GRAPH_SY  ((tot("Na")-NaO))          # NaOH added in M retrieved
from increase in Na in solution
 -end
END

USE SOLUTION 1
USE REACTION_TEMPERATURE 25     # 25 deg C
USE EQUILIBRIUM_PHASES 15       #4 minerals non-fixed pH X
USE REACTION 2                  #HCL
USER GRAPH 12
-headings %P-removal pH NaOH
-start
05 P0  = 9.714e-04                      # initial P in moles
10 Cl0 = 2.828e-02                      # initial Cl in moles
20 pH = -LA("H+")
30 GRAPH Y    ((P0-tot("P"))/P0)*100    # P removal in %
40 GRAPH_X    pH
```



```
50 GRAPH SY   ((tot("Cl")-Cl0))
 -end
END
USER_GRAPH 12
-detach
```

Explanation Halite in Equilibrium Phase according to (Parkhurst, 2019)

"You put "Halite -20 10" so that there would be a little Cl- available to make the HCl reactant. You made the target saturation index strongly negative so that only a little Cl- and Na+ could be there, just enough to provide the necessary Cl-. Since K is being used to balance charge, its concentration can be reduced in order to allow a little Na+ to be in solution.

Adding the Halite equilibrium phase allows NaOH to be added instead of HCl if necessary to arrive at the specified pH.
If HCl is needed, HCl is added through the Fix_H+ reaction, and a tiny bit of NaCl dissolves to put enough Na+ in solution to have an SI of -20 for Halite.
If NaOH is needed, then NaCl dissolves and HCl is removed, leaving Na+ and OH- in solution.
Concentration of Cl wil be quite small to obtain the -20 SI.

NaCl + H2O = Na+ + OH- + HCl(l).
The (l) simply indicates it is removed from solution." - (Parkhurst, 2019)

Additional information on Fix_pH as explained by (Parkhurst, 2019)

"Fix_pH may not arrive at the correct pH when multiple minerals are defined in equilibrium phases. Use -force to require that the correct pH is attained." -(Parkhurst, 2019)

Graph 14, P removal (%) with temperature at different P concentrations including pH fixation at pH 7.2, temperature 23 °C. The P content in Indian Drain water is 30mgP/l.

```
USE SOLUTION 2                  #pH 7.2
USE REACTION TEMPERATURE 1
USE EQUILIBRIUM PHASES 2        #7.2
USER_GRAPH 19 SI4_Precip7.2F_Prem_LotusPO4T.png     #Shows the P removal
at different temperatures and the SI values of the corresponding phases
-active True
-batch G19_SI4_Precip7.2F_Prem_LotusPO4T.png  False True
 -headings                  Temperature  15mgP/l 30mgP/l 50mgP/l 70mgP/l
# Struvite  #OCP TCP HAP
 -axis_titles            "Temperature (C)" "P-removal (%)"
 -chart_title            "%P-removal with Temperature, for different P
concentrations, pH fixation"
 -initial_solutions       false
 -axis_scale x_axis      5 35                    #Temperature
 -axis_scale y_axis      50 100                  #P removal %
```

```
 -connect_simulations     false
 -active                  true                    #true or false, to
publish graph or not
 -start
110 GRAPH X TC                          #TC temperature in Celcius
190  P0  = 4.857e-04                    #initial amount of P
200 GRAPH Y ((P0-tot("P"))/P0)*100      #%P removal
   -end
END

USE SOLUTION  1
USE EQUILIBRIUM PHASES 2        #pH Fix 7.2
USE REACTION_TEMPERATURE 1
USER_GRAPH 19       #Shows the P removal at different temperatures and
the SI values of the corresponding phases
# 110 GRAPH X TC                        #TC temperature in Celcius
10  P0  = 9.714e-04                     #initial amount of P
20 plot_xy TC, ((P0-tot("P"))/P0)*100
# 200 GRAPH_Y ((P0-tot("P"))/P0)*100    #%P removal
-end
END

USE SOLUTION  3
USE EQUILIBRIUM PHASES 2        #pH Fix 7.2
USE REACTION_TEMPERATURE 1
USER_GRAPH 19       #Shows the P removal at different temperatures and
the SI values of the corresponding phases
# 110 GRAPH X TC                        #TC temperature in Celcius
10  P0  = 1.619e-03                     #initial amount of P
20 plot_xy TC, ((P0-tot("P"))/P0)*100
# 200 GRAPH_Y ((P0-tot("P"))/P0)*100    #%P removal
-end
END

USE SOLUTION  4
USE EQUILIBRIUM_PHASES 2        #pH Fix 7.2
USE REACTION_TEMPERATURE 1
USER_GRAPH 19       #Shows the P removal at different temperatures and
the SI values of the corresponding phases
-start
# 110 GRAPH_X TC                        #TC temperature in Celcius
10  P0  = 2.267e-03                     #initial amount of P
20 plot_xy TC, ((P0-tot("P"))/P0)*100,
# 200 GRAPH_Y ((P0-tot("P"))/P0)*100    #%P removal
-end
END

USER_GRAPH 19
-detach
```

```
END
```

Graph 15, %P removal with increasing CaCl2 at different pH concentrations, including pH fixation, temperature 23 °C. The Ca of Indian Drain water is 7.28 mmol/l

```
#Calcium addition
# Separate script with different SOLUTION and REACTION.
Solution 3 is lowered in Ca, Reaction 2 adds CaCl2.

SOLUTION  3 Lotus Water
-units   mg/l
-temp    23          # Chiara
pH       7.2         # Afzal et al 2000 8.5, Lotus/Chiara 7.6 mgP/l
P        30          # mgPO4-P/l Lotus/Chiara      30, 50 average, 15-111
mgP/l
Amm      29          # mgN/l     Lotus/Chiara     # average 28, 2-104mgN/l
K        48          #48   Taskeena Hassan ##  22 # Afzal et al 2000,
Hudiara Drain June 1998, 22 mg/l
Na       406         #406  Taskeena Hassan ## 255 # Afzal et al 2000,
Hudiara Drain india-pakistan June 1998, 255mg/l
Mg       77          #77   Taskeena Hassan ##  24 # Afzal et al 2000,
Hudiara Drain June 1998, 24mg/l
S(6)     217         #217  Taskeena Hassan
Cl       1424        #1424 Taskeena Hassan
Ca       0         #291  Taskeena Hassan ##  56 # Afzal et al 2000,
Hudiara Drain June 1998, 56mg/l
Alkalinity    452
END



REACTION 2
CaCl2.H2O
0.010 moles in 20 steps #   (1mg/l = 2.502e-05 )(56mg/l = 1.398e-03
mol/l) (291mg/l = 7.282e-03 mol/l) (400mg/l =  1.001e-02 mol/l)
END


USE SOLUTION 3
USE REACTION 2
USE EQUILIBRIUM_PHASES 1 #6.8
USER_GRAPH 14
-headings pH6.8 %P-removal  #NaOHmM
-active true
#-batch G14 Prem 4pH CALCIUM LotusCa.png  False True
-axis_titles  "CaCl2 added (mmol/L)" "P-Removal (%)" # "NaOH added
```

```
(mmol/L)" #
-initial_solutions false
-chart_title "P removal by Ca addition"
-plot_concentration_vs x                    # xy plot where dosage
of chemicals added are plotted versus x defined further below as
calculated P removal
-axis_scale x_axis       auto auto          # P removal in %
axis_scale y_axis        0 100              # CaCl2 added in mM

-start
05 P0  = 9.712e-04      #3.237e-05                  # initial P in
moles
10 Ca0 = 0                                  # initial Cl in moles
40 graph_x ((tot("Ca")-Ca0))*1000           # P removal in %
30 graph_y      ((P0-tot("P"))/P0)*100      #  CaCl2 added in mM
retrieved from increase in Cl in solution

-end
END

USE SOLUTION 3
USE REACTION 2
USE EQUILIBRIUM PHASES 2 #7.2
USER GRAPH 14
-headings       pH7.2 %P-removal
-initial_solutions false
-plot_concentration_vs x                    # xy plot where dosage
of chemicals added are plotted versus x defined further below as
calculated P removal
-axis_scale y_axis       0 100              # P removal in %
-axis_scale x_axis       auto auto          # CaCl2 added in mM
-start
05 P0  = 9.712e-04      #3.237e-05                  # initial P in
moles
10 Ca0 = 0                                  # initial Cl in moles
40 graph_x       ((tot("Ca")-Ca0))*1000             # P removal in %
30 graph_y      ((P0-tot("P"))/P0)*100      #  CaCl2 added in mM
retrieved from increase in Cl in solution
-end
END

USE SOLUTION 3
USE REACTION 2
USE EQUILIBRIUM_PHASES 3 #7.8
USER GRAPH 14
-headings       pH7.8 %P-removal
-plot_concentration_vs x                    # xy plot where dosage
of chemicals added are plotted versus x defined further below as
calculated P removal
```

```
-initial_solutions false
-axis_scale y_axis       0 100              # P removal in %
-axis_scale y_axis       auto auto          # CaCl2 added in mM
-start
05 P0  = 9.712e-04      #3.237e-05                  # initial P in
moles
10 Ca0 = 0                                  # initial Cl in moles
40 graph_x (    (tot("Ca")-Ca0))*1000       # P removal in %
30 graph_y      ((P0-tot("P"))/P0)*100      #  CaCl2 added in mM
retrieved from increase in Cl in solution
END

USE SOLUTION 3
USE REACTION 2
USE EQUILIBRIUM_PHASES 4 #8.8
USER GRAPH 14
-headings       pH8.8 %P-removal
-plot_concentration_vs x                    # xy plot where dosage
of chemicals added are plotted versus x defined further below as
calculated P removal
-initial_solutions false
-axis_scale y_axis       0 100              # P removal in %
-axis_scale x_axis       auto auto          # CaCl2 added in mM
-start
05 P0  = 9.712e-04      #3.237e-05
# initial P in moles
10 Ca0 = 0                                  # initial Cl in moles
30 graph_y      ((P0-tot("P"))/P0)*100      # P removal in %
40 graph_x      ((tot("Ca")-Ca0))*1000  # CaCl2 added in mM retrieved
from increase in Cl in solution
-end
END

USER GRAPH 14
-detach
END
```

I. IV. Black Water Analysis

The chemical composition of Black Water as implemented in phreeqc:

```
TITLE Nicole Black Water, Temperature & pH effect
#Black water composition as defined by De Graaff 2010.

SOLUTION  1 Black Water  @De Graaff 2010
-units  mg/l
-temp   23
pH      7.2         # 7.2
P       25          # 25 mgPO4-P/l
Amm     286         # 286 mgN/l
K       116         # 116 mg/l
Na      221         # 221 mg/l
Mg      24          # 24 mg/l  = 0.504mmoles
S(6)    31.6        # 31.6
Cl      246         # 246
N(5)    11.4        # 11.4
Ca      54.6        # 54.6 mg/l
Alkalinity    1525  as HCO3    #as HCO3 mg/l)
SAVE SOLUTION 1
END
```

The reaction temperatures used for Black Water Analysis

```
REACTION TEMPERATURE 1 #increase in temperature by degree Celcius
5.0 35.0 in 21 steps
END

REACTION_TEMPERATURE 10 #set temperature of 10 degC
10
END

REACTION_TEMPERATURE 15 #set temperature of 15 degC
15
END

REACTION TEMPERATURE 25 #set temperature of 25 degC
25
END
```

The reactions for the increase or decrease of pH for Black Water.

```
REACTION 1
NaOH
0.0 0.004 0.004 0.008 0.008 0.01 0.01 0.025 0.025 0.04 0.04 0.04
0.08 0.08 #increases the pH in 14 steps by adding a total of 1.4M
NaOH
END

REACTION 2
HCl
0.0 0.004 0.004 0.006 0.006 0.008 0.008 0.01 0.01 0.02 0.02 0.03
END
```

The equilibrium phases at different fixed pHs and non fixed pH for Black Water analysis

```
EQUILIBRIUM PHASES 1    #pH 6.8
ATCP                    0 0
DCPD                    0 0
DCP                     0 0
Struvite                0 0
#K-Struvite              0 0
#Na-Struvite             0 0
Fix_pH                  -6.8 HCl #10
-force
Halite                  -10  10
END

EQUILIBRIUM_PHASES 2    #pH 7.2
ATCP                    0 0
DCPD                    0 0
DCP                     0 0
Struvite                0 0
Fix pH                  -7.2  HCl #10
-force
Halite                  -20  20
END

EQUILIBRIUM PHASES 3    #pH 7.8
ATCP                    0 0
DCPD                    0 0
DCP                     0 0
Struvite                0 0
Fix pH                  -7.8  HCl #10
-force
Halite                  -20  20
END
```

```
EQUILIBRIUM PHASES 4     #pH 8.8
ATCP                     0 0
DCPD                     0 0
DCP                      0 0
Struvite                 0 0
Fix pH                   -8.8  HCl #10
-force
Halite                   -20  20
END

EQUILIBRIUM PHASES 15    #4 minerals non-fixed pH X
ATCP                     0 0
DCPD                     0 0
DCP                      0 0
Struvite                 0 0
END
```

Graph 17, Saturation Index of minerals for increasing temperature at pH 8.8.

```
USE SOLUTION 1
USE REACTION TEMPERATURE 1              # 5 to 25 degC
USER GRAPH 2     SIAll NOPrecip 88 BWT.png
-batch G2b_SIall_noPrecip_88_BWT.png  False True
-active True
-headings Temperature  DCPD DCP ATCP Struvite HAP
-axis_titles            "Temperature (C)" "SI (-)"
-chart_title            "Black Water: Saturation Index vs.
Temperature (pH8.8)"
-initial_solutions      false
-axis_scale x_axis      5 35    # X Temperature
-axis_scale y_axis     auto auto        # Y SI
-connect_simulations    true
-start
20 GRAPH X TC
30 GRAPH_Y SI ("DCPD")
45 GRAPH_Y SI ("DCP")
50 GRAPH_Y SI ("ATCP")
60 GRAPH_Y SI ("Struvite")
90 GRAPH_Y SI ("Hydroxyapatite")
  -end
END
USER_GRAPH 2
-detach
```

Graph 18, Saturation Index of minerals for increasing pH at temperature 25 °C.

```
USE SOLUTION 1
USE REACTION  1
USE REACTION_TEMPERATURE 25
USER_GRAPH 10   G10b_SI4_noPrecip_T25BWpH.png
-active true
-batch G10b_SI4_noPrecip_T25_BWpH.png False True
-headings pH DCPD DCP ATCP Struvite
-axis_titles            "pH" "SI (-)"
-chart_title            "Black Water: SI vs. pH, at 25 °C"
-initial_solutions      false
-axis_scale x_axis      5 13            # X pH
-axis_scale y_axis      -6 6            # Y SI
-connect_simulations    true
-start
10 pH = -LA("H+")
20 GRAPH_X pH
30 GRAPH_Y SI ("DCPD")
45 GRAPH_Y SI ("DCP")
60 GRAPH_Y SI ("ATCP")
70 GRAPH_Y SI ("Struvite")
-end
END

USE SOLUTION 1
USE REACTION  2
USE REACTION TEMPERATURE 25
USER_GRAPH 10  G10b_SI4_noPrecip_T25_BWpH.png
-headings pH DCPD DCP ATCP Struvite
-initial_solutions      false
-connect_simulations    false
-start
10 pH = -LA("H+")
20 GRAPH_X pH
30 GRAPH_Y SI ("DCPD")
45 GRAPH_Y SI ("DCP")
60 GRAPH_Y SI ("ATCP")
70 GRAPH_Y SI ("Struvite")
-end

END
USER GRAPH 10
-detach
```

Graph 19, SI of Black water at pH 8.8 for increasing temperature

```
USE SOLUTION 1                          #pH 7.2
USE REACTION TEMPERATURE 1              # 5 to 25 degC
USE EQUILIBRIUM PHASES 4                #8.8 pH fixed
USER GRAPH 5 G5 SI6 Precip8.8F Prem BWT.png         # Shows the P
removal at different temperatures and the SI values of the
```

```
corresponding phases
-active True                                          #
-batch G5_SI6_Precip8.8F_Prem_BWT.png  False True    # name of png
output
-headings                Temperature DCPD DCP ATCP Struvite P-
removal8.8
-axis_titles            "Temperature (C)" "SI (-)" "P-removal (%)"
-chart_title            "Black Water: SI vs. Temperature with
precipitation, pH 8.8"
-initial_solutions      false
-axis_scale x_axis       5 35           #Temperature
-axis_scale y_axis       -4 1           #SI
-axis_scale sy_axis     0 100,  #P removal %
-connect_simulations    true
-start
110 GRAPH X TC                          #TC temperature in Celcius
130 GRAPH_Y SI("DCPD")
140 GRAPH_Y SI("DCP")
150 GRAPH_Y SI("ATCP")
160 GRAPH_Y SI("Struvite")
190 P0  = 8.092e-04                     #initial amount of P
200 GRAPH SY ((P0-tot("P"))/P0)*100     #%P removal
  -end
END
USER_GRAPH 5
-detach
```

Graph 20, Percentage P removal with increasing temperature under fixed pH conditions for Black Water, forcing precipitation.

```
## P removal with fixed pH and with all Minerals precipitating at
same time
USE SOLUTION  1
USE EQUILIBRIUM_PHASES 1                #pH Fix 6.8
USE REACTION_TEMPERATURE 1              #5 to 25degC
USER_GRAPH 7 G7_Prem_FpH_4pH_BWT.png #Shows the P removal at
different temperatures and the SI values of the corresponding phases
-active True
-batch G7_Prem_FpH_4pH_BWT.png  False True      # name png output
-headings               Temperature  pH6.8 pH7.2 pH7.8  pH8.8
-axis_titles            "Temperature (C)" "P-removal (%)"
-chart_title            "Black Water: %P-removal with Temperature,
pH fixation"
-initial_solutions      false
-axis_scale x_axis      5 35           #Temperature
-axis_scale y_axis      0 100          #P removal %
-connect_simulations    false
```

```
-active                  true           #true or false, to publish
graph or not
-start
10 GRAPH_X TC                           #TC temperature in Celcius
20 P0  =   8.092e-04                    #initial amount of P
30 GRAPH Y ((P0-tot("P"))/P0)*100       #%P removal
   -end
END

USE SOLUTION  1
USE REACTION TEMPERATURE 1
USE EQUILIBRIUM PHASES 2                #pH Fix 7.2
USER_GRAPH 7                            #Shows the P removal at
different temperatures and the SI values of the corresponding phases
10 P0  =   8.092e-04                    #initial amount of P
20 plot_xy TC, ((P0-tot("P"))/P0)*100   #TC temperature in Celcius,
%P removal
-end
END

USE SOLUTION  1
USE REACTION TEMPERATURE 1
USE EQUILIBRIUM PHASES 3                #pH Fix 7.8
USER GRAPH 7                            #Shows the P removal at
different temperatures and the SI values of the corresponding phases
10 P0  =   8.092e-04                      #initial amount of P
20 plot_xy TC, ((P0-tot("P"))/P0)*100   #TC temperature in Celcius,
%P removal
-end
END

USE SOLUTION  1
USE REACTION TEMPERATURE 1
USE EQUILIBRIUM PHASES 4                #pH Fix 8.8
USER GRAPH 7                            #Shows the P removal at
different temperatures and the SI values of the corresponding phases
-start
10 P0  =   8.092e-04                    #initial amount of P
20 plot_xy TC, ((P0-tot("P"))/P0)*100   #TC temperature in Celcius,
%P removal
-end
END
USER_GRAPH 7
-detach
END
```

Graph 21, Simultaneous precipitation of phosphorus minerals DCPD,

DCP, ATCP, and Struvite at 25 °C, Black Water

```
USE SOLUTION 1
USE REACTION 1
USE EQUILIBRIUM PHASES 15
USER_GRAPH 11 G11_SI4_Prem_Precip_T25_BWpH.png
-active True
-batch G11_SI4_Prem_Precip_T25_BWpH.png False True
-headings pH  DCPD DCP  ATCP Struvite %P-removal
-axis_titles             "pH" "SI (-)" "P-removal (%)"
-chart_title             "Black Water: P removal with SI vs. pH, Temp
25 C"
-initial_solutions       true
-axis_scale x_axis       5 13            # pH
-axis_scale y_axis       -6 1            # SI
-axis_scale sy_axis      0 100           # %P removal
-connect_simulations     true
-start
10 pH = -LA("H+")
20 GRAPH_X pH
30 GRAPH_Y SI("DCPD")
40 GRAPH_Y SI("DCP")
50 GRAPH_Y SI("ATCP")
60 GRAPH_Y SI("Struvite")
70 P0  =  8.092e-04
80 GRAPH_SY ((P0-tot("P"))/P0)*100,     # P removal in %
  -end
END

USE SOLUTION 1
USE REACTION 2
USE EQUILIBRIUM PHASES 15
USER_GRAPH 11 G11_SI4_Prem_Precip_T25_BWpH.png
-headings pH  DCPD DCP ATCP Struvite %P-removal
-initial_solutions       true
-connect_simulations    false
-start
10 pH = -LA("H+")
20 GRAPH_X pH
30 GRAPH_Y SI("DCPD")
40 GRAPH_Y SI("DCP")
50 GRAPH_Y SI("ATCP")
60 GRAPH_Y SI("Struvite")
70 P0  =  8.092e-04
80 GRAPH_SY ((P0-tot("P"))/P0)*100,     # P removal in %
  -end
END

USER_GRAPH 11
-detach
```

Graph 22, P removal by simultaneous precipitation at different pH for 25°C, including the amount of NaOH and HCl added to fixate the pH, Black Water.

```
USE SOLUTION  1
USE REACTION  1
USE REACTION_TEMPERATURE 25
USE EQUILIBRIUM_PHASES 15
 USER_GRAPH 12 G12_NaOH_noPrecip_T25_BWpH.png
-active True
-batch G12_NaOH_noPrecip_T10_25_BWpH.png False True
-headings %P-removal-NaOH pH NaOH
-axis_titles "pH" "P-removal (%)" "Chemical dosing (mol)" #
-initial_solutions true
-chart_title "P removal at different pH with pH dosing, at Temp 25"
-connect_simulations true
-axis_scale x_axis       5 13                    # pH
-axis_scale y_axis       0 100                   # %P removal
-axis_scale sy_axis     0 auto                   # NaOH added in M
-start
05 P0  =  8.092e-04                              # initial P in moles
10 Cl0 =  6.956e-03                              # initial Cl in
moles
15 Na0 =  9.637e-03                              # initial Na in
moles  (200mgNa/l)
20 pH = -LA("H+")
30 GRAPH Y    ((P0-tot("P"))/P0)*100             # P removal in %
40 GRAPH X    pH                                 # pH
50 GRAPH SY   ((tot("Na")-Na0))                          # NaOH added
in M retrieved from increase in Na in solution
 -end
 END

USE SOLUTION  1
USE REACTION  2
USE REACTION_TEMPERATURE 25
USE EQUILIBRIUM_PHASES 15
USER_GRAPH 12 G12_NaOH_noPrecip_T25LotuspH.png
-initial_solutions true
-connect_simulations false
-headings %P-removal-HCl pH HCL
05 P0  =  8.092e-04                              # initial P in moles
10 Cl0 =  6.956e-03                              # initial Cl in
moles
15 Na0 =  9.637e-03                              # initial Na in
moles  (200mgNa/l)
20 pH = -LA("H+")
```

```
30 GRAPH Y     ((P0-tot("P"))/P0)*100            # P removal in %
40 GRAPH X     pH                                # pH
50 GRAPH_SY    ((tot("Cl")-Cl0))                         # NaOH added
in M retrieved from increase in Na in solution
 -end
 END

USER_GRAPH 12
```

```
-detach
```

I. V. Validation PHREEQC and Experiment II

The following script was used to model the results of the Validation Experiment and Experiment II. The final pH and temperature were used as input. The different equilibrium phases let precipitation occur without pH fixation for all minerals and ATPC, DCP. HAP was also implemented as it's Ca:P molar ratio is close to the measured ratio. For Experiment II Lotus Like water was used as base composition, and the phosphorus as measured bu the test kit was adjusted, after which the Ca reduction was determined and adjusted. After running the model the output gives results which were then processed in Excel. The results were incorporated in in Table 22 and Graph 25.

```
SOLUTION  1 Lotus Like Water Validation and Experiment II
#Adjust the solution composition accordingly to the measured ICPOES
results, temperature, pH, and Alkalinity
-units  mg/l
-temp   22.8         # ADJUST
pH      7.74         # ADJUST
P       30.8         # ADJUST
Amm     27.00        # ADJUST
K       40.25        # ADJUST
Na      432.96       # ADJUST
Mg      77.19        # ADJUST
S(6)    210.55       # ADJUST
Cl      1321.11      # ADJUST
Ca      296.95       # ADJUST
Alkalinity    73.15   as HCO2   # ADJUST
END
```

```
EQUILIBRIUM_PHASES 1     all minerals
ATCP                     0 0
DCPD                     0 0
DCP                      0 0
Struvite                 0 0
CO2(g)                   -3.4
END
```

```
EQUILIBRIUM_PHASES 2     # only DCP
DCP                      0 0
CO2(g)                   -3.4
END

EQUILIBRIUM_PHASES 3     # only ATCP
ATCP                     0 0
CO2(g)                   -3.4
END

EQUILIBRIUM_PHASES 4     # only HAP
Hydroxyapatite           0 0
CO2(g)                   -3.4
END

REACTION_TEMPERATURE 1
24.8                      #ADJUST #Keeping the temp(degC) constant
END
```

```
The four runs performed
USE SOLUTION 1
USE EQUILIBRIUM_PHASES 1         #all minerals
USE REACTION_TEMPERATURE 1
SAVE SOLUTION 2
END

USE SOLUTION 1
USE EQUILIBRIUM_PHASES 2         # only DCP
USE REACTION_TEMPERATURE 1
SAVE SOLUTION 3
END

USE SOLUTION 1
USE EQUILIBRIUM_PHASES 3         # only ATCP
USE REACTION_TEMPERATURE 1
SAVE SOLUTION 4
END

USE SOLUTION 1
USE EQUILIBRIUM_PHASES 4         # only HAP
USE REACTION_TEMPERATURE 1
SAVE SOLUTION 5
END
```